Optimal control of non-invasive neuromodulation for the treatment of sleep apnea syndromes

Diego Oswaldo Pérez Trenard

▶ To cite this version:

UNIVERSITÉ DE
RENNES 1

UNIVERSITE
BRETAGNE
LOIRE

THÈSE / UNIVERSITÉ DE RENNES 1

sous le sceau de l'Université Bretagne Loire

pour le grade de

DOCTEUR DE L'UNIVERSITÉ DE RENNES 1

Mention : Signal, Image, Vision

Ecole doctorale MATHSTIC

présentée par

Diego Oswaldo Pérez Trenard

préparée à l'unité de recherche INSERM, U1099
Laboratoire Traitement du signal et de l'image
UFR ISTIC: Informatique et Électronique

Optimal Control of Non-Invasive Neuromodulation for the Treatment of Sleep Apnea Syndromes

Acknowledgements

I would like to express my sincere gratitude to my supervisor, *Alfredo Hernández*, for the continuous support not only during my Ph.D study but from the first moment we started working together during my engineering internship. His guidance, motivation and immense knowledge helped me all the time during my research and while writing this thesis. More than my supervisor, I consider him a friend. I would also like to express my sincere appreciation to my co-supervisor, *Lotfi Senhadji*, for his constant availability and cheerfulness that motivates the entire laboratory team. My deepest sense of gratitude to all the members of the LTSI for making me feel part of the team and supporting me at every moment. To my office colleague, *Thomas Janvier*, for our extremely interesting conversations and brainstorming moments that always result in brilliant ideas. To *Fabrice Tudoret* who always, with smiles and jokes, helped me with anything I needed. To *Patricia*, *Soizic* and *Muriel* for their logistic support and pleasant disposition. To my colleagues *Nadine*, *Matthieu* and *Daniel* for becoming my friends and for all the moments of joy that we shared together.

I want to seize this moment to thank all my old venezuelan friends that despite the distance we support each other with the same friendship as always. Special thanks to a friend who has become my brother, *Ragde*, who has been my friend during all my life and who has supported me in every moment since I've been here. A big thanks to all the new friends I have made in this wonderful country for showing me a new culture and another sense of seeing life.

No tengo palabras para describir el agradecimiento que tengo a mi querida familia que sin ellos nada de esto hubiese sido posible. Gracias a mi padre, *Oswaldo*, que con sus consejos, experiencia, extrema inteligencia y comprensión me ha guiado en cada paso de mi vida. A mi madre, *Carolina*, que con su infinito amor y dedicación me convirtieron en la persona que soy, no puedo imaginar una mejor madre. A mi hermano, *Andrés*, con su contagiosa alegría y apoyo incondicional me motivan a seguir adelante, créeme hermano, no tengo palabras para expresarte el orgullo y admiración que siento hacia ti. A *Mireia*, que con su amor y comprensión inigualable se ha convertido en uno de los pilares más importantes de mi vida, grandes aventuras aún nos deparan. Por último, quiero agradecer a mis abuelos y tíos que siempre con sus palabras de aliento me han acompañado en cada momento. Un agradecimiento especial a mi nana, *Pura*, que siempre la tengo en mis pensamientos.

Abstract

Sleep apnea syndrome (SAS) is a multifactorial disease characterized by recurrent episodes of breathing pauses or significant reductions in respiratory amplitude during sleep. Typically, these episodes are followed by events of significant drops of oxygen levels in the blood (hypoxemia) that may provoke acute cardiorespiratory responses along with alterations of the sleep structure, which may be deleterious in the long term. Several therapies have been proposed for the treatment of SAS, being continuous positive airway pressure (CPAP) the gold standard treatment. Despite their excellent results in symptomatic patients, there is a 15% initial refusal rate and long term adherence is difficult to achieve in minimally symptomatic patients. Therefore, the development of non-invasive SAS treatment methods, with improved acceptability, is thus of major importance. The objective of this PhD thesis is to propose new signal processing and control methods of non-invasive neuromodulation for the treatment of SAS. The hypothesis underlying this work is that bursts of kinesthetic stimulation delivered during the early phase of apneas or hypopneas may elicit a controlled startle response that can activate sub-cortical centers controlling upper airways muscles and the autonomic nervous system, stopping respiratory events without generating a cortical arousal.

In this context, the first part of this manuscript is dedicated to the description of a novel real-time monitoring and therapeutic neuromodulation system (PASITHEA system), which functions as a multi-purpose device for SAS diagnosis and treatment through kinesthetic stimulation. This system has been developed in the framework of an ANR TecSan project (PASITHEA project), led by our laboratory, with the participation of Sorin CRM SAS. The main contributions in this thesis are focused on the signal processing and control aspects of this system, as well as the electronics associated with one of the main system components. Another contribution is related to the evaluation of these methods and devices through specific clinical protocols.

In the second part of this work, we propose a first control method for delivering triggered kinesthetic stimulation. An On/Off control method using as control variable the output of a real-time respiratory event detector is proposed. When respiratory event detection is confirmed, a command is sent to the kinesthetic stimulator to activate it and it is stopped when the respiration flow is resumed. A unique stimulation strategy where a constant stimulation amplitude is applied upon event detention was implemented in a first clinical protocol (HYPNOS study), dedicated to assessing the patient response to therapy

implementing the previously mentioned control method. Several signal processing methods were developed and applied to estimate the patient response. Results showed that 75% of the patients responded correctly to the proposed therapy in terms of respiratory event duration. Moreover, significant decreases in the SaO_2 variability were also found in more than half of the patients when implementing a novel method for the estimation of the variations in the SaO_2 signal.

Since we hypothesized that inappropriate patient selection could be one of the factors that could explain the observed lack of response in 25% of patients. The next chapter proposes a method to differentiate patients who could benefit from kinesthetic stimulation therapy, based on the estimation of complexity-based indexes of heart rate variability (HRV). The results of these analyses showed that the effectiveness of this therapy seems correlated to a functional autonomic nervous system (ANS) and that future developments should be focused on the description of predictive models based on the combination of heart rate variability (HRV) and heart rate complexity (HRC) parameters, in order to identify appropriate candidates.

Finally, the last part of this thesis proposes an improved closed-loop control method, integrating concurrent, coupled proportional-derivative (PD) controllers in order to adaptively change the kinesthetic stimulation amplitude delivered to the patient by the therapeutic system, using as control variables three physiological signals recorded in real-time: Nasal pressure (NP), oxygen saturation (SaO2) and the electrocardiogram signal (ECG). A second clinical protocol comprising 40 patients (EKINOX study) with the main objective of validating the control algorithm for patient-specific adaptive kinesthetic stimulation was launched. Several improvements to the first version of the system were developed to allow the integration of the proposed controller. The last chapter presents preliminary results from the first phase of this study, where 10 patients were analyzed in order to validate the correct functioning of the controller and determine the set of optimal control parameters to be used for the second phase. The obtained results validated the proposed controller operation and showed that the controller was able to provide adaptive kinesthetic stimulation in function of the patient-specific responses. In addition, qualitative results show that the control algorithm tends to minimize the delivered amplitude of stimulation while eliciting the desired physiological response. A second phase of this study implementing the proposed controller and the set of the selected control parameters from the first phase is currently ongoing with the inclusion of the remaining 30 patients.

This manuscript ends with a chapter presenting the general conclusions and perspectives of this work.

Résumé

Le syndrome d'apnée du sommeil (SAS) est une maladie sous-diagnostiquée qui affecte environ 5% des hommes et des femmes d'âge moyen. Elle se caractérise par des épisodes récurrents de collapsus des voies respiratoires supérieures (apnée) ou par des réductions importantes de l'amplitude du flux d'air respiratoire (hypopnée), suivis d'un réveil transitoire qui entraîne le rétablissement de la perméabilité des voies respiratoires supérieures. Ces épisodes sont répétés plusieurs fois pendant le sommeil, ce qui entraîne une fragmentation du sommeil ainsi que des altérations cardiorespiratoires aiguës associées au développement de l'hypertension, des maladies coronariennes, des accidents vasculaires cérébraux et d'autres complications cardiovasculaires à long terme. Les effets délétères du SAS sur les manifestations cardiovasculaires sont principalement déclenchés par la gravité de l'hypoxie intermittente (HI) causée par les pauses respiratoires, induisant l'activation subséquente du système nerveux autonome.

Parmi les thérapies proposées pour le traitement des SAS, la thérapie de référence dans la prise en charge des SAS modérés à sévères est la pression positive continue des voies aériennes (CPAP), suivie de l'utilisation de dispositifs d'avancement mandibulaire (MAD). La CPAP est associée à d'excellents résultats chez les patients symptomatiques. Cependant, il y a un taux de refus initial de 15% et il est difficile d'atteindre une adhérence à long terme chez les patients présentant des symptômes minimaux. Des études récentes sur des patients traités par CPAP ont montré un taux relativement élevé d'abandon et de faible conformité avec des taux moyens d'adhérence entre 39% et 50%. La compliance à la MAD est plus élevée que la CPAP, mais les traitements ne sont pas aussi efficaces et les thérapies à base de MAD dépendent fortement de la morphologie du patient. Des améliorations à la CPAP classique, telles que la pression positive continue automatique des voies aériennes (Auto-CPAP), ont été proposées. Néanmoins, une méta-étude récente a montré que la méthode Auto-CPAP n'apporte pas de valeur ajoutée significative en ce qui concerne l'acceptation ou la conformité à la thérapie par rapport à la CPAP classique à titrage manuel. Les thérapies alternatives sont donc souhaitables dans le domaine des SAS.

En plus de la CPAP, de la MAD et de la chirurgie pour élargir les voies respiratoires supérieures, les thérapies basées par stimulation ont gagné de l'intérêt pour le traitement des SAS. Un mécanisme clé sous-jacent aux collapsus pharyngés répétés pendant le sommeil est la réduction de l'activité des muscles dilatateurs du pharynx à un niveau qui n'est pas en mesure de maintenir la perméabilité des voies respiratoires supérieures dans le contexte d'un

affaiblissement de l'anatomie des voies respiratoires supérieures. De nouvelles approches de stimulation dédiées à l'augmentation du débit neural vers les muscles dilatateurs des voies respiratoires supérieures comme la stimulation du nerf hypoglosse ou la stimulation électrique directe des muscles transcutanés sub-mentaux sont en cours d'évaluation. En outre, des dispositifs de stimulation directe du nerf phrénique ont été développés pour le traitement de l'apnée centrale. Ces thérapies font actuellement l'objet de recherches cliniques et, bien que prometteuses, elles nécessitent une intervention invasive qui peut entraîner des effets secondaires importants.

Les paragraphes ci-dessus soulignent le fait qu'une grande partie de la population des SAS reste encore insuffisamment traitée, voire non traitée. Le développement de méthodes de traitement SAS non invasives, avec une meilleure acceptabilité, est donc d'une importance majeure. Dans des études antérieures, il a été démontré que la stimulation kinesthésique déclenche un réflexe physiologique appelé réflexe de sursaut, capable d'entraîner des réponses motrices systémiques et une activation cardiaque autonome. L'hypothèse qui sous-tend ce travail de thèse est que des poussées de stimulation kinesthésique, délivrées au cours de la phase précoce de l'apnée ou de l'hypopnée, peuvent réduire la durée des événements respiratoires et, par la suite, limiter les désaturations d'oxygène associées, par une activation contrôlée du réflexe de sursaut.

Le premier chapitre de ce travail décrit le contexte clinique dans lequel s'inscrit cette thèse. Un aperçu général du SAS, comprenant la pathogenèse, l'épidémiologie, la stratification des risques, la gestion clinique, ainsi qu'un examen des thérapies actuelles, est présenté. De plus, ce chapitre inclut également une présentation de la physiologie du système cardiorespiratoire et de sa régulation par le système nerveux autonome ainsi que la structure du sommeil humain. Le deuxième chapitre présente le cadre théorique général des méthodes de traitement du signal et de théorie du contrôle, utilisées tout au long de ce travail. La terminologie et les définitions liées à ces domaines sont introduites, ainsi que leurs applications dans le domaine biomédical.

Dans ce contexte, la première partie de ce manuscrit est consacrée à la description d'un nouveau système de surveillance et de neuromodulation thérapeutique en temps réel (système PASITHEA), qui fonctionne comme un appareil multifonctionnel pour le diagnostic et le traitement du SAS par stimulation kinesthésique. Ce système a été développé dans le cadre d'un projet ANR TecSan (projet PASITHEA), piloté par notre laboratoire, avec la participation de Sorin CRM SAS. Les principales contributions de cette thèse se concentrent sur les aspects du traitement des signaux et contrôle de ce système, ainsi que sur l'électronique associée à l'un des principaux composants du système. Une autre contribution est liée à l'évaluation des dispositifs et des méthodes développées par de protocoles cliniques spécifiques.

Le troisième chapitre présente une description complète de la première version de ce nouveau système de surveillance et de neuromodulation thérapeutique pour le SAS, basé sur la stimulation kinesthésique adaptative non invasive proposée dans cette thèse. Dans ce chapitre, on décrit la première version du système (PASITHEA v1) qui a été conçu

pour détecter, surveiller et traiter les désordres respiratoires. Le système est composé de trois éléments : i) un enregistreur ambulatoire cardiorespiratoire (Holter), ii) un système de stimulation kinesthésique et iii) une application de contrôle en temps réel pour la stimulation kinesthésique adaptative, fonctionnant sur un ordinateur standard. Ces éléments communiquent entre eux par un protocole de communication sans fil basé sur la technologie Bluetooth (BT). Dans cette première version, nous proposons une première méthode de contrôle de la stimulation kinesthésique. Une méthode de contrôle On/Off utilisant comme variable de contrôle la sortie d'un détecteur d'événements respiratoires en temps réel est proposée. Lorsque la détection d'événements respiratoires est confirmée, un ordre est envoyé au stimulateur kinesthésique pour l'activer et il est arrêté lorsque le flux respiratoire reprend. Une stratégie de stimulation où une amplitude de stimulation constante est appliquée lors de la détention d'un événement, a été mise en œuvre dans le cadre d'un premier protocole clinique (étude HYPNOS), dédié à l'évaluation de la réponse du patient à la thérapie, mettant en œuvre la méthode de contrôle précédemment mentionnée.

Dans le cadre de ce premier étude clinique, le système a été testée sur 46 patients qui ont effectué une nuit complète d'enregistrement avec une polysomnographie (PSG). Ce test était constitué de périodes de stimulation intermittentes de 30 minutes suivies de périodes de 30 minutes pendant lesquelles le stimulateur était inactif. Une analyse qualitative, patient par patient, des réponses cardiorespiratoires obtenues lors de la thérapie kinesthésique a été réalisée, dans le but d'évaluer la réponse de chaque patient à la stimulation. Une réponse correcte a été définie comme un retour à une respiration normale, pendant ou immédiatement après la stimulation kinesthésique. L'absence de retour à une respiration normale après la fin de la troisième poussée de stimulation a été considérée comme une non-réponse. Les résultats préliminaires ont montré que le système a fonctionné de façon satisfaisante lors de cette première évaluation clinique. Dans le groupe de patients répondeurs, les conséquences cardiorespiratoires aiguës aux événements respiratoires observés pendant les périodes non stimulées, pouvant être délétères pour le patient à long terme, sont interrompues ou significativement atténuées pendant les périodes où la stimulation a été délivrée.

Les résultats quantitatifs obtenus à partir de cette première phase d'étude sont exposés dans le quatrième chapitre, afin d'analyser l'une des hypothèses principales de notre travail. Les poussées de stimulation kinesthésique délivrées au cours de la phase précoce de l'apnée ou de l'hypopnée peuvent provoquer une activation contrôlée du réflexe de sursaut. Les centres sous-corticaux, contrôlant les muscles des voies respiratoires supérieures et le système nerveux autonome, sont alors activés stoppant ainsi les événements respiratoires sans générer un réveil cortical. Plusieurs méthodes de traitement des signaux ont été appliquées pour estimer la réponse du patient. Les résultats montrent que le traitement proposé diminue significativement la durée des apnées ou des hypopnées (environ 5 secondes) chez 75% des patients inclus dans l'analyse. De plus, ils montrent que lors de la implémentation d'une nouvelle méthode d'estimation des variations du signal de SaO_2, le traitement diminue également l'amplitude des chutes de SaO_2 chez 54.2% des patients étudiés avec une réduction moyenne de la variance de SaO_2 de 55.44% pour l'apnée et de 37.61% pour les épisodes

d'hypopnée. La plupart des patients n'ont montré aucune différence significative entre les périodes de stimulation (stimulées et non stimulées) ni pour le stade de sommeil, ni en ce qui concerne l'indice micro-arousal. Dans ce chapitre, nous avons émis l'hypothèse que l'un des facteurs expliquant l'absence de réponse observée chez 25% des patients pourrait être attribuable à une sélection inappropriée de patients. Les individus, susceptibles de répondre de manière optimale à la thérapie, pourraient être sélectionnés en analysant certains indices de la fonction autonomique lors d'un test préliminaire.

Le cinquième chapitre présente les résultats obtenus à partir d'une nouvelle méthode permettant de différencier les patients qui pourraient bénéficier d'une thérapie de stimulation kinesthésique. Nous pensons que le mécanisme principal qui sous-tend l'efficacité de ce traitement est le bon état de fonctionnement du système nerveux autonome (SNA) des patients admissibles. Par conséquent, une analyse comparative de la fonction du SNA, basée sur des paramètres de variabilité (HRV) et de complexité (HRC) de la fréquence cardiaque, a été réalisée sur des données de patients souffrant de SAS avec des réponses différentes à la thérapie de stimulation kinesthésique. Les résultats de ces analyses ont montré que l'efficacité de cette thérapie dépend d'un SNA fonctionnant correctement et que les développements futurs devraient être centrés sur la description de modèles prédictifs basés sur la combinaison des paramètres HRV et HRC, afin d'identifier les candidats pouvant bénéficier de la thérapie de stimulation kinesthésique.

Le dernier chapitre propose une méthode améliorée de contrôle en boucle fermée, intégrant des contrôleurs proportionnels-dérivés (PD) couplés et simultanés, afin de modifier de façon adaptative l'amplitude de stimulation kinesthésique délivrée au patient par le système thérapeutique, en utilisant comme variables de contrôle trois signaux physiologiques enregistrés en temps réel : Pression nasale (NP), saturation en oxygène (SaO_2) et signal électrocardiographique (ECG). Un deuxième protocole clinique comprenant 40 patients (étude EKINOX) avec l'objectif principal de valider l'algorithme de contrôle de la stimulation kinesthésique adaptative spécifique au patient a été initié. Plusieurs améliorations de la première version du système ont été réalisées. Ce chapitre présente aussi les résultats préliminaires de la première phase de cette étude, où les données de 10 patients ont été analysées afin de valider le bon fonctionnement du contrôleur et de déterminer l'ensemble des paramètres de contrôle à utiliser pour la deuxième phase. Les résultats ont permis de valider le fonctionnement du contrôleur en boucle fermée proposé et sa capacité à fournir une stimulation kinesthésique adaptative en fonction des réponses spécifiques au patient. De plus, les résultats qualitatifs démontrent que l'algorithme de contrôle tend à minimiser l'amplitude de stimulation délivrée, tout en induisant la réponse physiologique désirée. Certaines préoccupations d'ordre technique ainsi que les travaux futurs prévus sont également exposés dans ce chapitre. Une deuxième phase de cette étude mettant en œuvre le contrôleur proposé et l'ensemble des paramètres de contrôle sélectionnés pour la première phase est actuellement en cours avec l'inclusion des 30 patients restants.

Enfin, un chapitre de conclusion est présenté dans lequel les principales conclusions et contributions de ce travail de thèse sont exposées.

Contents

List of acronyms

AHR	Apnea or hypopnea responder
ANS	Autonomic nervous system
AUC	Area under the ROC curve
AR	Apnea responder
Auto-CPAP	Automatic continuous positive airway pressure
BT	Bluetooth technology
BTLE	Bluetooth Low Energy
CNS	Central nervous system
CPAP	Continuous positive airway pressure
CVS	Cardiovascular system
EA	Evolutionary algorithms
ECG	Electrocardiogram
HF	High frequency
HR	Heart rate
HR	Hypopnea responder
HRC	Heart rate complexity
HRV	Heart rate variability
IH	Intermittent hypoxia
LF	Low frequency
MAD	mandibular advancement device
NP	Nasal pressure

NR   No responder

NREM   Non rapid eye movement

OSA   Obstructive sleep apnea

PASITHEA   Personalized and Adaptive kinesthetic StImulation Therapy, based on cardiorespiratory Holter monitoring, for slEep Apnea syndromes

$\mathbf{P}_{CO_2}$ Partial carbon dioxide pressure

PVC   Premature ventricular contractions

$\mathbf{P}_{O_2}$ Partial oxygen pressure

PNS   Peripheral nervous system

REM   Rapid eye movement

RS   Respiratory system

$\mathbf{SaO}_2$ Oxygen saturation

SAS   Sleep apnea syndrome

SNS   Somatic nervous system

SOP   Sleep-onset period

CHAPTER 1 ■

Introduction

Sleep apnea syndromes (SAS) is an under-diagnosed disease affecting up to 5% of middle-aged men and women (Heinzer et al., 2015; Jennum et al., 2009; Peppard et al., 2013). It is characterized by recurrent episodes of upper airway collapse (apnea) or significant reductions in respiratory airflow amplitude (hypopnea), followed by transient awakening that leads to the restoration of upper airway permeability. These episodes are repeated several times every hour, leading to sleep fragmentation along with acute cardio-respiratory alterations which are associated with the development of hypertension, coronary heart diseases, stroke and other cardiovascular complications in the long term (Lévy et al., 2014; Somers et al., 2008; Stansbury et al., 2015). The deleterious effects of SAS on cardiovascular outcomes are mainly triggered by the intermittent hypoxia (IH) severity caused by the respiratory pauses, inducing the subsequent activation of the autonomic nervous system (Dick et al., 2007; Drager et al., 2010; Kasai et al., 2011).

Patients with SAS have varying degrees of symptomatology and SAS-related co-morbid conditions (Bailly et al., 2016; Deacon et al., 2016). Several therapies have been proposed for the treatment of SAS, being the gold standard therapy in the management of moderate to severe SAS, the continuous positive airway pressure (CPAP) (Berkani et al., 2015; Marin et al., 2005), followed by the use of mandibular advancement devices (MAD) (Bratton et al., 2015; Hoffstein, 2007). CPAP, the first line therapy, is associated with excellent results in highly symptomatic patients. However, there is a 15% initial refusal rate and long term adherence is difficult to achieve in mildly symptomatic patients (Craig et al., 2012). Recent studies on CPAP-treated patients have shown a relatively high rate of abandonment and poor compliance with average adherence rates between 39% and 50% (Kushida et al., 2012). Compliance with MAD is higher than CPAP, yet treatments are not as effective (Phillips et al., 2013). In addition, the efficacy of MAD-based therapies strongly depends on the morphology of the patient (Fritsch et al., 2001) and more than 30% of SAS patients are contraindicated to MAD owing to dental or joint problems (Petit et al., 2002). Improvements to the classical CPAP, such as the automatic continuous

1

positive airway pressure (Auto-CPAP), have been proposed. However, a recent meta-study has shown that the Auto-CPAP method does not provide significant added value concerning the acceptance or compliance to the therapy, with respect to classical, manually titrated CPAP (Gao et al., 2012). Thus, alternative therapies are desirable for the appropriate treatment of SAS.

In addition to CPAP, MAD and surgery to enlarge the upper airways, stimulation therapies have recently gained interest in the treatment of SAS (Strollo et al., 2016). A key mechanism underlying repeated pharyngeal collapse during sleep is the reduction of pharyngeal dilator muscle activity to a level that is not able to maintain upper airway patency in the context of impaired upper airway anatomy. New stimulation approaches dedicated to increase the neural output to upper airway dilator muscles as hypoglossal nerve stimulation (Strollo Jr et al., 2014) or direct electrical stimulation of submental transcutaneous muscles are currently under evaluation (Pengo et al., 2016). Also, devices for the direct stimulation of the phrenic nerve have been developed, which may be useful for the treatment of central apnea (Ponikowski et al., 2011). These therapies are currently under clinical investigation and, although promising, they require an invasive procedure that may cause significant side effects (Eastwood et al., 2011). MRI incompatibility may also be a limitation to the widespread use of these systems.

The above paragraphs underline the fact that there is still a large portion of the SAS population that remains inadequately treated or even untreated. The development of non-invasive SAS treatment methods, with improved acceptability, is thus of major importance. In this context, the objective of this PhD thesis is to propose new signal processing and control methods of non-invasive neuromodulation for the treatment of SAS, based on kinesthetic stimulation. Additional objectives are the development of an integrated system prototype, embedding the proposed methods, and the evaluation of this prototype system in a clinical setup. Indeed, previous studies have shown that kinesthetic stimulation may trigger a physiological reflex, called the "startle reflex", which is capable of eliciting systemic motor responses and cardiac autonomic activation (Taylor et al., 1991; Yeomans et al., 2002). The hypothesis underlying this thesis is that bursts of kinesthetic stimulation, delivered during the early phase of apneas or hypopneas, may reduce respiratory event duration and subsequently limit related oxygen desaturations, through a controlled activation of the startle reflex.

This manuscript is divided into eight chapters. The first chapter provides the clinical context in which this thesis is framed. A general overview of the SAS, including pathogenesis, epidemiology, risk stratification, clinical management, as well as a state-of-the-art review of the current therapies, is presented. Also, a brief review about the cardiorespiratory system physiology and its regulation through the autonomic nervous system along with the human sleep nature is also presented. Chapter 3 introduces the general signal processing and control theory framework that is consistently employed throughout this work. It details the terminology and formalized definitions related to the context of control and signal processing, and presents some applications of the state of the art in the biomedical domain.

After these introductory chapters, chapter 4, provides a complete description of a novel real-time monitoring and therapeutic neuromodulation system (PASITHEA system), which serves as a multi-purpose device for delivering kinesthetic stimulation (HERNANDEZ et al., 2016). The different control methods that are proposed throughout this work were embedded into this device, which was then validated in clinical protocols. In the first stage of this thesis, we proposed a first control algorithm for delivering kinesthetic stimulation. An On/Off control method using as control variable the output of a real-time respiratory event detector was integrated. Briefly, when respiratory event detection is confirmed, a command is sent to the kinesthetic stimulator to activate it and it is stopped when the respiration flow is resumed. A unique stimulation strategy with a constant stimulation amplitude was applied upon event detention. The complete system was tested in a first clinical protocol (HYPNOS study), dedicated to assessing the patient response to therapy implementing the previously mentioned control method. Several signal processing methods were developed to estimate the patient response. Chapter 5 presents the implemented methods and the main results obtained from this first clinical protocol. In addition, a novel method developed in the context of this thesis for the analysis of the variations in the SaO_2 signal is also presented in that chapter.

In chapter 6, we propose a new method to estimate patients who could benefit from kinesthetic stimulation therapy. Several analyses in the time and frequency domains were implemented in order to extract heart rate variability (HRV) and heart rate complexity (HRC) markers from heart rate time series. Beat detection was obtained from the recorded electrocardiogram (ECG), through a wavelet-based algorithm previously proposed in our laboratory and adapted to this signals. Results from the retrospective application of this method for the estimation of patient response on the data obtained from the previously mentioned clinical protocol are also presented.

Finally, the last part of this thesis proposes a novel closed-loop control method, integrating concurrent, coupled proportional-derivative (PD) controllers in order to manage the kinesthetic stimulation amplitude delivered to the patient by the therapeutic system, using as control variables three physiological signals recorded in real-time: Nasal pressure (NP), oxygen saturation (SaO_2) and the ECG signal. A complete description of a second clinical protocol comprising 40 patients (EKINOX study) with the main objective of validating the control algorithm for patient-specific adaptive kinesthetic stimulation is presented in chapter 7. This chapter also describes the different improvements to the first version of the system that were developed to allow the integration of the proposed controller. Preliminary results from the first phase of this study, where 10 patients were analyzed in order to validate the correct functioning of the controller and determine the set of optimal control parameters to be used for the second phase with the inclusion of the remaining 30 patients are also presented.

References

BAILLY, S., M. DESTORS, Y. GRILLET, P. RICHARD, B. STACH, I. VIVODTZEV, J.-F. TIMSIT, P. LÉVY, R. TAMISIER, J.-L. PÉPIN, et al. (2016). "Obstructive sleep apnea: a cluster analysis at time of diagnosis". In: *PLoS One* 11.6, e0157318.

BERKANI, K. and J. DIMET (2015). "[Acceptability and compliance to long-term continuous positive pressure treatment]". In: *Revue des maladies respiratoires* 32.3, pp. 249–255.

BRATTON, D. J., T. GAISL, A. M. WONS, and M. KOHLER (2015). "CPAP vs mandibular advancement devices and blood pressure in patients with obstructive sleep apnea: a systematic review and meta-analysis". In: *Jama* 314.21, pp. 2280–2293.

CRAIG, S. E., M. KOHLER, D. NICOLL, D. J. BRATTON, A. NUNN, R. DAVIES, and J. STRADLING (2012). "Continuous positive airway pressure improves sleepiness but not calculated vascular risk in patients with minimally symptomatic obstructive sleep apnoea: the MOSAIC randomised controlled trial". In: *Thorax*, thoraxjnl–2012.

DEACON, N. L., R. JEN, Y. LI, and A. MALHOTRA (2016). "Treatment of obstructive sleep apnea. Prospects for personalized combined modality therapy". In: *Annals of the American Thoracic Society* 13.1, pp. 101–108.

DICK, T. E., Y.-H. HSIEH, N. WANG, and N. PRABHAKAR (2007). "Acute intermittent hypoxia increases both phrenic and sympathetic nerve activities in the rat". In: *Experimental physiology* 92.1, pp. 87–97.

DRAGER, L. F., J. C. JUN, and V. Y. POLOTSKY (2010). "Metabolic consequences of intermittent hypoxia: relevance to obstructive sleep apnea". In: *Best practice & research Clinical endocrinology & metabolism* 24.5, pp. 843–851.

EASTWOOD, P. R., M. BARNES, J. H. WALSH, K. J. MADDISON, G. HEE, A. R. SCHWARTZ, P. L. SMITH, A. MALHOTRA, R. D. McEVOY, J. R. WHEATLEY, et al. (2011). "Treating obstructive sleep apnea with hypoglossal nerve stimulation". In: *Sleep* 34.11, pp. 1479–1486.

FRITSCH, K. M., A. ISELI, E. W. RUSSI, and K. E. BLOCH (2001). "Side effects of mandibular advancement devices for sleep apnea treatment". In: *American journal of respiratory and critical care medicine* 164.5, pp. 813–818.

GAO, W., Y. JIN, Y. WANG, M. SUN, B. CHEN, N. ZHOU, and Y. DENG (2012). "Is automatic CPAP titration as effective as manual CPAP titration in OSAHS patients? A meta-analysis". In: *Sleep and Breathing* 16.2, pp. 329–340.

HEINZER, R., S. VAT, P. MARQUES-VIDAL, H. MARTI-SOLER, D. ANDRIES, N. TOBBACK, V. MOOSER, M. PREISIG, A. MALHOTRA, G. WAEBER, et al. (2015). "Prevalence of sleep-disordered breathing in the general population: the HypnoLaus study". In: *The Lancet Respiratory Medicine* 3.4, pp. 310–318.

HERNANDEZ, A., G. GUERRERO, D. FEUERSTEIN, L. GRAINDORGE, D. PEREZ, A. AMBLARD, P. MABO, J.-L. PÉPIN, and L. SENHADJI (2016). "Pasithea: An integrated monitoring and therapeutic system for sleep apnea syndromes based on adaptive kinesthetic stimulation". In: *IRBM* 37.2, pp. 81–89.

HOFFSTEIN, V. (2007). "Review of oral appliances for treatment of sleep-disordered breathing". In: *Sleep and Breathing* 11.1, pp. 1–22.

JENNUM, P. and R. L. RIHA (2009). "Epidemiology of sleep apnoea/hypopnoea syndrome and sleep-disordered breathing". In: *European Respiratory Journal* 33.4, pp. 907–914.

KASAI, T. and T. D. BRADLEY (2011). "Obstructive sleep apnea and heart failure: pathophysiologic and therapeutic implications". In: *Journal of the American College of Cardiology* 57.2, pp. 119–127.

KUSHIDA, C. A., D. A. NICHOLS, T. H. HOLMES, S. F. QUAN, J. K. WALSH, D. J. GOTTLIEB, R. D. SIMON JR, C. GUILLEMINAULT, D. P. WHITE, J. L. GOODWIN, et al. (2012). "Effects of continuous positive airway pressure on neurocognitive function in obstructive sleep apnea patients: the Apnea Positive Pressure Long-term Efficacy Study (APPLES)". In: *Sleep* 35.12, pp. 1593–1602.

LÉVY, P., M. KOHLER, W. T. McNICHOLAS, F. BARBÉ, R. D. McEVOY, V. K. SOMERS, L. LAVIE, and J.-L. PEPIN (2014). "Obstructive sleep apnoea syndrome." In: *Nature reviews. Disease primers* 1, pp. 15015–15015.

MARIN, J. M., S. J. CARRIZO, E. VICENTE, and A. G. AGUSTI (2005). "Long-term cardiovascular outcomes in men with obstructive sleep apnoea-hypopnoea with or without treatment with continuous positive airway pressure: an observational study". In: *The Lancet* 365.9464, pp. 1046–1053.

PENGO, M. F., S. XIAO, C. RATNESWARAN, K. REED, N. SHAH, T. CHEN, A. DOUIRI, N. HART, Y. LUO, G. F. RAFFERTY, et al. (2016). "Randomised sham-controlled trial of transcutaneous electrical stimulation in obstructive sleep apnoea". In: *Thorax*, thoraxjnl–2016.

PEPPARD, P. E., T. YOUNG, J. H. BARNET, M. PALTA, E. W. HAGEN, and K. M. HLA (2013). "Increased prevalence of sleep-disordered breathing in adults". In: *American journal of epidemiology* 177.9, pp. 1006–1014.

PETIT, F.-X., J.-L. PÉPIN, G. BETTEGA, H. SADEK, B. RAPHAËL, and P. LÉVY (2002). "Mandibular advancement devices: rate of contraindications in 100 consecutive obstructive sleep apnea patients". In: *American journal of respiratory and critical care medicine* 166.3, pp. 274–278.

PHILLIPS, C. L., R. R. GRUNSTEIN, M. A. DARENDELILER, A. S. MIHAILIDOU, V. K. SRINIVASAN, B. J. YEE, G. B. MARKS, and P. A. CISTULLI (2013). "Health outcomes of continuous positive airway pressure versus oral appliance treatment for obstructive sleep apnea: a randomized controlled trial". In: *American journal of respiratory and critical care medicine* 187.8, pp. 879–887.

PONIKOWSKI, P., S. JAVAHERI, D. MICHALKIEWICZ, B. A. BART, D. CZARNECKA, M. JASTRZEBSKI, A. KUSIAK, R. AUGOSTINI, D. JAGIELSKI, T. WITKOWSKI, et al. (2011). "Transvenous phrenic nerve stimulation for the treatment of central sleep apnoea in heart failure". In: *European heart journal* 33.7, pp. 889–894.

SOMERS, V. K., D. P. WHITE, R. AMIN, W. T. ABRAHAM, F. COSTA, A. CULEBRAS, S. DANIELS, J. S. FLORAS, C. E. HUNT, L. J. OLSON, et al. (2008). "Sleep apnea and

cardiovascular disease: An American heart association/American college of cardiology foundation scientific statement from the American heart association council for high blood pressure research professional education committee, council on clinical cardiology, stroke council, and council on cardiovascular nursing in collaboration with the national heart, lung, and blood institute national center on sleep disorders research (national institutes of health)". In: *Journal of the American College of Cardiology* 52.8, pp. 686–717.

Stansbury, R. C. and P. J. Strollo (2015). "Clinical manifestations of sleep apnea". In: *Journal of thoracic disease* 7.9, E298.

Strollo Jr, P. J., R. J. Soose, J. T. Maurer, N. De Vries, J. Cornelius, O. Froymovich, R. D. Hanson, T. A. Padhya, D. L. Steward, M. B. Gillespie, et al. (2014). "Upper-airway stimulation for obstructive sleep apnea". In: *New England Journal of Medicine* 370.2, pp. 139–149.

Strollo, P. J. and A. Malhotra (2016). *Stimulating therapy for obstructive sleep apnoea.*

Taylor, B. K., R. Casto, and M. P. Printz (1991). "Dissociation of tactile and acoustic components in air puff startle". In: *Physiology & behavior* 49.3, pp. 527–532.

Yeomans, J. S., L. Li, B. W. Scott, and P. W. Frankland (2002). "Tactile, acoustic and vestibular systems sum to elicit the startle reflex". In: *Neuroscience & Biobehavioral Reviews* 26.1, pp. 1–11.

General context: Sleep apnea syndrome (SAS)

This chapter describes the clinical context in which this thesis is framed. First, a general overview of the disease under study, the sleep apnea syndrome (SAS), is presented. This frequent syndrome is characterized by repeated episodes of breathing pauses, associated with acute cardiorespiratory responses, that may be deleterious in the long term. Since the upper airway anatomy plays a significant role in the pathophysiology, a description of this structure is presented in section 2.2.1. An explanation of the physiological sub-systems that are involved in the pathogenesis of SAS is also resented in section 2.2. Then, a brief review on the physiological basis of the cardiorespiratory system and its modulation through the autonomic nervous system is introduced. Finally, the last sections are dedicated to the description of the different physiological concepts that will be evoked in this work.

2.1. Sleep apnea syndrome (SAS)

Sleep apnea syndrome (SAS) is characterized by repeated episodes of breathing pauses (apnea) or reductions in respiratory amplitude (hypopnea) during sleep. These episodes often induce significant arterial hypoxemia and hypercapnia that usually lead to transient sleep arousals, sleep fragmentation and acute over compensatory responses of the autonomic nervous system, that may be deleterious in the long term, being associated with higher cardiovascular and metabolic morbidities (PEPPARD et al., 2013; SOMERS et al., 2008; STANSBURY et al., 2015). SAS represent a major healthcare issue, affecting more than 5% of the middle-aged population (HEINZER et al., 2015; JENNUM et al., 2009; PEPPARD et al., 2013). Commonly, SAS is divided into two event categories:

- **Central events:** Central apnea (CA) or hypopnea (CH) are denoted by an absence or marked reduction of brain stem respiratory output, and thus, neuromuscular respiratory drive to respiratory pump muscles.

- **Obstructive events:** Obstructive apnea (OA) or hypopnea (OH) are characterized by an extra-thoracic upper airway obstruction along with respiratory efforts.

- **Mixed events:** Mixed apnea or hypopnea result from a combination of central and obstructive events.

Population-based studies have shown that most SAS events are driven by anatomical and neurochemical anomalies in the control of the upper airway and chest wall respiratory musculature. The dominant risk factors are the body weight, followed by male gender and craniofacial structure and aging (DEMPSEY et al., 2002; PARTINEN et al., 1988a; PEPPARD et al., 2000; YOUNG et al., 2003). Figure 2.2 presents an example of the typical physiological signals recorded during the night from patients suffering from severe SAS. In this example, the consequences of the repeated respiratory events in each signal can be observed.

Three biological systems are primarily involved in SAS: i) the respiratory system, ii) the cardiovascular system and iii) the autonomic nervous system (ANS). The next sections will present a brief description of these systems and their relation to SAS, in order to fix the clinical framework of this work.

2.1.1.   Pathogenesis of Sleep Apnea

In humans, one of the major structures that comprise the respiratory system are the upper airways (description in section 2.2.1). This structure performs complex motor behaviors required to generate speech and are possible because the hyoid bone, which is a key anchoring site for pharyngeal dilator muscles which is not rigidly attached to skeletal structures, leaving the human pharynx with no rigid support unlike in other animals (MORGAN et al., 2007). This attribute gives to the upper airway the chance to narrow or collapse when the compensatory neural activation of dilator muscles is lost at sleep onset. However, these compensatory processes are the product of multiple factors and vary markedly among individuals (DEMPSEY et al., 2010). A diagram of the pathogenesis of SAS is shown in figure 2.1. First, the diagram shows the principal structural and functional determinants of an anatomical predisposition for airway closure. Generally, a patient having any of them is more prone to suffer from SAS. Then, after sleep, two paths to develop either an obstructive or central apnea are presented. The diagram emphasizes the mechanisms underlying both types of respiratory events, and integrates anatomical deficits with mechanisms for central neurochemical control of breathing stability and compensatory neuromuscular control of upper airway muscles in order to explain the cyclical nature of SAS.

An illustration of these different mechanisms can also be appreciated in figure 2.2. Figure 2.2-A shows the nasal pressure (NP) signal with the presence of several respiratory events. These events are provoked, as previously described, by a decrease of the tonic activity of the upper airway dilator muscles causing the upper airway to narrow/collapse (obstructive apnea) or by an unstable central respiratory motor output leading to a stoppage
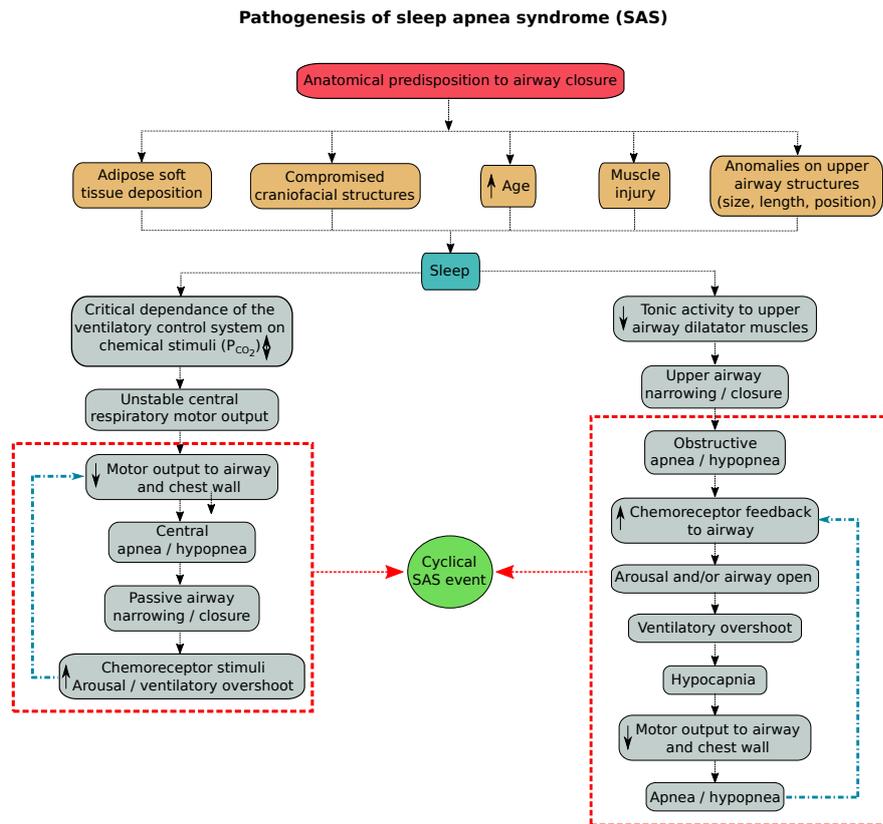
Figure 2.1: Scheme of the sleep apnea syndrome cyclical pathogenesis. Modified figure from (DEMPSEY et al., 2010).

of the respiration (central apnea). After these alterations in the respiratory system, the lack of uptake of oxygen produces a decrease of oxygen concentration in the blood (hypoxemia) which induces intermittent hemodynamic variations in the cardiovascular system, this behavior can be observed in figure 2.2-B, where the oxygen saturation (SaO_2) signal is presented. Moreover, acute autonomic responses can also be seen in the heart rate (HR) signal (figure 2.2-C), where regulating mechanisms in the cardiovascular system are induced by recurrent activations of the baroreflex and chemoreflex as a response to hypoxia. Additionally, these respiratory events may provoke sleep micro-arousals (figure 2.2-D) which are the main factor of the sleep fragmentation related to SAS. The next sections will describe the different physiological concepts previously mentioned.

2.1.2. Consequences of sleep apnea

As previously introduced in section 2.1, SAS is recognized as a risk factor for the development of hypertension and other cardiovascular diseases. Recurrent episodes of SAS produce arterial oxygen desaturation, hypercapnia, significant intrathoracic pressure oscillations, and sleep disruption. They are also characterized by a marked, transient increase in systemic arterial pressure caused by sympathetic nervous system activation
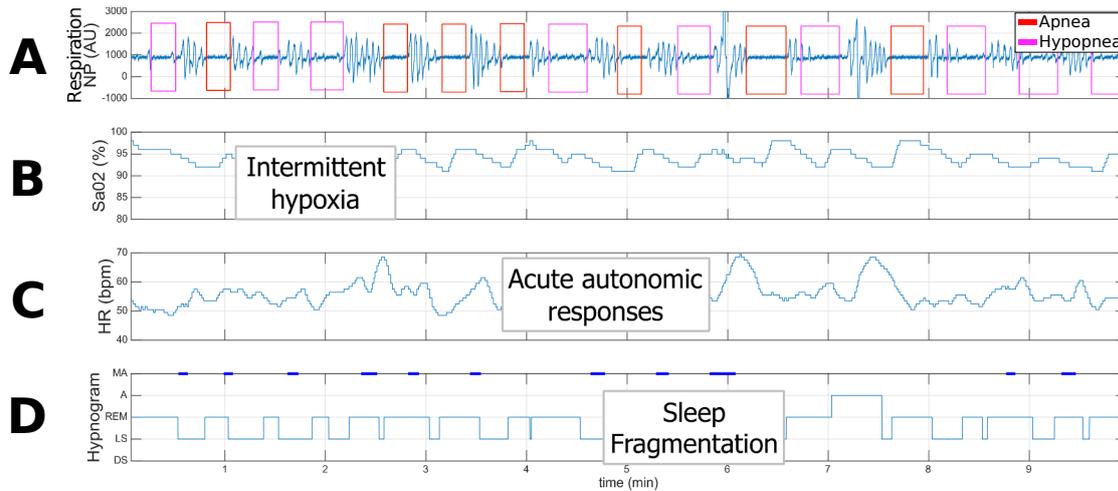
Figure 2.2: Example of a typical recording of a patient suffering from sleep apnea syndrome (HYPNOS study). The first panel shows the nasal pressure (NP) signal, where the different apnea and hypopnea events are highlighted. The second panel represents the oxygen saturation (SaO$_2$) signal with the intermittent hypoxia events associated with SAS. The third panel, presents the instantaneous heart rate (HR) signal, showing recurrent acute autonomic responses that are due to the respiratory events. Finally, the fourth panel presents a hypnogram signal (MA = micro-arousal, A = Awake, REM = Rapid eye movement, LS = Light sleep and DS = Deep sleep) representing the sleep structure of the patient during the recording. The hypnogram shows the presence of sleep arousals and sleep fragmentation produced by respiratory events.

(Katragadda et al., 1997; O'Donnell et al., 1996). Such responses can occur a significant number of times for severe SAS patients, as shown in figure 2.2. These acute over compensatory responses of the autonomic nervous system, due to the effects of SAS, are deleterious in the long-term and they may induce the following consequences:

- **Cardiovascular and metabolic defects:** One of the most well-known risk factors for hypertension is SAS. The causal link between SAS and hypertension has been firmly established via animal models (Brooks et al., 1997; Fletcher et al., 1992) and studies that have shown that blood pressure decreases in hypertensive patients when SAS is treated (Becker et al., 2003; Pepperell et al., 2002). Other diseases, such as left ventricular dysfunction, cardiac arrhythmias and stroke have been also associated with SAS (Arzt et al., 2005; Guilleminault et al., 1983; Shahar et al., 2001). In addition, recent studies have associated SAS with metabolic defects and to the predisposition to the eventual development of Type 2 diabetes (McArdle et al., 2007; Punjabi et al., 2005).

- **Sleep fragmentation:** Sleep deprivation, or sleep restriction, may not reflect the disturbances in sleep that occur in SAS. Typically, total sleep time is not significantly restricted in SAS, but rather sleep is fragmented by repetitive arousals resulting

from the impaired breathing during sleep. Common symptoms associated with sleep fragmentation include decreased psychomotor performance on task involving short term memory, reaction time, vigilance and degraded mood (BONNET et al., 2003; MARTIN et al., 1996). These symptoms lead to daytime sleepiness which is one of the main risk factors to suffer everyday accidents (NODA et al., 1998; STOOHS et al., 1994).

2.2. The cardio-respiratory system response to SAS

This section presents a brief description of the main components of the cardio-respiratory system and its control, in order to introduce the main physiological concepts needed for the understanding of the rest of the manuscript. Figure 2.3 presents a modular diagram of the three biological systems that are involved in response to SAS and the general interactions among them.

The blue module represents the respiratory system, where the airflow coming from the upper airways interacts with the lungs in order to allow for gas exchange and transport of oxygen (O_2) and carbon dioxide (CO_2) to the rest of the body. The red module represents the cardiovascular system, comprising the heart and the circulatory system. Moreover, the sinoatrial node in charge of the heart rhythm control has been represented separately. The heart acts upon the circulatory system and its different components: pulmonary, systemic and cerebral. Finally, the purple module represents the nervous system, comprised by central respiratory and ANS controls and three sensory receptors (chemoreceptors, baroreceptors and pulmonary stretch receptors).

The respiratory system is affected by the cardiovascular system due to alterations in blood flow and, more importantly, by the nervous system. The central nervous system induces the ventilatory activity by sending electrical impulses through the phrenic and abdominal nerves, which will generate a negative intra-thoracic pressure, allowing for airflow intake. In turn, the nervous system receives mechanical feedback from the lungs captured by pulmonary stretch receptors. On the other hand, sympathetic and parasympathetic branches of the autonomic nervous system regulate the cardiovascular system function. Baroreceptors and chemoreceptors measure arterial blood pressure and gases in circulation respectively in order to close the loop between these two systems.

In the case of SAS, the balance among systems is lost by a narrow/collapse of the upper airways (obstructive apnea) or by unstable central respiratory motor drive (central apnea) as described in section 2.1.1. These alterations limit the gas exchange and activate peripheral chemoreceptors and pulmonary stretch receptors due to the lack of air and therefore oxygen. In turn, these activations produce an increase of the sympathetic tone which leads to an increase in HR and thus in arterial blood pressure. They also induce an activation of the neural controller that forces respiration to resume by controlling lung mechanics and in consequence generating a cortical arousal. A general physiological

description of each of the previously mentioned modules are described in the following sections.
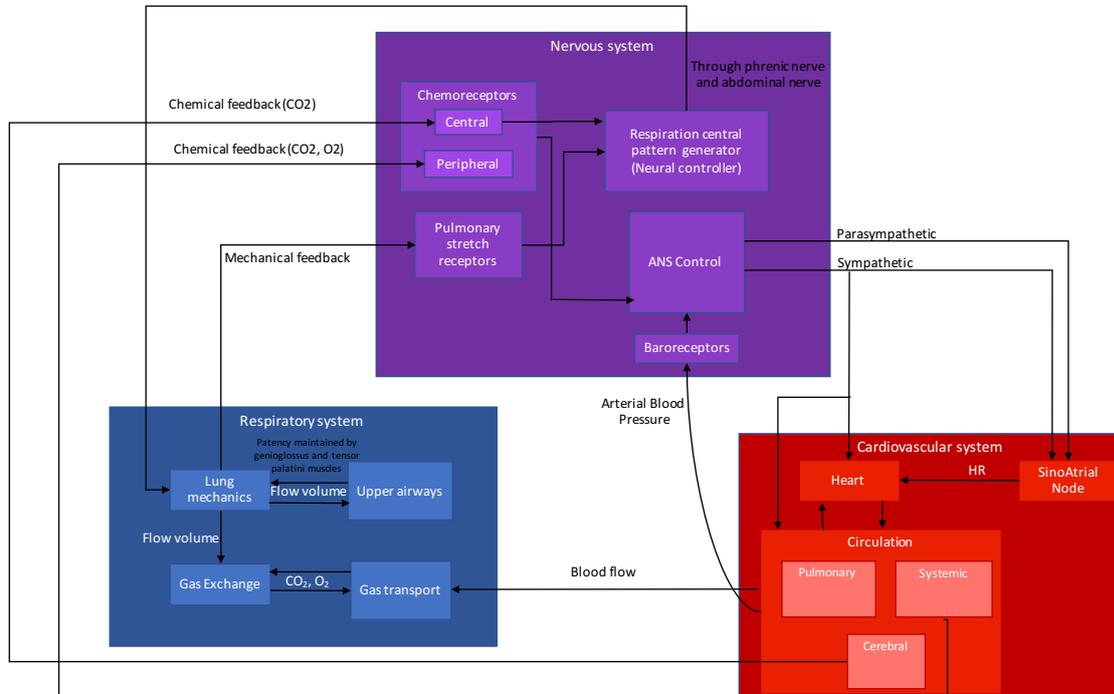

Figure 2.3: Diagram of the three biological systems that are involved in response to SAS. Figure adapted from the ongoing PhD thesis work of Gustavo Guerrero, SEPIA team - LTSI.

2.2.1.   The respiratory system

The respiratory system (RS) (see figure 2.4) is a biological system composed by three major structures: the airways, the lungs, and different respiratory muscles. Its main function is to perform the gas exchange that is required by the human body to maintain a constant stream of oxygen, in order to sustain the cellular lifecycle. Gas exchange is particularly important for respiration, which involves the uptake of oxygen (O_2) and release of carbon dioxide (CO_2).

As illustrated in figure 2.4, the RS is divided in two main parts: the upper and the lower airway tracts. The latter is comprised by the lungs and the diaphragm. The lungs are the largest organs in the respiratory system and their function is to extract O_2 from the outside and to transfer it into the bloodstream to then release CO_2 from the bloodstream to the outside in a process know as gas exchange. On the other hand, the diaphragm is a muscle capable of voluntarily contracting in order to pull or push the membrane surrounding the lungs facilitating air to flow inside or outside them.

The upper airway is a multipurpose structure composed by the pharynx and nasal
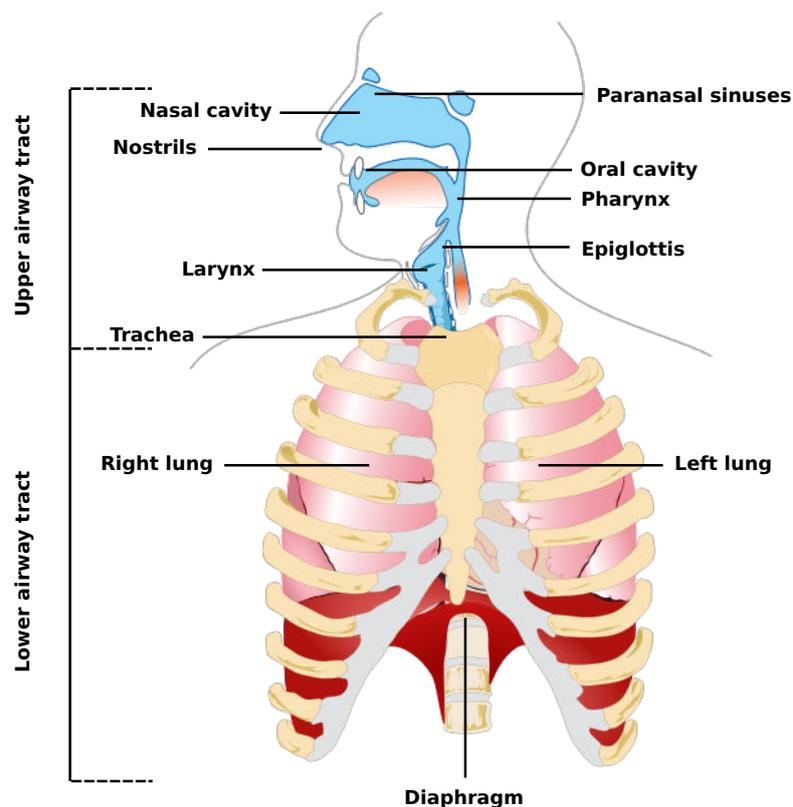
Figure 2.4: The respiratory system. Adapted from "Human respiratory system pedagogical fr" by Michka B licensed under CC BY 4.0.

cavities (POHUNEK, 2004). However, some authors also include the larynx, trachea and oral cavity because of their role in the RS. These structures are involved in performing functional tasks such as air warming and humidification, pathways for olfaction, speech, swallowing and allowing the passage of air for breathing. It is composed of numerous muscles and soft tissue which allows the upper airway to change shape in order to grant to humans the ability to speak and swallow. Although these features are widely used during wakefulness, the lack of rigid or bony support creates a collapsible portion that extends from the hard palate to the larynx, that may collapse during sleep due to a significantly reduced muscle tone (PIERCE et al., 1999).

The upper airway patency is maintained by activation of dilator muscles driven by chemoreceptors responding to chemical stimuli (hypercapnia and hypoxia) and by mechanoreceptor feedback responding to negative pharyngeal pressure (LOEWEN et al., 2011). In the case of SAS, during airways obstruction an increase in negative pharyngeal pressure is due to an elevation of the respiratory effort against the obstructed airway, which in turn is provoked due to chemical stimulation. The most well studied muscles are the genioglossus and tensor palatini (MALHOTRA et al., 2000). Anatomic airway narrowing is compensated by increased activation of upper airway muscles in awake patients.

However, an important mechanism in the pathogenesis of OSA relates to the interaction between pharyngeal anatomy and a diminished ability of the upper airway dilator muscles to maintain a patent airway during sleep (Mezzanotte et al., 1992). Consequently, several studies have shown that whereas healthy individuals experience a loss of upper airway muscle tone at sleep onset, an individual reliant on muscle tone due to an anatomic vulnerability will be particularly susceptible to developing OSA (Mezzanotte et al., 1996; Worsnop et al., 1998).

In addition, as previously mentioned, the genioglossus is importantly modulated by locally mediated mechanoreceptive reflex mechanisms that respond to negative pharyngeal pressure (Pillar et al., 2001). One such mechanism is the genioglossus negative pressure reflex, whereby the muscle is activated in response to rapid changes in negative intrapharyngeal pressure (Horner et al., 1991). Nevertheless, although genioglossus muscle responsiveness may be impaired during sleep compared with wakefulness, studies have shown that the muscle does respond to sustained negative pressure and potentially hypercapnia (Lo et al., 2006; Stanchina et al., 2002). However, there is a substantial interindividual variability in the effectiveness of these compensatory responses to restore airflow during sleep (Jordan et al., 2007).

2.2.2. Autonomic regulation of the cardiovascular system

The cardiovascular system (CVS) is a closed circulatory system mainly composed of the heart, blood vessels and blood (figure 2.5). Its function is to maintain an adequate supply of oxygen to all tissues of the body and to transport nutrients, carbon dioxide, hormones and blood cells throughout the organism. However, in order to maintain this function, the autonomic system must process visceral information and coordinate neural elements that innervate the heart, blood vessels, and the respiratory system. Regarding SAS, this system is closely involved in the responses to the breathing pauses as figure 2.3 shows. During a SAS event, activations of the nervous system are primarily elicited by activations on chemoreceptors due to the lack of oxygen. These activations trigger different over compensatory responses in the cardiovascular system such as: increased HR, changes in cardiac contractility and changes in the intrathoracic pressure due to the airway occlusion. As mentioned in section 2.1, these responses may be deleterious in the long term, being associated with cardiovascular diseases.

On the other hand, the nervous system is a network of nerve cells and fibres which, along the brain and spinal cord, receives and interprets information from the entire organism and transmits impulses to the effector organs. It is subdivided in four different subsystems:

- **Central Nervous System (CNS):** It is composed of the brain and spinal cord and it behaves as the processing center of the nervous system. It integrates and coordinates the information that it receives and also influences the activity of the organism.
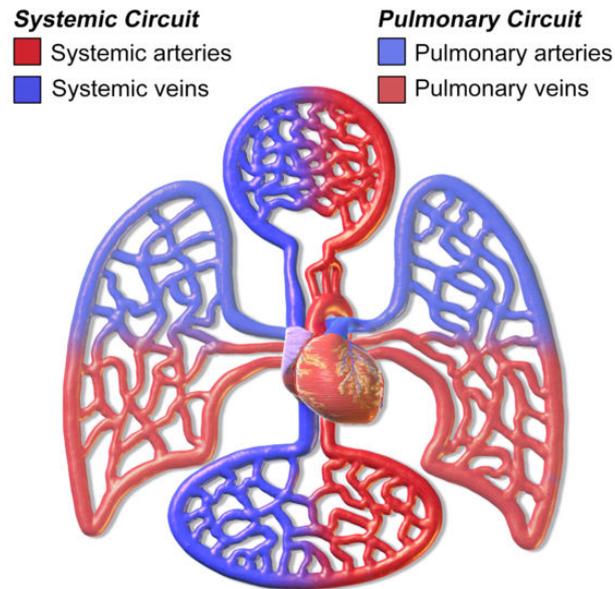
Figure 2.5: Cardiovascular system, composed of the heart and the pulmonary and systemic circulations. Adapted from "CardiovascularSystem" by Dcoetzee licensed under CC BY 4.0.

- **Peripheral Nervous System (PNS):** It consists on nerves and glands outside of the brain and spinal cord, and it is responsible of the connection and information transport between CNS and the rest of the body. This subsystem is also subdivided in two parts:

  - **The somatic nervous system (SNS):** Comprising the nerves associated with the voluntary control of body movements, and innervating skeletal muscles and external sensory organs.

  - **The autonomic nervous system (ANS):** Innervating smooth muscles and glands in order to influence the function of internal organs, and thus regulate involuntary body functions. It is subdivided in three branches: the sympathetic, parasympathetic and enteric nervous systems. The sympathetic and parasympathetic nervous systems have opposite actions, where the former is often considered as the "fight or flight" system and is generally activated in cases of stress whereas the latter is mainly activated when organisms are in a relaxed state. Finally, the enteric nervous system is responsible of the intestinal motility in digestion and is capable of acting independent of the sympathetic and parasympathetic nervous systems.

2.2.2.1. Mechanoreceptors

Mechanoreceptors are sensory receptors that respond to mechanical forces applied to the body (Biswas et al., 2015; Catton, 1970). These receptors allow animals to perceive the different mechanical stimuli coming from outside, by initiating nerve impulses in sensory neurons when they are physically deformed by an outside force such as: touch, pressure, motion and stretching. There are four main types of mechanoreceptors in glabrous mammalian skin, depending of their function (Parvizi, 2010):

- **Pacinian corpuscles:** They are egg-shaped structures embedding free nerve endings responsible for sensitive to vibration and pressure.

- **Meissner's corpuscles:** This type of nerve endings are located near the surface of the skin and they are responsible for sensitivity to light touch and vibration.

- **Merkel nerve endings:** They consist of large cells with lobulated nuclei and dense-core granules in the cytoplasm facing the associated afferent nerve terminal. They are slowly adapting mechanoreceptors responsible of adapting to maintained stimuli.

- **Ruffini corpuscle:** These nerve endings are located in the dermis, subcutaneous tissues, and connective tissues. They are slowly adapting endings that respond when skin is stretched.

2.2.2.2. Human reflexes

A reflex is one of the simplest kind of neural activity in which a stimulus leads to an immediate automatic response that does not receive or need conscious thought. The anatomical pathway of a reflex is called the reflex arc and it consists of an afferent (or sensory) nerve, usually one or more interneurons within the central nervous system, and an efferent (motor, secretory, or secreto-motor) nerve.

The cardiorespiratory system is regulated by sets of neurons that form two major types of reflex circuit. The first type is called baroreflex or baroreceptor reflex, which causes a decrease in the discharge of sympathetic vasomotor and cardiac outflows whenever an increase in blood pressure occurs. The second major type is the chemoreflex or chemoreceptor reflex which regulates respiration, cardiac output, and regional blood flow, ensuring that proper amounts of oxygen are delivered to the brain and heart.

2.2.2.3. Baroreflex

The baroreflex is a mechanism that regulates acute blood pressure changes via controlling heart rate, contractility, and peripheral resistance. These blood pressure changes are sensed by baroreceptors, which are mechanoreceptors located in the carotid sinus and in the aortic arch. Impulses sent from the baroreceptors are relayed to the nucleus of the tractus solitarius and ultimately to the vasomotor center of the brain. A sudden increase in blood

pressure stretches the baroreceptors and the increased firing results in the vasomotor center inhibiting sympathetic drive and increasing vagal tone. On the other hand, in a sudden drop in blood pressure, baroreceptors will decrease the firing of impulses provoking the vasomotor center to uninhibit sympathetic activity in the heart and blood vessels and decrease vagal tone causing an increase in heart rate.

2.2.2.4. Chemoreflex

The chemoreflex is a mechanism that regulates respiratory activity in order to maintain arterial blood partial oxygen pressure (P_{O_2}), partial carbon dioxide pressure (P_{CO_2}), and pH within appropriate physiological ranges. Falls in arterial P_{O_2} are called hypoxemia whereas increases in arterial P_{CO_2} are called hypercapnia. Both phenomenon are sensed by chemoreceptors which are sensory extensions located in carotid and aortic bodies (Peripheral chemoreceptors) and in medullary neurons (central chemoreceptors). They send impulses in order to increase the rate and depth of respiration, however, they also affect cardiovascular function either directly (by interacting with medullary vasomotor centers) or indirectly (via altered pulmonary stretch receptor activity).

2.3. Sleep structure

Sleep is a complex process in which the body rests and where the consciousness is in partial or complete abeyance along with a partial suspension of body functions, including sensory activity. This process is required in humans in order to maintain proper function and health, and it is influenced by two interacting biological mechanisms: the circadian rhythm and the sleep-wake homeostasis. The former, which is the main mechanism that coordinates the day-night / light-dark cycle and regulates the body's sleep patterns and brainwave activity among other biological processes, interacts together with the latter which is an internal biochemical system that operates as a timer, generating a homeostatic sleep drive or pressure to sleep, in order to determine the timing of the transitions from wakefulness to sleep and vice-versa (typically 8 hours of sleep).

Usually, the sleep process is divided into four stages: rapid eye movement (REM), stage 1, stage 2 and stage 3. However, some studies separate these stages into two categories: REM and non-REM (NREM) sleep. These stages progress cyclically and represent brain activity during sleep, which is estimated among other factors, by synchronized electrical pulses from masses of neurons communicating with each other called brainwaves. Figure 2.6 shows the different brainwaves and their associated sleep stages.

- **Stage 1:** is a light transition sleep stage where brainwave activity gradually slows down, drifting form sleep to awake. During this stage, eye movement decreases as well as muscle activity. However, it is an easily disrupted stage where sudden changes in brainwave activity pattern accompanied by shifts from deep sleep to light sleep

or from sleep to wakefulness may occur. These sudden changes are know as sleep arousals.

- **Stage 2:** it is a stage where the body begins to prepare for deep sleep. Muscle activity decreases still further and conscious awareness begins to fade completely. Eye movement stops and brainwaves become slower with only an occasional burst of rapid brainwaves. It is also accompanied by a drop on body's temperature and a heart rate (HR) decrease.

- **Stage 3:** It is the deepest sleep stage and it is characterized by extremely slow brainwaves. During this period, the sleeper is even less responsive and essentially, it is unaware of any sounds or other stimuli.

- **REM:** is a sleep stage where brainwaves activity increases and mimic activity during the waking state. It is called REM stage because eyes in spite of being closed, they move rapidly from side-to-side. It is in this stage where dreams occurs, and it is related with an increase in respiration and HR.
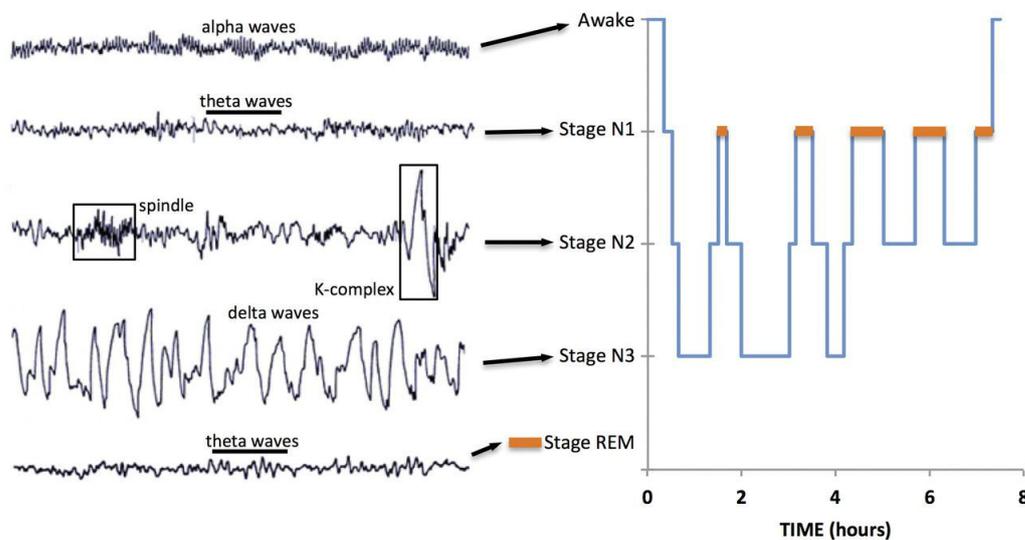

Figure 2.6: EEG features of sleep/wake stages (left) and typical temporal organization of healthy nocturnal sleep in an adult (right) (Carley et al., 2016).

Concerning SAS, as described in section 2.1.2, sleep deprivation or sleep restriction are not the principal consequences of SAS regarding sleep, but rather sleep fragmentation by repetitive arousals which are abrupt changes in the pattern of the brainwave activity representing a shift from a deep sleep to light sleep. These arousals result from the impaired breathing during sleep that activates the autonomic nervous system as a critical defense mechanism that activates upper airway dilator muscles and prevents asphyxiation.

2.4. Conclusion

This chapter briefly described the main physiological knowledge underlying this work. Sleep apnea syndrome (SAS) is a multifactorial disease characterized by recurrent breathing pauses that usually provoke significant arterial hypoxemia and hypercapnia leading to over compensatory responses. Many physiological sub-systems are involved in the pathogenesis of SAS and further development of this syndrome.

The autonomic nervous system (ANS) innervates the cardiorespiratory system with both sympathetic and parasympathetic branches, in order to regulate respiration, heart rate and blood pressure. One of the primary sensory receptors in the physiological closed-loop control involving the autonomic and cardiorespiratory systems are the arterial baroreceptors and chemoreceptors. In the context of SAS, there is increasing evidence that recurrent respiratory events that evoke over compensatory autonomic activations, significantly contribute to the development of serious pathological conditions in the long term.

Patients with structural and anatomical irregularities in the upper airway are more prone to suffer from narrow or collapse of the upper airway when the compensatory neural activation of dilator muscles is lost at sleep onset. These irregularities are key factors for the understanding of the pathogenesis of SAS.

The next chapter will present a state of the art of the current therapies for the treatment of SAS and the different control algorithms implemented, the limitations of these therapies and the hypothesis that support this work.

References

ARZT, M., T. YOUNG, L. FINN, J. B. SKATRUD, and T. D. BRADLEY (2005). "Association of sleep-disordered breathing and the occurrence of stroke". In: *American journal of respiratory and critical care medicine* 172.11, pp. 1447–1451.

BECKER, H. F., A. JERRENTRUP, T. PLOCH, L. GROTE, T. PENZEL, C. E. SULLIVAN, and J. H. PETER (2003). "Effect of nasal continuous positive airway pressure treatment on blood pressure in patients with obstructive sleep apnea". In: *circulation* 107.1, pp. 68–73.

BISWAS, A., M. MANIVANNAN, and M. A. SRINIVASAN (2015). "Vibrotactile sensitivity threshold: Nonlinear stochastic mechanotransduction model of the Pacinian corpuscle". In: *IEEE transactions on haptics* 8.1, pp. 102–113.

BONNET, M. H. and D. L. ARAND (2003). "Clinical effects of sleep fragmentation versus sleep deprivation". In: *Sleep medicine reviews* 7.4, pp. 297–310.

BROOKS, D., R. L. HORNER, L. F. KOZAR, C. L. RENDER-TEIXEIRA, and E. A. PHILLIPSON (1997). "Obstructive sleep apnea as a cause of systemic hypertension. Evidence from a canine model." In: *Journal of Clinical Investigation* 99.1, p. 106.

Carley, D. W. and S. S. Farabi (2016). "Physiology of Sleep". In: *Diabetes Spectrum* 29.1, pp. 5–9.

Catton, W. (1970). "Mechanoreceptor function." In: *Physiological reviews* 50.3, pp. 297–318.

Dempsey, J. A., J. B. Skatrud, A. J. Jacques, S. J. Ewanowski, B. T. Woodson, P. R. Hanson, and B. Goodman (2002). "Anatomic determinants of sleep-disordered breathing across the spectrum of clinical and nonclinical male subjects". In: *CHEST Journal* 122.3, pp. 840–851.

Dempsey, J. A., S. C. Veasey, B. J. Morgan, and C. P. O'Donnell (2010). "Pathophysiology of sleep apnea". In: *Physiological reviews* 90.1, pp. 47–112.

Fletcher, E. C., J. Lesske, W. Qian, C. C. Miller, and T. Unger (1992). "Repetitive, episodic hypoxia causes diurnal elevation of blood pressure in rats." In: *Hypertension* 19.6 Pt 1, pp. 555–561.

Guilleminault, C., S. J. Connolly, and R. A. Winkle (1983). "Cardiac arrhythmia and conduction disturbances during sleep in 400 patients with sleep apnea syndrome". In: *The American journal of cardiology* 52.5, pp. 490–494.

Heinzer, R., S. Vat, P. Marques-Vidal, H. Marti-Soler, D. Andries, N. Tobback, V. Mooser, M. Preisig, A. Malhotra, G. Waeber, et al. (2015). "Prevalence of sleep-disordered breathing in the general population: the HypnoLaus study". In: *The Lancet Respiratory Medicine* 3.4, pp. 310–318.

Horner, R., J. Innes, K. Murphy, and A. Guz (1991). "Evidence for reflex upper airway dilator muscle activation by sudden negative airway pressure in man." In: *The Journal of Physiology* 436.1, pp. 15–29.

Jennum, P. and R. L. Riha (2009). "Epidemiology of sleep apnoea/hypopnoea syndrome and sleep-disordered breathing". In: *European Respiratory Journal* 33.4, pp. 907–914.

Jordan, A. S., A. Wellman, R. C. Heinzer, Y.-L. Lo, K. Schory, L. Dover, S. Gautam, A. Malhotra, and D. P. White (2007). "Mechanisms used to restore ventilation after partial upper airway collapse during sleep in humans." In: *Thorax*.

Katragadda, S., A. Xie, D. Puleo, J. B. Skatrud, and B. J. Morgan (1997). "Neural mechanism of the pressor response to obstructive and nonobstructive apnea". In: *Journal of Applied Physiology* 83.6, pp. 2048–2054.

Lo, Y.-L., A. S. Jordan, A. Malhotra, A. Wellman, R. C. Heinzer, K. Schory, L. Dover, R. B. Fogel, and D. P. White (2006). "Genioglossal muscle response to CO2 stimulation during NREM sleep". In: *Sleep* 29.4, pp. 470–477.

Loewen, A. H., M. Ostrowski, J. Laprairie, F. Maturino, P. J. Hanly, and M. Younes (2011). "Response of genioglossus muscle to increasing chemical drive in sleeping obstructive apnea patients". In: *Sleep* 34.8, pp. 1061–1073.

Malhotra, A., G. Pillar, R. B. Fogel, J. Beauregard, J. K. Edwards, D. I. Slamowitz, S. A. Shea, and D. P. White (2000). "Genioglossal but not palatal muscle activity relates closely to pharyngeal pressure". In: *American journal of respiratory and critical care medicine* 162.3, pp. 1058–1062.

MARTIN, S. E., H. M. ENGLEMAN, I. J. DEARY, and N. J. DOUGLAS (1996). "The effect of sleep fragmentation on daytime function." In: *American journal of respiratory and critical care medicine* 153.4, pp. 1328–1332.

MCARDLE, N., D. HILLMAN, L. BEILIN, and G. WATTS (2007). "Metabolic risk factors for vascular disease in obstructive sleep apnea: a matched controlled study". In: *American journal of respiratory and critical care medicine* 175.2, pp. 190–195.

MEZZANOTTE, W. S., D. J. TANGEL, and D. P. WHITE (1996). "Influence of sleep onset on upper-airway muscle activity in apnea patients versus normal controls." In: *American journal of respiratory and critical care medicine* 153.6, pp. 1880–1887.

MEZZANOTTE, W. S., D. J. TANGEL, and D. P. WHITE (1992). "Waking genioglossal electromyogram in sleep apnea patients versus normal controls (a neuromuscular compensatory mechanism)." In: *Journal of Clinical Investigation* 89.5, p. 1571.

MORGAN, T. D. and J. E. REMMERS (2007). "Phylogeny and animal models: An uninhibited survey". In: *Obstructive Sleep Apnea.*

NODA, A., T. YAGI, M. YOKOTA, Y. KAYUKAWA, T. OHTA, and T. OKADA (1998). "Daytime sleepiness and automobile accidents in patients with obstructive sleep apnea syndrome". In: *Psychiatry and clinical neurosciences* 52.2, pp. 221–222.

O'DONNELL, C., T. AYUSE, E. KING, A. SCHWARTZ, P. SMITH, and J. ROBOTHAM (1996). "Airway obstruction during sleep increases blood pressure without arousal". In: *Journal of Applied Physiology* 80.3, pp. 773–781.

PARTINEN, M., C. GUILLEMINAULT, M.-A. QUERA-SALVA, and A. JAMIESON (1988a). "Obstructive sleep apnea and cephalometric roentgenograms: the role of anatomic upper airway abnormalities in the definition of abnormal breathing during sleep". In: *Chest* 93.6, pp. 1199–1205.

PARVIZI, J. (2010). *High Yield Orthopaedics E-Book.* Elsevier Health Sciences.

PEPPARD, P. E., T. YOUNG, J. H. BARNET, M. PALTA, E. W. HAGEN, and K. M. HLA (2013). "Increased prevalence of sleep-disordered breathing in adults". In: *American journal of epidemiology* 177.9, pp. 1006–1014.

PEPPARD, P. E., T. YOUNG, M. PALTA, J. DEMPSEY, and J. SKATRUD (2000). "Longitudinal study of moderate weight change and sleep-disordered breathing". In: *Jama* 284.23, pp. 3015–3021.

PEPPERELL, J. C., S. RAMDASSINGH-DOW, N. CROSTHWAITE, R. MULLINS, C. JENKINSON, J. R. STRADLING, and R. J. DAVIES (2002). "Ambulatory blood pressure after therapeutic and subtherapeutic nasal continuous positive airway pressure for obstructive sleep apnoea: a randomised parallel trial". In: *The Lancet* 359.9302, pp. 204–210.

PIERCE, R. J. and C. J. WORSNOP (1999). "Upper airway function and dysfunction in respiration". In: *Clinical and experimental pharmacology and physiology* 26.1, pp. 1–10.

PILLAR, G., R. B. FOGEL, A. MALHOTRA, J. BEAUREGARD, J. K. EDWARDS, S. A. SHEA, and D. P. WHITE (2001). "Genioglossal inspiratory activation: central respiratory vs mechanoreceptive influences". In: *Respiration physiology* 127.1, pp. 23–38.

Pohunek, P. (2004). "Development, structure and function of the upper airways". In: *Paediatric respiratory reviews* 5.1, pp. 2–8.

Punjabi, N. M. and V. Y. Polotsky (2005). "Disorders of glucose metabolism in sleep apnea". In: *Journal of Applied Physiology* 99.5, pp. 1998–2007.

Shahar, E., C. W. Whitney, S. REdline, E. T. Lee, A. B. Newman, F. Javier Nieto, G. T. O'Connor, L. L. Boland, J. E. Schwartz, and J. M. Samet (2001). "Sleep-disordered breathing and cardiovascular disease: cross-sectional results of the Sleep Heart Health Study". In: *American journal of respiratory and critical care medicine* 163.1, pp. 19–25.

Somers, V. K., D. P. White, R. Amin, W. T. Abraham, F. Costa, A. Culebras, S. Daniels, J. S. Floras, C. E. Hunt, L. J. Olson, et al. (2008). "Sleep apnea and cardiovascular disease: An American heart association/American college of cardiology foundation scientific statement from the American heart association council for high blood pressure research professional education committee, council on clinical cardiology, stroke council, and council on cardiovascular nursing in collaboration with the national heart, lung, and blood institute national center on sleep disorders research (national institutes of health)". In: *Journal of the American College of Cardiology* 52.8, pp. 686–717.

Stanchina, M. L., A. Malhotra, R. B. Fogel, N. Ayas, J. K. Edwards, K. Schory, and D. P. White (2002). "Genioglossus muscle responsiveness to chemical and mechanical stimuli during non–rapid eye movement sleep". In: *American journal of respiratory and critical care medicine* 165.7, pp. 945–949.

Stansbury, R. C. and P. J. Strollo (2015). "Clinical manifestations of sleep apnea". In: *Journal of thoracic disease* 7.9, E298.

Stoohs, R. A., C. Guilleminault, A. Itoi, and W. C. Dement (1994). "Traffic accidents in commercial long-haul truck drivers: the influence of sleep-disordered breathing and obesity". In: *Sleep* 17.7, pp. 619–623.

Worsnop, C., A. Kay, R. Pierce, Y. Kim, and J. Trinder (1998). "Activity of respiratory pump and upper airway muscles during sleep onset". In: *Journal of Applied Physiology* 85.3, pp. 908–920.

Young, T., L. Finn, D. Austin, and A. Peterson (2003). "Menopausal status and sleep-disordered breathing in the Wisconsin Sleep Cohort Study". In: *American journal of respiratory and critical care medicine* 167.9, pp. 1181–1185.

Problem statement and general methodological approach

As mentioned in chapter 2, SAS is a major healthcare issue that affects more than 5% of the middle-aged population. The acute over compensatory responses induced by the breathing pauses have been associated with a higher risk of development of cardiovascular and metabolic morbidities in the long term. The goal of this chapter is to present the problem statement and the general methodological approach adopted in this work along with a brief state of the art of the current therapies for the treatment of SAS and how they operate from a control point of view. A description of the different control algorithms that are usually implemented in biomedical applications are also presented. Since the objective of this PhD work was to develop an optimal controller of non-invasive neuromodulation for the treatment of SAS, a description of optimal control theory and an explanation of why in certain cases, the different controllers that are presented in this chapter can be considered as optimal is presented in section 3.2.3.

3.1. Problem statement: patient-specific treatment of SAS

Although there is increasing evidence suggesting SAS can adversely affect health in a variety of ways as is explained in section 2.1.2, this common disease remains underdiagnosed (ABDELSATTAR et al., 2015; COSTA et al., 2015). Patient suffering from severe SAS show more than 30 respiratory events per hour of sleep (MARIN et al., 2005; RUEHLAND et al., 2009), with durations ranging from 10 seconds to several minutes, producing severe hypoxemias, exaggerated negative intrathoracic pressure against the occluded pharynx and sleep arousals (LEUNG et al., 2001). As a consequence of these repetitive pathophysiological features, the cardiovascular autonomic activity oscillates between the respiratory event and the ventilatory phase, counteracting the regular HR and blood pressure (BP) that accompanies sleep in normal conditions (SHEPARD, 1985; TILKIAN et al., 1976; TOLLE

et al., 1983). These abrupt changes are key factors for the development of the adverse cardiovascular outcomes associated with SAS (Partinen et al., 1988b, 1992).

The above paragraph highlights the need for new reliable automatic diagnostic and treatment strategies for improving the management of patients suffering from SAS. These systems should include advanced data processing and control methods since as mentioned in section 2.1.1, there are different structural and functional determinants of an anatomical predisposition for airway closure and they differ among patients. Therefore, patient-specific therapies for SAS are of major importance. The next subsections present the current therapies that have been developed and the underlying hypothesis that motivated this work, to develop a novel optimal controlled therapy for the treatment of SAS.

3.1.1.   Current therapies for sleep apnea syndrome

A number of therapies have been proposed to treat SAS. Nowadays, continuous positive airway pressure (CPAP) is the reference treatment in the management of moderate to severe SAS (Berkani et al., 2015; Marin et al., 2005). Basically, this therapy consists on a compressor that pressurizes the air in order to deliver the amount of air pressure that the patient needs to clear the upper airway obstruction. However, although CPAP is associated with excellent results in symptomatic patients, it is a binding long-term therapy, with relatively high rate of abandonment and poor compliance, associated with side effects or intolerance (Antone et al., 2015; Galetke et al., 2011). Recent studies have reported that the average adherence rates of the CPAP are between 39% and 50% (Kushida et al., 2012).

Improvements to the classical CPAP, such as the automatic continuous positive airway pressure (Auto-CPAP), have been proposed. However, a recent meta-study has shown that the Auto-CPAP method does not provide significant added value concerning the acceptance or compliance to the therapy, with respect to classical, manually titrated CPAP (Gao et al., 2012). Other treatment approaches are available, such as the oral appliance therapy and the mandibular advancement devices (MAD), that are considered less cumbersome than CPAP (Hoffstein, 2007). Nevertheless, these devices also show side effects and their efficacy strongly depends on the morphology of the patient (Fritsch et al., 2001; Petit et al., 2002).

More recently, modulation of nerve activity through targeted delivery of a stimulus, such as electrical stimulation or chemical agents, to specific neurological sites in the body, have been also implemented as alternative therapies for the treatment of SAS. These sort of therapies are commonly known as neuromodulation strategies. A variety of these strategies for the treatment of SAS have been recently proposed and are currently under clinical evaluation.

These strategies can be divided into two categories: i) invasive treatment methods and ii) non-invasive treatment methods. The former consists in implantable devices that deliver electrical stimulation to certain nerves on the human body. The neuromodulation

of the hypoglossal nerve has been presented as a way to increase the neuromuscular activity of the upper airways and reduce obstructive apnea events (DEDHIA et al., 2015). Preliminary results of the evaluation of this therapy have shown significant improvements in objective and subjective measurements of the severity of obstructive sleep apnea (OSA) (STROLLO JR et al., 2014; WOODSON et al., 2016; ZAIDI et al., 2013). Also, devices for the direct stimulation of the phrenic nerve have been developed, which may be useful for the treatment of central sleep apnea (CSA) (ABRAHAM et al., 2015; PONIKOWSKI et al., 2011). Nonetheless, these implantable therapies are currently under clinical investigation and, although promising, they require an invasive procedure that may cause significant side effects. MRI incompatibility may also be a limitation to the widespread use of these systems.

On the other hand, non-invasive treatment methods, such as lingual musculature (hyoglossus, styloglossus and genioglossus muscles) stimulation have proven their effectiveness decreasing the frequency of OSA episodes without causing sleep arousals (SCHWARTZ et al., 1996).

The main limitation of most of the previously mentioned therapies is that they are not designed with a patient-specific approach and therefore, they present low rates of compliance and poor effectiveness in certain patients. Control strategies for the management of therapies intended to treat SAS are thus needed. The typical control method implemented for SAS treatment is an On/Off control algorithm, where with the inclusion of a respiratory event detector, a stimulation is sent to the patient when an apnea is detected and it stops when respiration is resumed. Examples of therapies implementing this approach are the hypoglossal and the phrenic nerve stimulation. A more advanced control approach has been employed by Auto-CPAP therapy, where a non-invasive method for determining the level of air flow resistance in the upper airways is applied (RANDERATH et al., 2001). This resistance is then used as a control variable for a proportional (P) controller that regulates the level of air pressure to be administrated to the patient according to the upper airways resistance in a given moment.

More advanced control strategies should be developed in order to provide more adapted therapies for each patient, improving acceptability and effectiveness. The following subsection presents a novel approach that have been developed in the context of this work for a patient-specific therapy of SAS.

3.1.2. Proposed approach, objectives and underlying hypotheses

A novel non-invasive neuromodulation strategy capable of treating both OSA and CSA has been recently developed by our team (AMBLARD et al., 2016; GRAINDORGE et al., 2015; HERNÁNDEZ et al., 2007a). This therapy is based on the delivering of adaptive kinesthetic stimulation on regions with large concentration of mechanoreceptors that elicit startle responses. The selected region in this study was the mastoid bone behind the ear. This region is particularly interesting not only from an ergonomic point of view but also since it

allows the activation of both a tactile and an auditory startle reflex.

The startle reflex is one of the most important reflex functions in mammals, providing a protective response to a sudden acoustic, tactile or vestibular stimuli. This reflex is initiated by mechanoreceptors that detect mechanical forces applied to the body (Yeomans et al., 2002). In mammals, stimulation of these sensory receptors elicits acoustic startle responses (ASR) and tactile startle responses (TSR), through activation of small clusters of giant neurons located in the pontine reticular nucleus (PnC) that project directly and indirectly to motor neurons in the facial motor nucleus and the spinal cord, leading to a fast activation of a number of facial and peripheral muscles, as well as a positive autonomic activation (Li et al., 2001; Lingenhohl et al., 1994; Sandrini et al., 2001; Simons-Weidenmaier et al., 2006). The startle response has a non-zero baseline, that is, the response magnitude can be increased or decreased by a variety of pathological conditions and experimental manipulations. Figure 3.1-A shows a diagram with the primary startle pathway and the most important physiological structures that are involved for this reflex in rodents, where tactile and acoustic stimulations are applied. In this work, adaptive stimulation therapy is designed not only for patient-specific purposes but also to indirectly adapt stimulation to the sleep stage of the patient since studies have shown that the startle reflex activation threshold changes upon these stages (see figure 3.1-B).
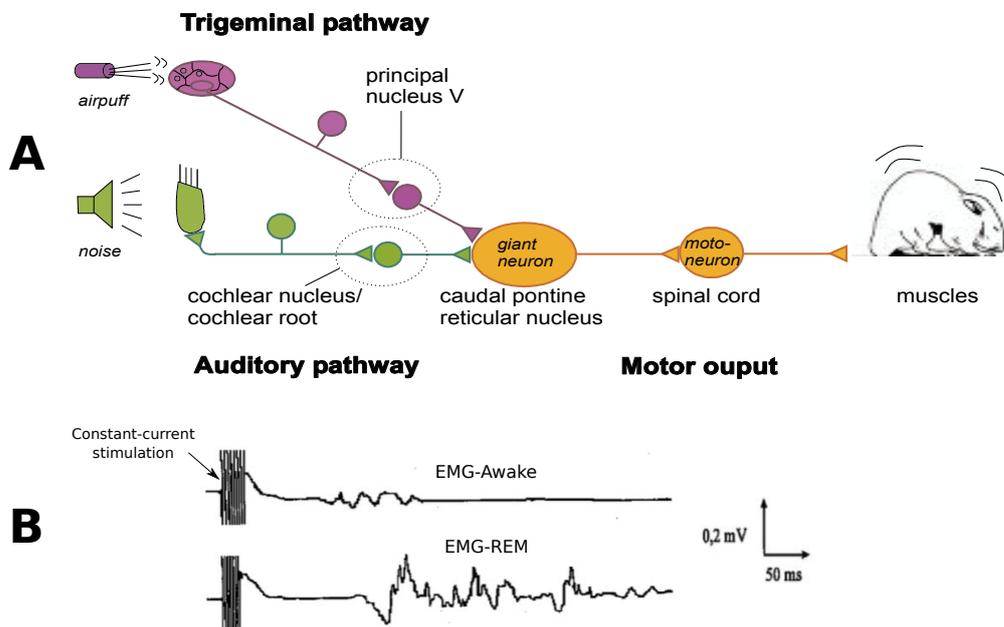
Figure 3.1: A) Scheme of the primary startle pathway in rodents (Simons-Weidenmaier et al., 2006). B) Typical EMG recording (case C.A.) of the RIII reflex before falling sleep (upper trace) and during REM sleep (lower trace). During REM sleep, a prolonged latency and enlarged reflex response are evident (Sandrini et al., 2001).

The hypothesis underlying this work is that bursts of kinesthetic stimulation delivered during the early phase of apneas or hypopneas may elicit a controlled startle response

that can activate sub-cortical centers controlling upper airways muscles and the autonomic nervous system, stopping respiratory events without generating a cortical arousal.

The following sections present a brief description of the control algorithms and definitions that are used in this work. All the controllers that are explained in this chapter are considered as alternatives of optimal controllers for the treatment of SAS. Section 3.2.3 describes why, in certain cases, classical control algorithms can be considered as optimal.

3.2. Brief presentation of classical control algorithms implemented in biomedical applications

Control theory is a root of both, engineering and mathematics that complement each other with the objective of design mechanisms that maintain certain to-be-controlled variables at constant values against external disturbances that act on the system to be treated. These systems are a collection of different elements with complex relationships that together produce results not obtainable by the elements alone. (MUNASINGHE, 2012; POLDERMAN et al., 1998)

One of the central concepts in control theory is feedback, which in a few words is the usage of the value of one variable in the system that is measured in order to take appropriate action through a control variable at another point in the system. The versatility of this concept makes control theory to not be limited to any engineering discipline but to be equally applicable to any area of science.

Following this idea, a control system is an interconnection of components forming a system configuration that will provide a desired system response. These control systems can be divided into two different types, depending if they have or not a feedback control. Figure 3.2 shows block diagrams of the principal types of control systems.

- **Open-loop control systems:** They implement a controller or control actuator to obtain the desired response from the process directly without using feedback.

- **Closed-loop control systems:** They use a measurement of the output variable called the feedback signal and compare it with a desired output (reference) in order to apply a function of a prescribed relationship between the output and reference input to control the process. Commonly, the difference between the output and the reference input is continually reduced.

This section presents a brief description of the control methods that are used in the context of this work, a more detailed explanation can be found in (GOLNARAGHI et al., 2010; OGATA et al., 2002).

3.2.1. Feedback strategies

As previously discussed, the idea of feedback control is simple and yet exceptionally powerful. The reason why these kind of controllers are of interest is because they make the
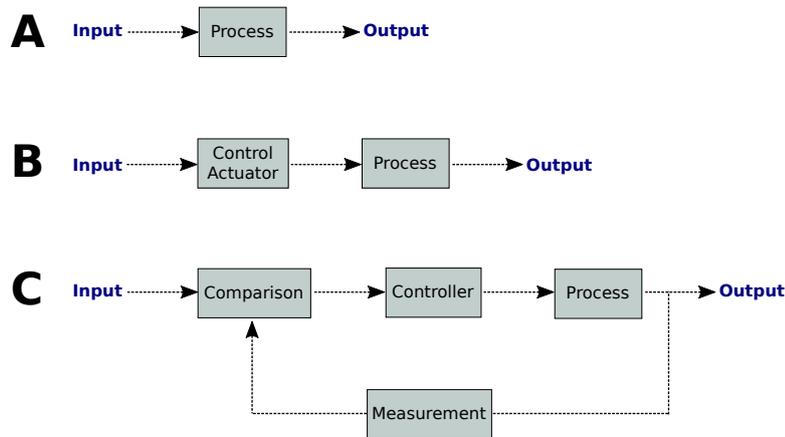
Figure 3.2: Block diagrams of the main types of control systems. A) System or process to be controlled, B) Open-loop control system (without feedback) and C) Closed-loop control system (with feedback).

to-be-controlled variable close to certain set-point in spite of disturbances or variations in the process characteristics. Moreover, the feedback can be arranged in different ways according to the requirements or the behavior of the system to be treated, being the following strategies the most implemented. Figure 3.3 shows a block diagram example of a system with simple feedback control.
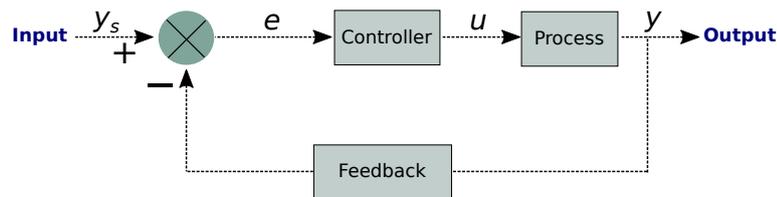
Figure 3.3: Block diagram of a system with simple feedback control. Being the control error $e = y_s - y$, y_s the target or expected value for the control variable, y the control variable and u the output of the controller.

From section 3.2.1.1 onwards, the use of an example of a system to be controlled will be provided in order to facilitate the explanation of each of the different controllers. The system consists in a transfer function of the process (or plant) $G(s) = 2 \cdot (s + 1)^{-3}$. Figure 3.4 shows a block diagram of the system to be controlled while figure 3.5 presents its response to the unit step in open loop. Notice that in this example, in steady state, the system converges to a value of 2. The controllers that will be explained next will be designed to bring the control variable to an expected value (y_s) of 1.
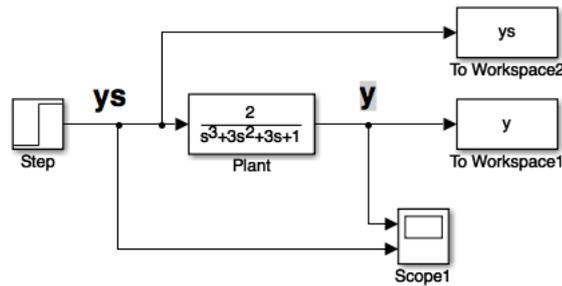
Figure 3.4: Open loop block diagram of the system to be controlled with a transfer function $G(s) = 2 \cdot (s+1)^{-3}$.
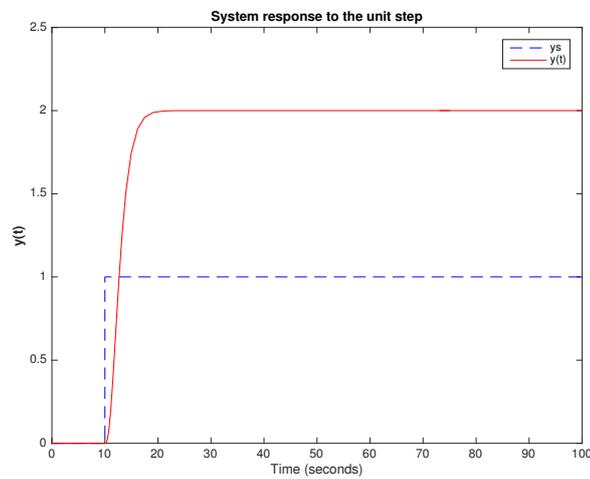

Figure 3.5: System response to the unit step in open loop, converging to a value of 2 in steady state.

3.2.1.1. On-Off control

This type of controller is the simplest feedback control mechanism and can be described mathematically as follows:

$$u = \begin{cases} u_{max}, & \text{if } e > 0 \\ u_{min}, & \text{if } e < 0 \end{cases} \tag{3.1}$$

where the control error, e, is $e = y_s - y$, being y_s the target or expected value for the control variable and y the control variable, as observed from the system. This kind of controller implies that the maximum corrective action is always applied. Therefore, the controlled variable has its largest value when the error is positive and its smallest otherwise.

It is important to notice that, other than u_{max} and u_{min}, there are no parameters values to define. However, in equation 3.1, the control variable is not defined for $e = 0$, thus, some modifications as introducing hysteresis or a dead zone are commonly used. A block diagram of the previously mentioned example system implementing an on-off control is illustrated in figure 3.6. The transfer function of the process remains as $G(s) = 2 \cdot (s+1)^{-3}$, the target (y_s) for the control variable (y) is set to 1. Figure 3.7 shows the system step response with the inclusion of the On-Off controller. Notice that the control variables oscillates around the set point $y_s = 1$.
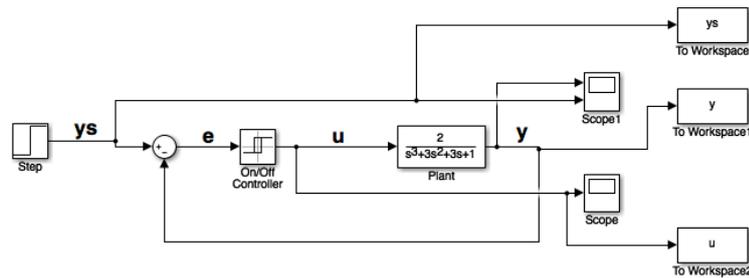
Figure 3.6:   Block diagram of the previously mentioned example system in figure 3.4 implementing an on-off control. Being e the control error, y_s the target or expected value for the control variable, y the control variable and u the output of the controller.
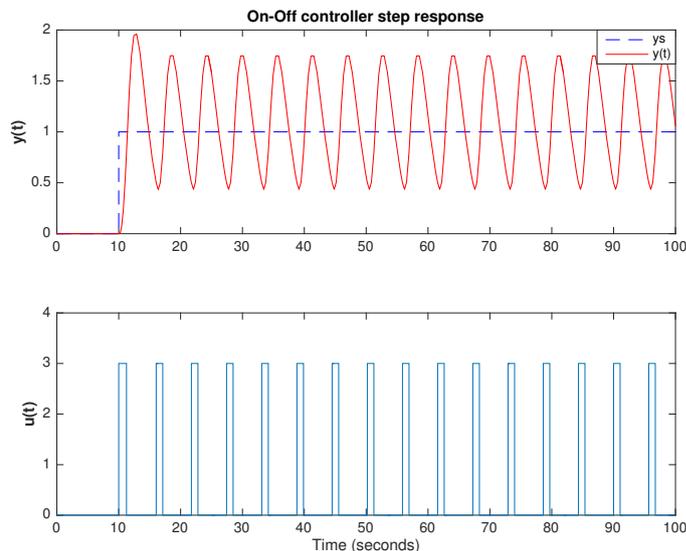
Figure 3.7:   Response of the closed-loop system with an On-Off control. The transfer function of the process is $G(s) = 2 \cdot (s+1)^{-3}$ with set-point of $y_s = 1$. Being $y(t)$ the control variable and $u(t)$ the output of the controller ($u_{max} = 3$ and $u_{min} = 0$).

3.2.1.2. Proportional control

The primary limitation of On-Off controllers is that they often give rise to oscillations because small changes in the error make the controlled variable to change over the full range, thus, making the system to overreact. This limitation is avoided with proportional controllers, where their outputs are proportional to the control error, for small error values. In other words, the output of a proportional controller is the product of the error signal and the proportional gain. This relation can be can be expressed as:

$$u(t) = K_p \cdot e(t) + P_n$$

being, $u(t)$ the proportional controller output, K_p the proportional gain, $e(t)$ the instantaneous process error at time t ($e(t) = y_s - y(t)$) and P_n the controller output with null value or zero error.

In addition, the characteristics of proportional controllers are given by the limits u_{max} and u_{min} of the control variable, where K_p can be specified by giving the range where the characteristics are linear or, in a few words, the range where the control variable will move from one extreme to another. This range is called proportional band (PB), and can be expressed mathematically as:

$$u_{max} - u_{min} = K_p \cdot PB \tag{3.2}$$

Conventionally, it is assumed that $u_{max} - u_{min} = 100\%$. Then,

$$K_p = \frac{100}{PB} \tag{3.3}$$

It is important to notice that proportional controllers act like On-Off controllers for high K_p values, because in those cases, the PB is very small which means that the range of the control variable from its maximum to its minimum is very small, therefore, for small errors, the control variable is driven from one extreme to another. Continuing with the system example mentioned above, figure 3.8 shows the system with the inclusion of a proportional control. In addition, figure 3.9 illustrates the system response with this controller, three values of K_p were tested in order to tune the controller.

Regardless the clear advantages of proportional controllers over On-Off controllers, they require certain error in order to generate an output, thus, they cannot eliminate the difference between the desired value (y_s) and the actual value ($y(t)$) as figure 3.9 shows. This phenomenon occurs because in purely proportional controls, any corrective control action will omit the error between the next steady state and the desired value, resulting in a residual error called offset error.
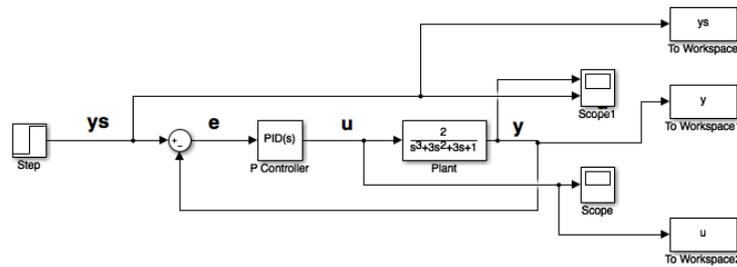
Figure 3.8: Block diagram of the previously mentioned example system in figure 3.4 implementing an on-off control. Being e the control error, y_s the target or expected value for the control variable, y the control variable and u the output of the controller.
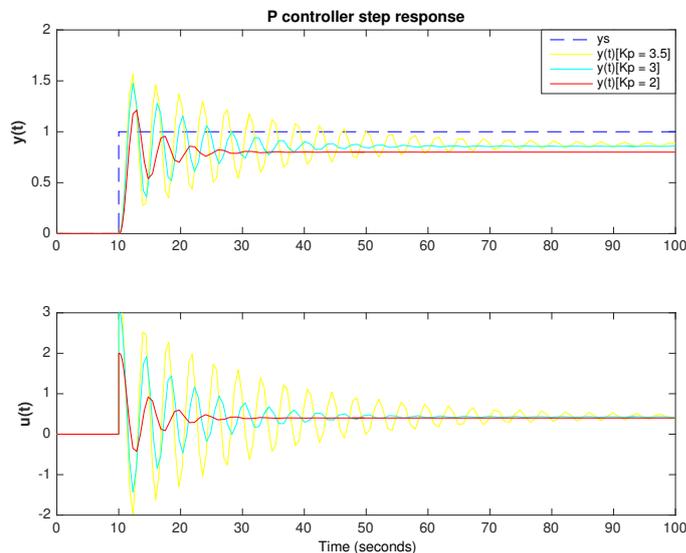

Figure 3.9: Response of the closed-loop system with proportional (P) control. The transfer function of the process is $G(s) = 2 \cdot (s+1)^{-3}$ with set-point of $y_s = 1$. Being $y(t)$ the control variable and $u(t)$ the output of the controller. Responses to different proportional gains (K_p) are shown.

3.2.1.3. Proportional-integrative-derivative (PID) control

Due to the purely proportional control limitations, some improvements were appended in order to implement certain control to more complex systems. The most important advances were the design of algorithms that represented the control variable as the sum of different terms linked to the error. These terms are: the previously explained P-term (proportional to the error), the I-term (proportional to the integral of the error) and the D-term (proportional to the derivative of the error). Each of these terms have their own control parameters which are: proportional gain (K_p), integral time (T_i) and derivative time (T_d). In this sense, the sum of these three terms for the representation of the control

variable is known as PID controller. Equation 3.4 shows the classic mathematical expression of a PID controller.

$$u(t) = K_p \left(e(t) + \frac{1}{T_i} \int_0^t e(\tau)d\tau + T_d \frac{de(t)}{dt} \right) \tag{3.4}$$

This equation is often simplified by taking $K_i = \frac{K_p}{T_i}$ and $K_d = K_p T_d$. Resulting in:

$$u(t) = K_p e(t) + K_i \int_0^t e(\tau)d\tau + K_d \frac{de(t)}{dt} \tag{3.5}$$

where K_p, K_i and K_d are non-negative and denote the coefficients for the proportional, integral, and derivative terms respectively.

Other controllers as the proportional-integrative (PI) and the proportional-derivative (PD) have been also proposed in order to simplify the control algorithm depending to the system requirements. These controllers are a particular case of the PID controller, with control coefficient (K_i or K_p) set to zero. Figure 3.10 shows a block diagram of a typical PID controller.
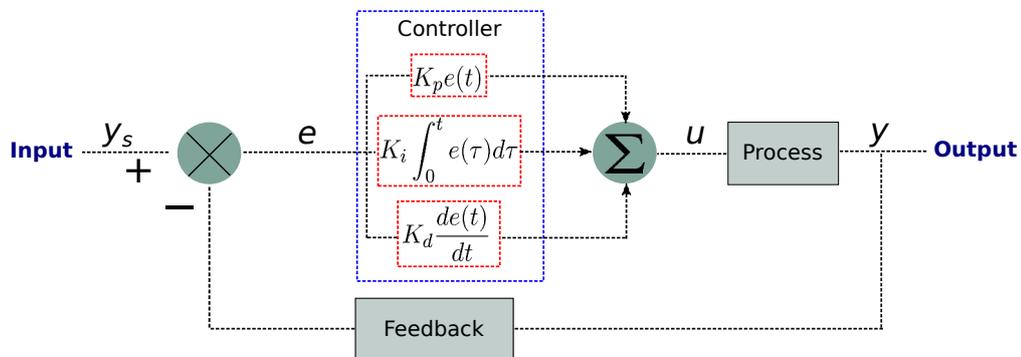
Figure 3.10: Block diagram of a system with typical PID control

As previously mentioned, the selection of the type of controller to use depends on the desired functioning of the system response. In a purely proportional case, the control action is simply to proportional to the error and therefore, it normally leads to an offset error in steady state. However, when an integrative action is added, the process output agrees with the set-point in steady state making this error equal to zero. This behavior can be observed in figure 3.12 which shows the response of the example system in figure 3.11 which has the inclusion of an I-term.

One of the functions of the derivative action is to improve the close-loop stability. Usually, the control system will show a phase delay in correcting the error, mainly due to
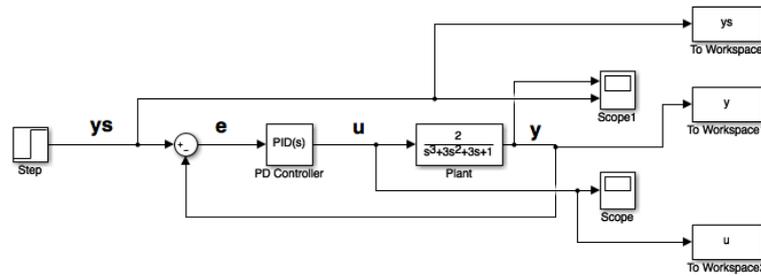
Figure 3.11:   Block diagram of the previously mentioned example system in figure 3.4 implementing a proportional-integrative control. Being e the control error, y_s the target or expected value for the control variable, y the control variable and u the output of the controller.
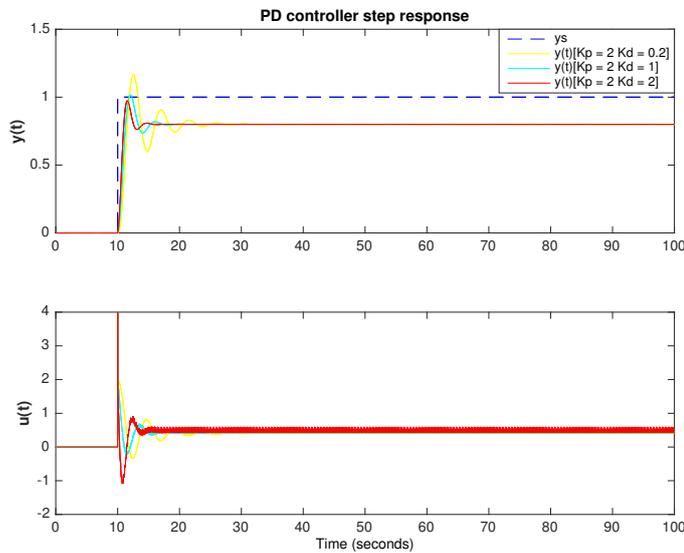

Figure 3.12:   Response of the closed-loop system with proportional-integrative (PI) control. The transfer function of the process is $G(s) = 2 \cdot (s+1)^{-3}$ with set-point of $y_s = 1$. Being $y(t)$ the control variable and $u(t)$ the output of the controller. Responses to fixed proportional gains (K_p) for different integral coefficients (K_i) are shown.

the fact that the control variable and the integrative component of the PID may introduce non-negligible phase delays. Pure derivative controllers are not capable of bringing the system to its set-point. However, they seek to bring the rate of change of the error to its minimum. These controllers aim to reduce the overshoot by flattening the trajectory of the error. Controllers that apply large amounts of energy to correct small errors are more prone to overshoot and, in the same sense, after this overshoot, large correction in the opposite direction will be applied leading to oscillations in the output of the controller. Depending on whether the amplitude of these oscillations remain constant or if they increase or decrease,

the systems are considered as marginally stable, unstable or stable respectively. Figure 3.13 presents a block diagram of the same system example treated previously with the inclusion of a PD controller. Moreover, figure 3.14 shows the response of the system with this controller, where different derivative coefficients (K_d) were applied. In this figure, it can be observed how damping decreases when derivative times increase.

Figure 3.13: Block diagram of the previously mentioned example system in figure 3.4 implementing a proportional-derivative control. Being e the control error, y_s the target or expected value for the control variable, y the control variable and u the output of the controller.
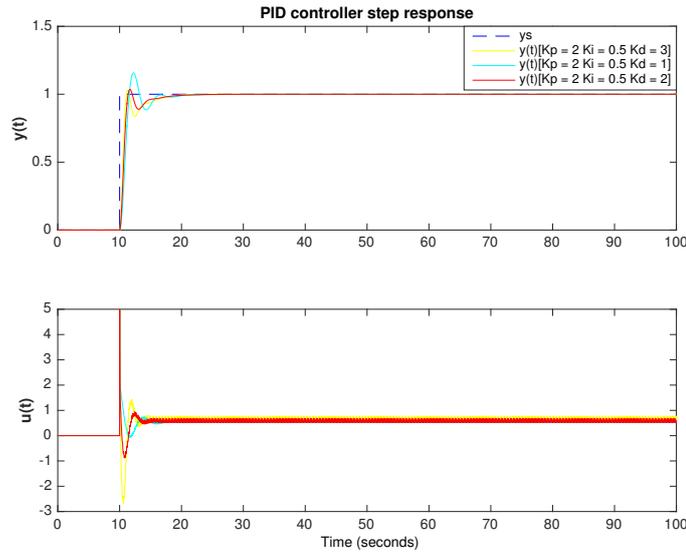

Figure 3.14: Response of the closed-loop system with proportional-derivative (PD) control. The transfer function of the process is $G(s) = 2 \cdot (s + 1)^{-3}$ with set-point of $y_s = 1$. Being $y(t)$ the control variable and $u(t)$ the output of the controller. Responses to fixed proportional gains (K_p) for different derivative coefficients (K_d) are shown.

In brief, PID controllers are capable of taking into account different states of the error. The P-term is set in proportion to the existing error, however, it is not able by itself to eliminate the offset error since any corrective control action will omit the error between the

next steady state and the desired value, resulting in a residual error. On the other hand, the I-term increases its action not only by the error itself but also by the time for which it has persisted. This behavior is the reason why this term is able to bring the error to zero, yet, it can lead to overshoot and oscillations of the controller output. Finally, as described above, the D-term seeks to correct the overshooting problem. The combination of these terms complement each other in order to correct the error of the system, bringing the control variable to the desired set-point and avoiding excessive overshooting and instability. Figure 3.15 presents the same block diagram example in figure 3.4 but with the inclusion of a PID controller. The response of this system with different control coefficients is presented in figure 3.16. Notice that the three alternatives bring the error to zero with minimal overshoot. However, the controller can be tuned by changing the different control coefficients depending of the control performance requirements.
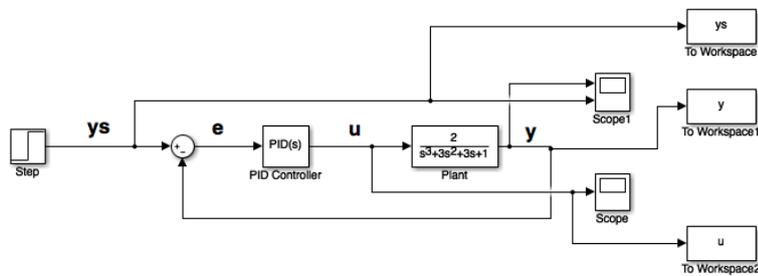
Figure 3.15:   Block diagram of the previously mentioned example system in figure 3.4 implementing a proportional-integrative-derivative control. Being e the control error, y_s the target or expected value for the control variable, y the control variable and u the output of the controller.

Although most of the industrial control problems are solved by PID control; there are certain domains in which the systems are very complex and more advanced controllers, which differ from classic PID control are therefore implemented by using more sophisticated methods such as adaptive and predictive controllers.

3.2.2.   Performance measurement of control methods

In order to quantify performance of control methods, the following indicators are commonly computed:

a. The settling time (t_s) which is the time required for the system to settle within a certain percentage δ of the set-point amplitude.

b. The peak (M_p) which is the maximum amplitude value reached by the system.

c. The peak time (T_p) is the instant in which the system reaches M_p.

Figure 3.16: Response of the closed-loop system with proportional-integrative-derivative
(PID) control. The transfer function of the process is $G(s) = 2 \cdot (s+1)^{-3}$ with set-point of
$y_s = 1$. Being $y(t)$ the control variable and $u(t)$ the output of the controller. Responses
to fixed proportional gains (K_p) and integrative coefficients (K_i) for different derivative
coefficients (K_d) are shown.

d. The percent overshoot (%OS) that corresponds to the amplitude of the overshoot
   response, expressed as a percentage of the steady-state value.

e. The rise time, B_r, as the time required for the waveform to go from 10% of the final
   value to 90% of the final value.

f. The mean squared error (MSE, ms^2), calculated from the instant in which the system
   arrived to the steady state (t_s) up to instant $M = t_s + W - 1$, with W being the temporal
   support of the MSE estimation:

$$\text{MSE} = \frac{1}{W} \sum_{t=t_s}^{M} \epsilon^2(t) \,. \tag{3.6}$$

g. the standard deviation of the error (σ, ms) during the steady-state :

$$\sigma = \sqrt{\frac{1}{W} \sum_{t=t_s}^{M} (\epsilon(t) - \bar{\epsilon})^2} \,, \tag{3.7}$$

where

$$\bar{\epsilon} = \frac{1}{W} \sum_{t=t_s}^{M} \epsilon(t) \,. \tag{3.8}$$

Figure 3.17 shows a representation of the performance indicators previously mentioned
based on the example system of section 3.2.1.3. Analyzing the previous sections, it seems

obvious that the most suitable controller for the presented example system (figure 3.4) are the PID controllers. However, the control coefficients can be adjusted in order to alter the behavior of the system. For this reason, performance measures are used to determine the values of the coefficients that should be used according to the system requirements. Returning to the figure 3.16, we can observe that although the error in steady state is similar between the different sets of coefficients, the percent of overshooting changes among them. This indicator could be important for some systems where stability is a concern.
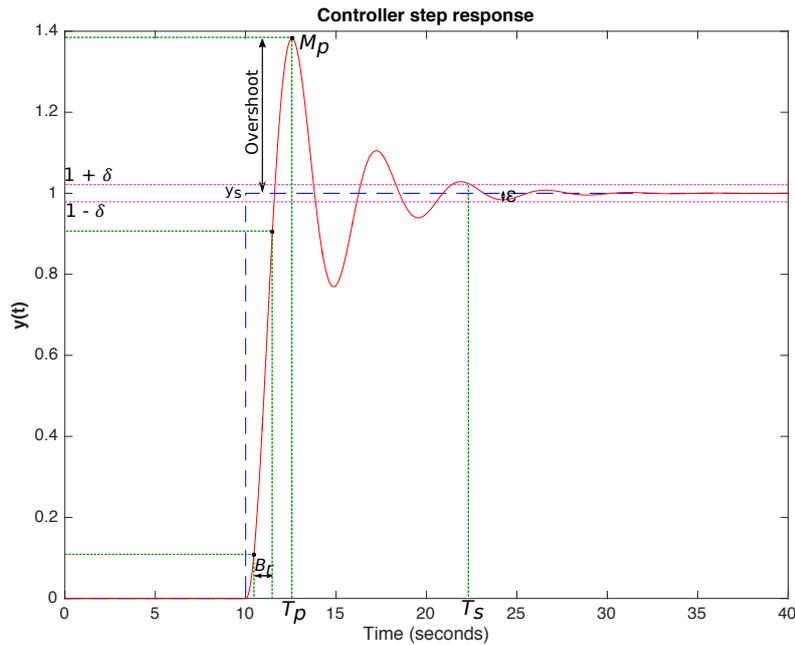
Figure 3.17: Representation of the performance indicators commonly computed for control methods. The response of the closed-loop system with proportional-integrative-derivative (PID) control is presented. The transfer function of the process is $G(s) = 2 \cdot (s+1)^{-3}$ with set-point of $y_s = 1$. Being $y(t)$ the control variable. The following indicators are illustrated: settling time (t_s), peak (M_p), peak time (T_p), rise time (B_r) and the error (ϵ).

3.2.3.   Optimal control

The above mentioned control methods are focused in the minimization of an error between a target value and an observed value, for a given control variable. Optimal control relies on a different approach, in which the objective is to minimize a cost, or to maximize a performance index, that may be a function of a number of observed or state variables. There are various types of optimal control problems, depending on the performance index, the type of time domain (continuous or discrete) and the presence of different types of constraints. Typically, the formulation of an optimal control problem requires the following:

- a mathematical model of the system to be controlled,

- specification of the performance index,

- specification of all boundary conditions and constraints to be satisfied by states and controls.

Notice that, in a biomedical context, these requirements present a great complexity for their formulation since the functioning of the human body results from a complex system which is not completely understood. The mathematical models that could represent the underlying mechanisms of certain pathologies are approximations that represent the knowledge of a system until a certain level of detail. Moreover, these models may also be significantly different between patients. In addition, the large number of variables involved in each process linked to the human body, further increase the complexity of the formulation of the problem.

The above mentioned paragraph, emphasizes the difficulty and complexity of implementing knowledge-driven optimal controllers in biomedical problems. However, in this sort of problems, a controller is considered as optimal if it maximizes the average performance that would be achieved with the ideal controller or if it minimizes certain cost function. The ideal controller is the controller that would be computed if the true system was known (MacGregor, 2005). Adaptive and predictive controls satisfy this definition. Nonetheless, mathematical models capable of representing up to a certain degree of detail the phenomenon to be controlled, are highly useful for the selection and optimization of the parameters of the controllers, that on the contrary they would have to be tested empirically.

The controllers that were described in this chapter are all considered as intrinsically optimal when applied in minimum-time problems. In some cases, where the objective is to reach certain point in the shortest possible time, the solution for the controller is to simply apply its maximum amplitude and stop it when the set-point is achieved. In optimal control theory, when a controller switches from one extreme to the other, it is known as a bang-bang solution or bang-bang controller. Concerning this PhD work, the principal objective was to develop an optimal control for the treatment of SAS. Therefore, we initially implemented this type of controllers since our goal is to stop respiratory events in the shortest possible time, based on the hypothesis that kinesthetic stimulation at a certain amplitude level may be able to stop these events. A complete description of this implementation will be presented in the next chapters.

3.3.   Conclusion

This chapter presented a state of the art of the current therapies for SAS and the control methods currently implemented in this domain. Several therapies have been proposed, being continuous positive airway pressure (CPAP) the reference treatment in the management of moderate to severe SAS. However, it has relatively high rate of abandonment and poor compliance. Other invasive therapies, based on neuromodulation strategies such as hypoglossal and phrenic nerve stimulation, have proven their effectiveness increasing the

neuromuscular activity of the upper airways and reducing the frequency of apnea events. Nonetheless, they remain under clinical investigation and their required invasive procedures may cause significant side effects.

This chapter presented the concept of the underlying hypothesis that motivated this work. This mechanism is a physiological reflex called startle reflex, which is a protective response to a sudden stimulus. A novel non-invasive neuromodulation strategy for the treatment of SAS based of the previously mentioned mechanism was also introduced. The following chapters will provide a detailed description of a novel closed-loop system for the diagnosis and therapy of SAS, based on kinesthetic stimulation as well as the different control methods that were implemented.

A brief description of the classical control methods implemented in biomedical application was also presented in this chapter. A general description of optimal control and its difficulty to be implemented in certain cases was presented in section 3.2.3. Since in a biomedical context, the systems to be analyzed are often complex and the mathematical models that can be implemented are only simplified representations of the knowledge of a system until a certain level of detail, the task of controlling such systems is not trivial. Therefore, adaptive control methods are necessary. The main contributions of this thesis are situated in this field, where the control methods that were designed are intrinsically optimal when applied with the objective of reducing respiratory event durations induced by SAS. Chapters 5 and 7 explain this principle as well as the results obtained after implementing these kind of controllers.

References

Abdelsattar, Z. M., S. Hendren, S. L. Wong, D. A. Campbell Jr, and S. K. Ramachandran (2015). "The impact of untreated obstructive sleep apnea on cardiopulmonary complications in general and vascular surgery: a cohort study". In: *Sleep* 38.8, pp. 1205–1210.

Abraham, W. T., D. Jagielski, O. Oldenburg, R. Augostini, S. Krueger, A. Kolodziej, K.-J. Gutleben, R. Khayat, A. Merliss, M. R. Harsch, et al. (2015). "Phrenic nerve stimulation for the treatment of central sleep apnea". In: *JACC: Heart Failure* 3.5, pp. 360–369.

Amblard, A., L. Graindorge, D. Feuerstein, A. Hernandez, and J.-L. Pépin (2016). *Device for optimization of sleep apnea syndrome therapy by kinesthetic stimulation.* US Patent App. 14/961,403.

Antone, E., M. Gilbert, V. Bironneau, and J. Meurice (2015). "[Continuous positive airways pressure treatment for obstructive sleep apnoea]". In: *Revue des maladies respiratoires* 32.4, pp. 447–460.

Berkani, K. and J. Dimet (2015). "[Acceptability and compliance to long-term continuous positive pressure treatment]". In: *Revue des maladies respiratoires* 32.3, pp. 249–255.

Costa, L. E., C. H. G. Uchôa, R. R. Harmon, L. A. Bortolotto, G. Lorenzi-Filho, and L. F. Drager (2015). "Potential underdiagnosis of obstructive sleep apnoea in the cardiology outpatient setting". In: *Heart* 101.16, pp. 1288–1292.

Dedhia, R. C., P. J. Strollo Jr, and R. J. Soose (2015). "Upper airway stimulation for obstructive sleep apnea: past, present, and future". In: *Sleep* 38.6, pp. 899–906.

Fritsch, K. M., A. Iseli, E. W. Russi, and K. E. Bloch (2001). "Side effects of mandibular advancement devices for sleep apnea treatment". In: *American journal of respiratory and critical care medicine* 164.5, pp. 813–818.

Galetke, W., L. Puzzo, C. Priegnitz, N. Anduleit, and W. J. Randerath (2011). "Long-term therapy with continuous positive airway pressure in obstructive sleep apnea: adherence, side effects and predictors of withdrawal–a 'real-life'study". In: *Respiration* 82.2, pp. 155–161.

Gao, W., Y. Jin, Y. Wang, M. Sun, B. Chen, N. Zhou, and Y. Deng (2012). "Is automatic CPAP titration as effective as manual CPAP titration in OSAHS patients? A meta-analysis". In: *Sleep and Breathing* 16.2, pp. 329–340.

Golnaraghi, F. and B. Kuo (2010). "Automatic control systems". In: *Complex Variables* 2, pp. 1–1.

Graindorge, L., A. Amblard, C. Henry, M. Limousin, L. Laporte, A. Hernández, and J. Pépin (2015). *Device for the treatment of sleep apnea syndrome in a patient by kinesthetic stimulation.* US Patent App. 14/617,534.

Hernández, A., J. Cruz, and G. Garrault (2007a). *Device for supervision and stimulation intended to fight sleep apnea.* Tech. rep. WO Patent App. PCT/EP2007/055,723.

Hoffstein, V. (2007). "Review of oral appliances for treatment of sleep-disordered breathing". In: *Sleep and Breathing* 11.1, pp. 1–22.

Kushida, C. A., D. A. Nichols, T. H. Holmes, S. F. Quan, J. K. Walsh, D. J. Gottlieb, R. D. Simon Jr, C. Guilleminault, D. P. White, J. L. Goodwin, et al. (2012). "Effects of continuous positive airway pressure on neurocognitive function in obstructive sleep apnea patients: the Apnea Positive Pressure Long-term Efficacy Study (APPLES)". In: *Sleep* 35.12, pp. 1593–1602.

Leung, R. S. and T. Douglas Bradley (2001). "Sleep apnea and cardiovascular disease". In: *American journal of respiratory and critical care medicine* 164.12, pp. 2147–2165.

Li, L., S. Steidl, and J. Yeomans (2001). "Contributions of the vestibular nucleus and vestibulospinal tract to the startle reflex". In: *Neuroscience* 106.4, pp. 811–821.

Lingenhohl, K. and E. Friauf (1994). "Giant neurons in the rat reticular formation: a sensorimotor interface in the elementary acoustic startle circuit?" In: *Journal of Neuroscience* 14.3, pp. 1176–1194.

MacGregor, J. F. (2005). *Dynamics and Control of Process Systems 2004.* Elsevier.

Marin, J. M., S. J. Carrizo, E. Vicente, and A. G. Agusti (2005). "Long-term cardiovascular outcomes in men with obstructive sleep apnoea-hypopnoea with or without treatment with continuous positive airway pressure: an observational study". In: *The Lancet* 365.9464, pp. 1046–1053.

Munasinghe, R. (2012). *Classical Control Systems: Design and Implementation.* Alpha science international.

Ogata, K. and Y. Yang (2002). *Modern control engineering.* Vol. 4. Prentice hall India.

Partinen, M., A. Jamieson, and C. Guilleminault (1988b). "Long-term outcome for obstructive sleep apnea syndrome patients: mortality". In: *Chest* 94.6, pp. 1200–1204.

Partinen, M. and T. Telakivi (1992). "Epidemiology of obstructive sleep apnea syndrome". In: *Sleep* 15.suppl_6, S1–S4.

Petit, F.-X., J.-L. Pépin, G. Bettega, H. Sadek, B. Raphaël, and P. Lévy (2002). "Mandibular advancement devices: rate of contraindications in 100 consecutive obstructive sleep apnea patients". In: *American journal of respiratory and critical care medicine* 166.3, pp. 274–278.

Polderman, J. W. and J. C. Willems (1998). "Introduction to the mathematical theory of systems and control". In: *New York* 434.

Ponikowski, P., S. Javaheri, D. Michalkiewicz, B. A. Bart, D. Czarnecka, M. Jastrzebski, A. Kusiak, R. Augostini, D. Jagielski, T. Witkowski, et al. (2011). "Transvenous phrenic nerve stimulation for the treatment of central sleep apnoea in heart failure". In: *European heart journal* 33.7, pp. 889–894.

Randerath, W. J., O. Schraeder, W. Galetke, F. Feldmeyer, and K.-H. Ruhle (2001). "Autoadjusting CPAP therapy based on impedance efficacy, compliance and acceptance". In: *American journal of respiratory and critical care medicine* 163.3, pp. 652–657.

Ruehland, W. R., P. D. Rochford, F. J. O'donoghue, R. J. Pierce, P. Singh, and A. T. Thornton (2009). "The new AASM criteria for scoring hypopneas: impact on the apnea hypopnea index". In: *Sleep* 32.2, pp. 150–157.

Sandrini, G., I. Milanov, B. Rossi, L. Murri, E. Alfonsi, A. Moglia, and G. Nappi (2001). "Effects of sleep on spinal nociceptive reflexes in humans". In: *Sleep* 24.1, pp. 13–17.

Schwartz, A. R., D. W. Eisele, A. Hari, R. Testerman, D. Erickson, and P. L. Smith (1996). "Electrical stimulation of the lingual musculature in obstructive sleep apnea". In: *Journal of Applied Physiology* 81.2, pp. 643–652.

Shepard, J. J. (1985). "Gas exchange and hemodynamics during sleep." In: *The Medical clinics of North America* 69.6, pp. 1243–1264.

Simons-Weidenmaier, N. S., M. Weber, C. F. Plappert, P. K. Pilz, and S. Schmid (2006). "Synaptic depression and short-term habituation are located in the sensory part of the mammalian startle pathway". In: *BMC neuroscience* 7.1, p. 38.

Strollo Jr, P. J., R. J. Soose, J. T. Maurer, N. De Vries, J. Cornelius, O. Froymovich, R. D. Hanson, T. A. Padhya, D. L. Steward, M. B. Gillespie, et al. (2014). "Upper-airway stimulation for obstructive sleep apnea". In: *New England Journal of Medicine* 370.2, pp. 139–149.

Tilkian, A. G., C. Guilleminault, J. S. Schroeder, K. L. Lehrman, F. B. Simmons, and W. C. Dement (1976). "Hemodynamics in sleep-induced apnea: studies during wakefulness and sleep". In: *Annals of Internal Medicine* 85.6, pp. 714–719.

Tolle, F. A., W. V. Judy, P. Yu, and O. N. Markand (1983). "Reduced stroke volume related to pleural pressure in obstructive sleep apnea". In: *Journal of Applied Physiology* 55.6, pp. 1718–1724.

Woodson, B. T., R. J. Soose, M. B. Gillespie, K. P. Strohl, J. T. Maurer, N. De Vries, D. L. Steward, J. Z. Baskin, M. S. Badr, H.-s. Lin, et al. (2016). "Three-year outcomes of cranial nerve stimulation for obstructive sleep apnea: the STAR trial". In: *Otolaryngology–Head and Neck Surgery* 154.1, pp. 181–188.

Yeomans, J. S., L. Li, B. W. Scott, and P. W. Frankland (2002). "Tactile, acoustic and vestibular systems sum to elicit the startle reflex". In: *Neuroscience & Biobehavioral Reviews* 26.1, pp. 1–11.

Zaidi, F. N., P. Meadows, O. Jacobowitz, and T. M. Davidson (2013). "Tongue anatomy and physiology, the scientific basis for a novel targeted neurostimulation system designed for the treatment of obstructive sleep apnea". In: *Neuromodulation: Technology at the Neural Interface* 16.4, pp. 376–386.

Novel kinesthetic stimulation system for the treatment of sleep apnea syndromes (PASITHEA system)

This chapter presents a novel system for real-time detection, monitoring and treatment of SAS, based on adaptive kinesthetic stimulation. This system has been developed within the framework of the ANR TecSan project entitled "Personalized and Adaptive kinesthetic StImulation Therapy, based on cardiorespiratory Holter monitoring, for slEep Apnea syndromes" (PASITHEA), supported by the French "Agence Nationale pour la Recherche". The first part, section 4.1, describes the global functioning and the most important components or modules of the system. Then a brief description of the on-off control method that was implemented is presented. Since this kind of controller requires certain control variable capable of indicating when to start or stop its functioning, a respiratory event detector that was developed in the framework of this project which output is taken by the controller as a control variable is also presented. Section 4.2.1 describes the functioning of such detector. A first clinical protocol which objective was to evaluate the performance of this respiratory event detector and to evaluate the preliminary qualitative results from the therapy is described in section 4.3.1. The quantitative results from this clinical protocol along with their analyses will be presented in chapter 5.

4.1. General description of the PASITHEA system

The PASITHEA system has been designed to detect, monitor and treat respiratory event disorders. The system is composed of three elements: i) a cardiorespiratory ambulatory recorder (Holter), ii) a kinesthetic stimulation system and iii) a real-time control application

for adaptive kinesthetic stimulation, running into a standard computer. These elements
communicate with each other through a wireless communication protocol based on the
Bluetooth (BT) technology. Figure 4.1 shows a general diagram of this system.
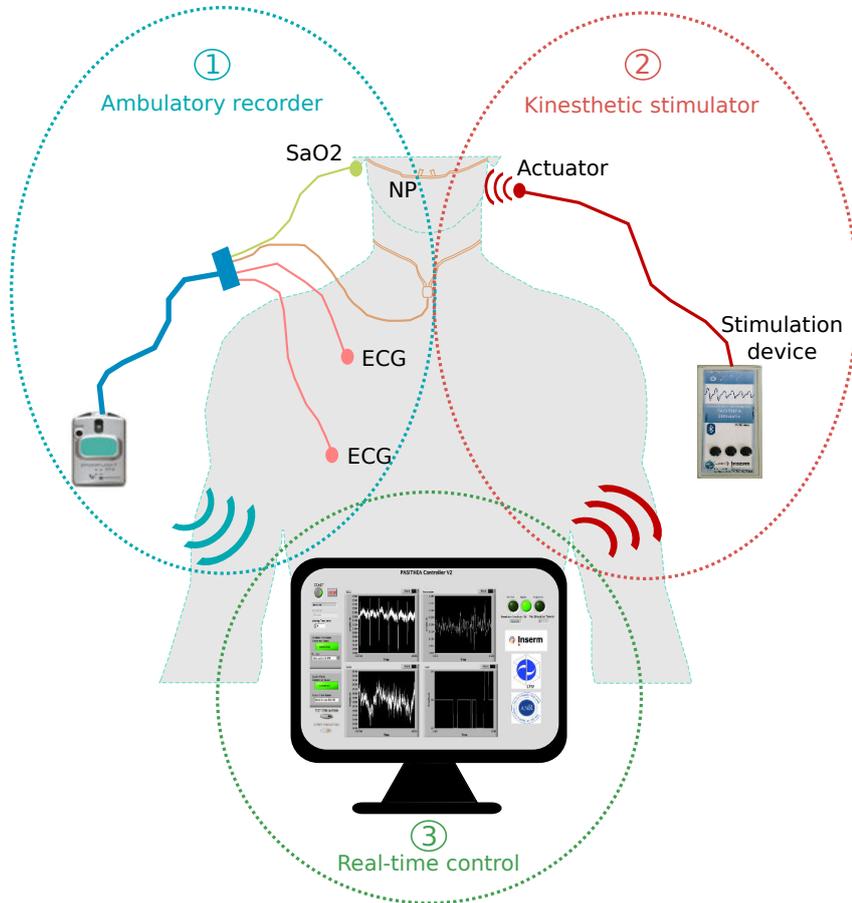
Figure 4.1: General diagram of the PASITHEA detection and stimulation system.

4.1.1.   Cardiorespiratory Holter

A commercially available Sorin Holter system (figure 4.2) was modified by partner
(SORIN CRM, Clamart, France) in order to meet the requirements of the project. This
cardiorespiratory Holter prototype is capable to perform acquisition, recording and real-time
wireless transmission of the following signals:

- Two ECG channels, with a sampling frequency of 256 Hz a resolution of 10 μV and a
  frequency response of [0.05-80 Hz].

- A nasal pressure (NP) signal, acquired at a sampling frequency of 256 Hz.

- A blood oxygen saturation (SaO$_2$) signal with sampling frequencies of 1 Hz.

The wireless transmission is performed through a Bluetooth Low Energy (BTLE) link, which transfers the data every 100 ms towards the real-time signal processing application for further processing. This device (without the real-time BTLE transmission function) is currently proposed as a new product by partner Sorin CRM, for ambulatory analysis and diagnosis of SAS.

Figure 4.2: The prototype cardiorespiratory Holter device with associated sensors (ECG electrodes, SaO$_2$ ear sensor and nasal pressure cannula).

4.1.2. Kinesthetic stimulation system

The kinesthetic stimulation system has been developed by partner LTSI (figure 4.3), based on previous prototypes already used for kinesthetic stimulation therapy for apnea-bradycardia on preterm newborns (HERNÁNDEZ et al., 2007b). The system consists in two parts: a command module in charge of the dynamic generation of the stimulation signals, and a linear resonant actuator. The command module is a battery-operated device based on an ATmega168 micro-controller, embedding a custom, multi-agent software that handles all its functionalities. In particular, the micro-controller can synthesize sinus signals with varying amplitudes and frequencies, to be presented as input to a driver circuit that will handle the kinesthetic actuator in order to generate dynamic stimulation signals in an adaptive fashion. Although this module can function either in an "autonomous" or a "slave" mode, within the framework of this project, the command module is intended to operate in the latter mode which requires establishing a BT connection with a master system (in this case, the real-time control application) that will manage the operation of the stimulator in real-time.

The actuator (stimulating device) is a resonant linear actuator with optimal resonance frequency of 175Hz (model C10-100, Precision Microdrives Ltd, London, UK). At 100% of the acceptable input signal amplitude (2V RMS), this actuator generates a typical normalized acceleration of 13.7 m/s^2. This actuator is attached on the mastoid bone

behind the ear of the patient as section 3.1.2 explained. Figure 4.4 shows the placement site of the kinesthetic actuator.
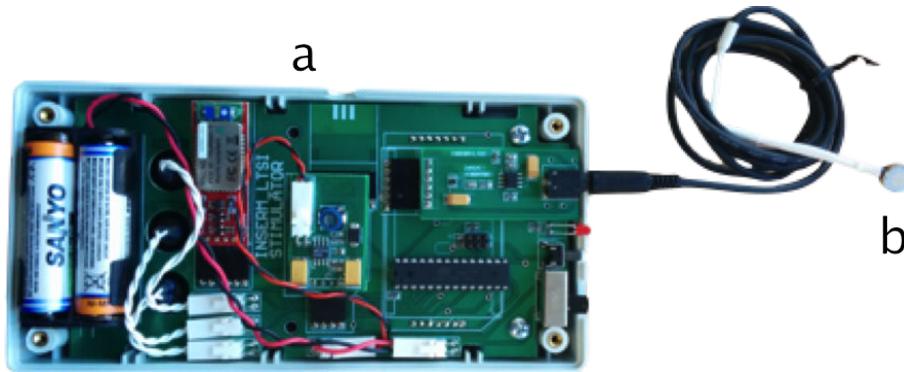
Figure 4.3: The kinesthetic stimulation system, showing (a) an opened control module and (b) and the kinesthetic actuator.

Figure 4.4: Placement site of the kinesthetic actuator. The selected region is on the mastoid bone behind the ear of the patient which is an area rich in mechanoreceptors, allowing a more effective activation of the startle reflex (see section 3.1.2).

4.1.3. Real time processing and control application

The control application, illustrated in figure 4.5, is in charge of: i) establishing wireless communication links with the Holter and the stimulator, ii) receiving data from the cardio-respiratory Holter, iii) performing real-time signal processing on the received signals and iv) according to the outputs of the signal processing stage, apply a given control method in real-time to define and send the appropriate command to the kinesthetic stimulator through a BT link.
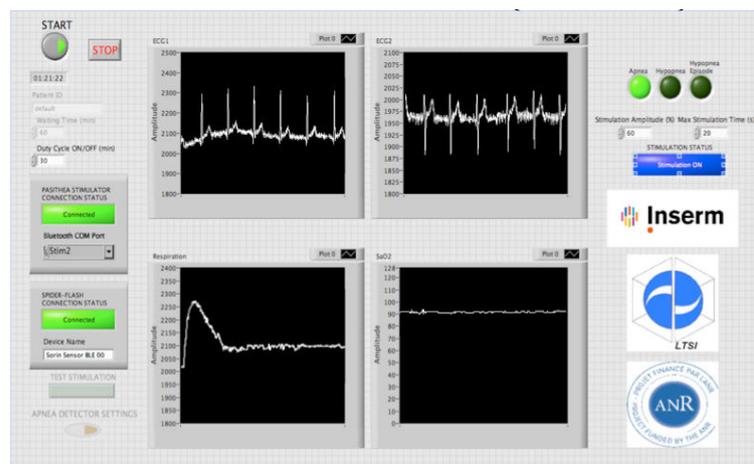
Figure 4.5: Real-time application for data acquisition, processing and control. User-defined configuration parameters and BT connexion with the Holter and the stimulator are placed in the left side of the application. Four screens showing real-time acquired data: 2 ECG channels (top), nasal pressure (bottom left), SaO2 (bottom right). The output of the real-time respiratory event detector (apnea or hypopnea) indicated by LEDs and the stimulation parameters are found in the right side of the application frame.

This application establishes wireless BT links with the Holter and the stimulator device and performs device initialization and management using specifically developed application-level communication protocols. Methods of error correction and verification of the integrity of the BT links have been integrated into the protocol and are also handled by the control application. Data acquisition is initiated and terminated by the application and all available signals are received in real-time from the Holter at their original sampling rates. The application was developed in the Labview software environment because of its multithread programming advantages and real-time processing capabilities. A portable application was also created in order to be distributed and installed on any computer.

Different signal processing and control methods have been proposed in this work and they were integrated into two different versions of the PASITHEA system. The rest of this chapter will be focused on the first version of the PASITHEA system, that implements an "on-off" controller for the kinesthetic stimulation.

Seven complete systems including the cardiorespiratory holter, the kinesthetic stimulation system and computers running the real time control application were developed in order to be distributed among the different centers of a first multi-center clinical protocol that will be described in section 4.3.1.

4.2. On-Off kinesthetic stimulation for the treatment of SAS

The first version of the PASITHEA system integrates an "on-off" controller which can be represented in figure 4.6.
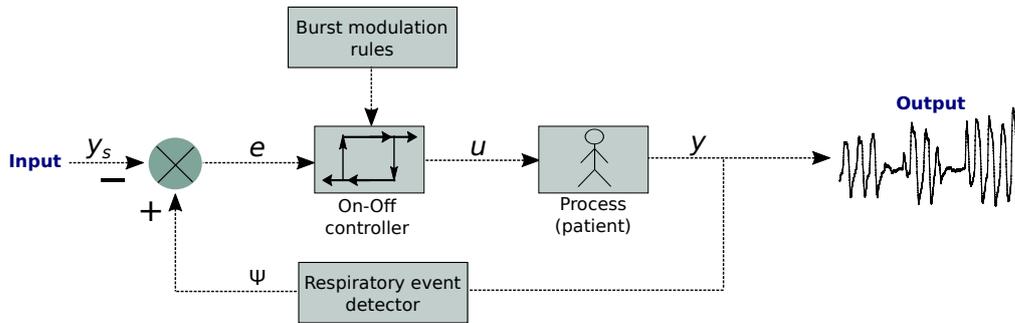
Figure 4.6: Block diagram of the PASITHEA system integrating an "on-off" controller, being, y_s the set-point or expected value, e the error, u the output of the controller, y the output of the system which, in this case is the patient, and its output the nasal pressure (NP) signal, and Ψ the output of the respiratory event detector.

The control variable is a binary value obtained from the output of a proposed respiratory event detector which receives as input the nasal pressure (NP) signal obtained from the patient. Detections (Ψ) are represented as:

$$\Psi(t) = \begin{cases} 0, & \text{if no event detected} \\ 1, & \text{if presence of event} \end{cases} \tag{4.1}$$

In this version, the desired value (y_s) is set to 0, which means that the controller should not stimulate if there are no detections. The following sections describe each of the components of this system.

4.2.1. Real-time respiratory event detector

The respiratory event detector is based on the segmentation of respiratory cycles from the acquired nasal pressure signal (Feuerstein et al., 2015). A full respiratory cycle is defined as inhalation followed by exhalation. Inhalation is detected when the nasal pressure signal exceeds a positive threshold value ($\lambda_I(t)$). Exhalation is detected when nasal pressure signal falls below a negative threshold value ($\lambda_E(t)$). Thresholds $\lambda_I(t)$ and $\lambda_E(t)$ are adaptively updated in an independent fashion, according to the breathing patterns of the patient. An apnea is detected as the absence of inhalation for more than $\delta_a \in [3, ..., 10]$ seconds. A hypopnea event is detected when inhalation amplitude falls 50% below inhalation baseline for more than $\delta_h \in [5, ..., 10]$ seconds. Normal breathing is detected when the inhalation is sufficient again, i.e. $NP > 85\%$ of the baseline or when

the NP amplitude is largely above the inhalation threshold ($NP > \lambda_I(t) \cdot \alpha$), being α a constant factor. Briefly, the decision of the detector is the result of a series of processing and decision rules which are illustrated in figure 4.7.
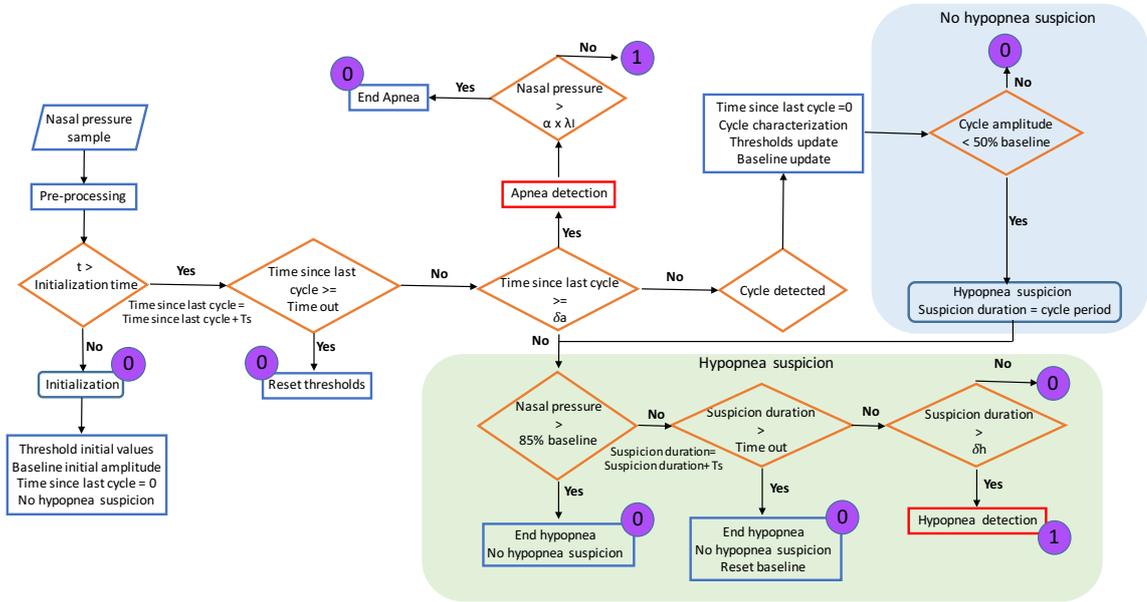
Figure 4.7: Block diagram of the functioning of the proposed real-time respiratory event detector. The input is the nasal pressure (NP) signal sampled at a frequency of $1/Ts$ (typically 8-200 Hz). The output is a signal Ψ with the same sample frequency with binary values between 0 and 1 (0 = no event detected and 1 = presence of a respiratory event). Adapted frigure from (FEUERSTEIN et al., 2015).

A prospective evaluation of the performance of this detector is described in section 4.3.3. Nevertheless, it is important to mention that two versions of this detector were developed. The original version which has been used as control variable for triggering kinesthetic stimulation for the patients included in a first clinical protocol (see section 4.3.1) and a second improved version, integrating the following modifications:

- an additional criterion was required for apnea detection: an apnea was detected not only as the absence of inhalation for a certain time but also as a "flat" breathing line, i.e. nasal pressure amplitude had to stay within the inhalation and exhalation thresholds

- the time to detect apneas (δ_a) was not a fixed parameter but would be set, within limits, as the average of the patient's latest respiratory cycle periods.

- the time to detect hypopnea (δ_h) was not a fixed parameter but linked to the amplitude of inhalation drop: a quicker detection for severe hypopnea (with a large drop) and a slower detection for less severe hypopnea

A retrospective assessment of this improved version (referred to as v2) is given in Table
4.1.

4.2.2.   On-off control of the kinesthetic stimulation

As is observed in figure 4.6, a burst modulation rules unit was added to the controller.
In this approach, when respiratory event detection is confirmed ($\Psi = 1$), around 8 seconds
after the beginning of the respiratory event, a command is sent to the kinesthetic stimulator
to activate it. Although the system is able to apply different stimulation strategies for
different types of respiratory events (Amblard et al., 2014a,b), the following unique
stimulation strategy was used in this chapter as figure 4.8 illustrates. A constant amplitude
of 80% of the maximum power of the stimulator (normalized acceleration of approx. 11
m/s^2) is applied to the patient at a frequency of 175 Hz. Kinesthetic stimulation is
organized into bursts of a maximum duration of 3 s each, followed by a silent period of 2 s.
A maximum of 3 bursts are applied in a given detected respiratory event. This burst-based
stimulation is applied in order to minimize patient habituation to the stimulation as well
as the fragmentation of the sleep of the patient. When the detector confirms the end of
the respiratory event (first detected deflection on the nasal pressure signal above a given
threshold during a respiratory event) a command is sent to stop kinesthetic stimulation.

4.3.   Evaluation methodology

4.3.1.   The HYPNOS study

A clinical study is necessary in order to evaluate closed-loop therapeutic methods, since
the patient response cannot be dissociated from the feedback loop. The evaluation of this
first version of the PASITHEA system has been performed within the framework of a
clinical protocol approved by the ethics committee of the Grenoble University Hospital
(Comité de Protection des Personnes, Grenoble, France, IRB 2014-A00339-38, HYPNOS
study) and registered at ClincalTrials.gov with the identifier NCT03300037. The study was
conducted in accordance with applicable good clinical practice requirements in Europe,
French law, ICH E6 recommendations, and the ethical principles of the Helsinki Declaration
(1996 and 2000). It involved five centers: the University Hospitals of Angers, Grenoble,
Montpellier, Rennes and Tours. Six complete PASITHEA systems were developed in order
to be distributed to these centers (plus one backup system).

The first objective of this study was to validate the on-line real-time methods for the
detection and characterization of apnea and hypopnea during sleep, taking the polysomnog-
raphy (PSG) as a gold standard. A secondary objective of this study was to obtain
preliminary results on the effect of the proposed on-off controlled kinesthetic stimulation
on respiratory events.
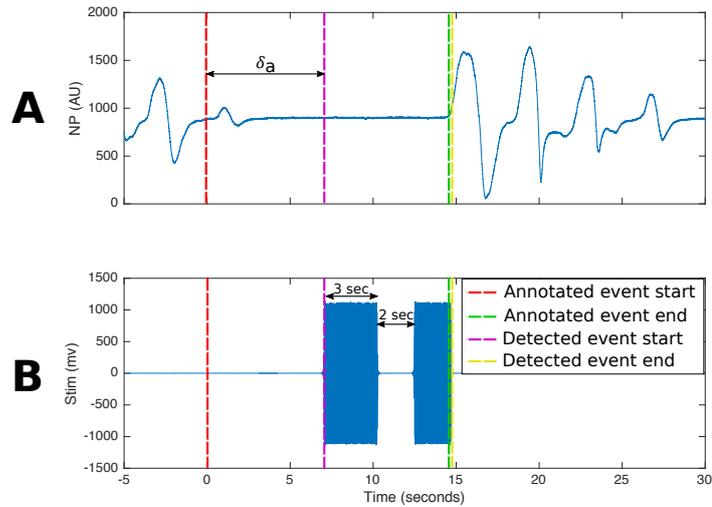
Figure 4.8: Example of a stimulated apnea event, showing the response to kinesthetic stimulation. A) the acquired nasal pressure (NP) signal and B) the signal driving the kinesthetic stimulator (Stim). Green and red segmented lines represent, respectively, the start and end of the event, as taken from the core-lab annotations. The violet segmented line represents the start of the stimulation when the presence of a respiratory event is detected by the automatic real-time detector ($\Psi = 1$). The yellow segmented line represents the end of the stimulation which is when the detector confirms the end of the respiratory event ($\Psi = 0$). One stimulation burst of 3 seconds followed by a silent period of 2 seconds is displayed. The second burst has a duration of less than 3 seconds since it was interrupted because of the breathing resumption. δ_a denotes the time to detect the apnea, where the delivered stimulation burst sequence starts just after the event confirmation (7 seconds after the annotated beginning of the respiratory event).

4.3.2. Data acquisition and patient population

After signing an informed consent, all patients underwent a full PSG (acquiring more than 25 different physiological signals at a sample frequency of 1024 Hz) during one whole night in a sleep laboratory. Nasal pressure (NP), electrocardiography (ECG) and oxygen saturation (SaO$_2$) were simultaneously acquired and processed by the PASITHEA system. Using a T-deviation tube, the same nasal pressure was presented as input to the sensors of both the cardiorespiratory Holter and the PSG systems. Central reading of PSG was performed by an expert, blinded core-lab (CHU Grenoble, France) who provided the overall AHI together with an accurate scoring of individual events (start, duration and type of event) for each patient.

A total of 46 severe obstructive sleep apnea (OSA) patients (mean age: 58.5, BMI: 30.1 kg/m2, AHI: 47.7 /h - with 92% of obstructive events, 75% male) were included in this study. 12 patients were included in a *titration phase*, dedicated to optimize the parameters of the respiratory event detector and to establish the amplitude of the kinesthetic bursts that were used for the rest of the study. 34 additional patients were included on the *study phase*, with a fixed stimulation amplitude of 80% of the maximum power of the

stimulator (normalized acceleration of approx. 11 m/s^2). This stimulation amplitude value
was determined during the titration phase.

Four patients were totally excluded from the analysis due to problems with the PSG
recording, or to a bad nasal cannula signal, preventing correct detection of respiratory events.
Additionally, 6 other patients were also excluded from the therapy analysis: 4 because
the stimulation therapy was not delivered (failure of the stimulator cable or connector)
and 2 due to dysautonomia (1 patient with fibromyalgia and 1 patient with periodic leg
movement). However, they could participate in the analysis of the detection performance.
In total, 30 patients were thus available for the analysis of detection performance and 24
patients were available for the analysis of the therapy. Figure 4.9 presents a summary of
the study flowchart.
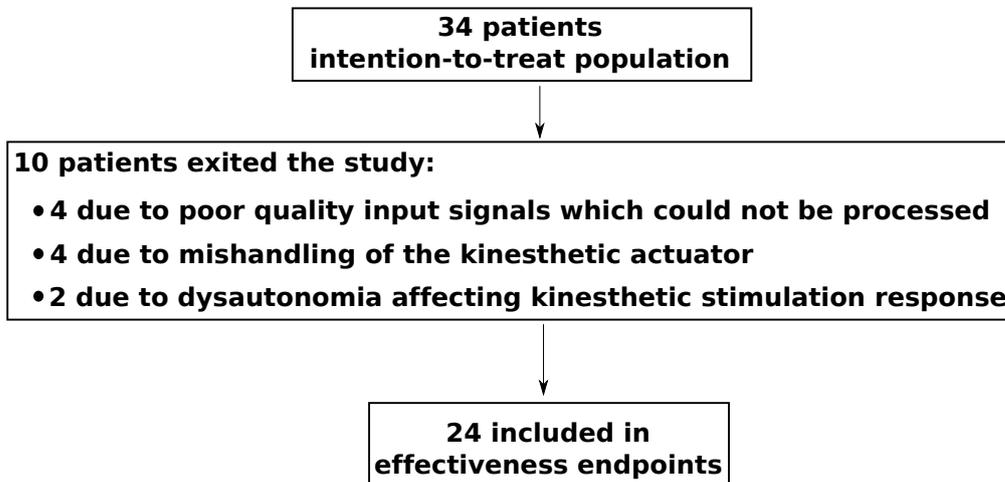
Figure 4.9: Study Flow Chart

4.3.3.   Evaluation of the respiratory event detector

Regarding the evaluation of the performance of the first version of the respiratory event
detector, a training set constituted of the first 12 patients included in the study was used
for the definition of the detector parameters. At the end of this phase, the parameters
were fixed to $\delta_a = 8$ seconds for the apneas, $\delta_h = 10$ seconds for hypopnea and $\alpha = 3$ (see
section above). A test set composed of the remaining 30 patients was used to assess the
detector performance.

Performance was assessed by matching PSG annotated events (blinded core-lab scoring)
with the PASITHEA detector output. A true positive (TP) event was defined as an event
detected less than 10 seconds before or within the duration of a PSG-annotated event. Note
that for a global assessment of respiratory event detection, apneas detected as hypopneas
(and reciprocally) were regarded as true positives.

Delay to the detection was defined as the time lag between the detector output and the start of the event, as per core-lab PSG annotation. The detector sensitivity (SE) and positive predictive value (PPV) were calculated as usual:

$$SE(\%) = TP/(TP + FN) \cdot 100 \qquad (4.2)$$

$$PPV(\%) = TP/(TP + FP) \cdot 100 \qquad (4.3)$$

Where FN and FP represent respectively the number of false negative and false positive detections. The 95% confidence intervals of the detector outputs were calculated using the Wilson score.

Detection delays were calculated as the median time between the start of the clinical annotation and the start of the detection. The same evaluation over the same population was retrospectively performed for the second version of the respiratory event detector.

4.3.4. Preliminary, qualitative evaluation of the therapy

As previously described, all patients underwent a full standard PSG. In order to let the patient to fall asleep, each PSG started with an initialization segment of 60 minutes during which no stimulation was delivered. After this period, intermittent stimulation was initiated during which the stimulator was inactive ($Ther_{dis}$) for 30 minutes and then active ($Ther_{en}$) for 30 minutes. Respiratory events that occurred during $Ther_{dis}$ and $Ther_{en}$ periods were compared within each patient; thus, each patient served as their own control/reference. Only complete $Ther_{en}$ and $Ther_{dis}$ periods (30 minutes) were analyzed. Figure 4.10 shows the different study segments (initialization, $Ther_{en}$, $Ther_{dis}$) collected during the one-night evaluation.

A qualitative patient-by-patient analysis of the obtained cardiorespiratory responses to the kinesthetic therapy was performed, with the objective of evaluating if a given patient correctly responds to the kinesthetic stimulation. A correct response has been defined as a return to normal breathing, during or immediately after the delivery of kinesthetic stimulation. The absence of a return to normal breathing after the end of the third stimulation burst was considered as a no-response. A partial response was defined when the patient intermittently showed a correct or a no-response to the therapy throughout the night. A quantitative evaluation of the proposed therapy is proposed in chapter 5.

4.4. Results

4.4.1. Evaluation of the apnea/hypopnea detector

The global performance of the real-time apnea/hypopnea detector is given in Table 4.1. Only the $Ther_{dis}$ periods were included in the analysis, to avoid any bias of potential events interrupted by kinesthetic stimulation. Overall, 2561 apneas and 1679 hypopneas were scored on the PSG. 3656 events were correctly detected within the 10-second window
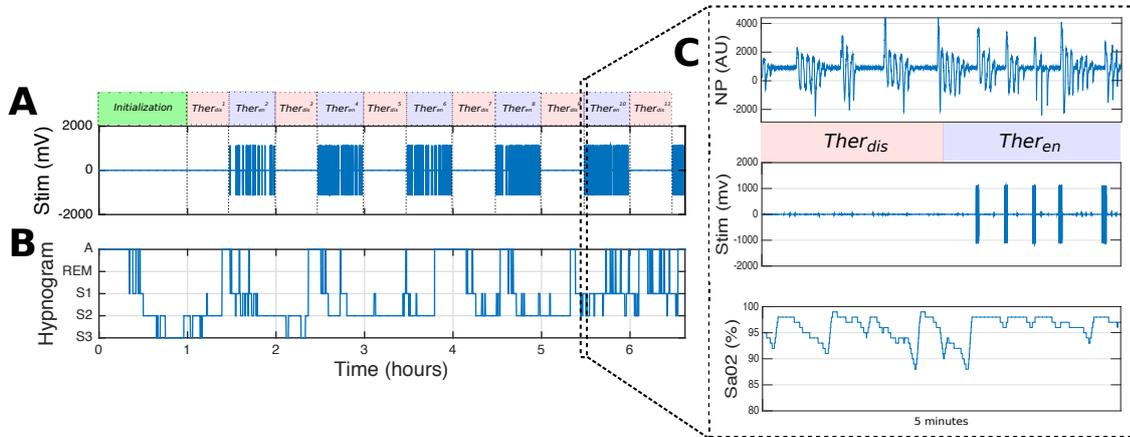
Figure 4.10: Sleep study with the distribution of the different study periods. A) Distribution of the kinesthetic stimulations (Stim) during a complete night: $Ther_{en}/Ther_{dis}$ (30 minutes each) periods alternate after therapy initialization (typically 60 minutes after the record start), B) Hypnogram obtained from Core-lab annotations (A = Awake, REM = rapid eye movement, S1 = stage 1, S2 = stage 2 and S3 = stage 3). C) Zoom on a transition from a $Ther_{dis}$ to a $Ther_{en}$ period, showing the acquired nasal pressure, the stimulation bursts and the SaO2 signal.

(see definition of a true positive above). 2367 false positive events were detected, among which 318 apneas and 697 hypopneas were wrongly detected while the patient was awake. Breathing baseline fluctuations due to movements during awake periods explain the high number of wrongly detected hypopneas, while nasal cannula withdrawal and physiological apneas at sleep onset (that are not scored on the PSG since they are not pathological) account for most of the false positive apneas during wakefulness. The use of a sleep detector, that would temporarily turn off the real-time event detection while the patient is awake, would significantly improve the PPV (second line of Table 4.1).

Apnea and hypopnea events were always detected well before the conventional 10 seconds requirement to define a respiratory event, with a mean delay of 6.0 seconds and 8.7 seconds for apneas and hypopneas respectively. The second version of the detector (v2), when tested retrospectively on the test set significantly reduced this detection delay (down to 4.1 seconds for apneas and 3.5 seconds for hypopneas on average) while sensitivity slightly improved and PPV remained similar.

4.4.2.   Qualitative preliminary responses of the kinesthetic stimulation

This section will present three case reports, describing the cardiorespiratory response to the proposed triggered kinesthetic therapy of a responder patient, a partially responder patient and a non-responder patient.

Table 4.1: Real-time respiratory event detector performances. Values are given as mean [95% Confidence intervals]. The first two lines give the performances of the on-line detector, as assessed prospectively on all 30 patients included in the evaluation phase of the study. The last line gives the performances of the improved detector (v2) on the same patients, but assessed retrospectively.

Analysis method	SE(%)	PPV(%)	Apnea detection delay (sec)	Hypopnea detection delay (sec)
Prospective Event-based	86.2 [85.2-87.2]	60.7 [59.5-61.9]	6.0	8.7
Prospective Event-based Asleep only	86.2 [85.2-87.2]	78.3 [77.1-79.4]	6.0	8.7
Retrospective (v2) Event-based	89.2 [88.4-89.8]	59.0 [58.1-59.9]	4.1	3.5

4.4.2.1. Responder patient

Figure 4.11 shows the cardiorespiratory effect of the therapy on one responder patient, using the PASITHEA system v1. The first 10 min in this figure correspond to a $Ther_{dis}$ segment and the following 10 min correspond to a $Ther_{en}$ phase. The nasal pressure (NP) signal shown in the upper panel (Fig. 4.11-A) was applied as input to the above-mentioned respiratory event detector.

Figure 4.11-B shows the stimulation signal (Stim), obtained as output from the on-off controller, used to activate the kinesthetic actuator. Note that, as expected, no stimulation is performed during the $Ther_{dis}$ phase and different stimulation bursts are delivered during the $Ther_{en}$ phase. As described above, all delivered stimulations have the same amplitude and the number of bursts delivered depends on the duration of the respiratory event. For this patient, in most cases, the respiratory episode is stopped during the first stimulation burst. However, some over-stimulations were observed on this patient, due to a lack of a correct detection of the end of the event for some hypopnea episodes.

The first effect that can be noticed from the therapy in this responder patient is that the duration of the apnea events is smaller during the $Ther_{en}$ phase than during the $Ther_{dis}$ phase. Also, due to these extended respiratory events, oxygen saturation (SaO$_2$) (Figure 4.11-C) shows significant hypoxia events (low oxygen saturation, some of them below 90%) during the $Ther_{dis}$ phase. These hypoxemia events are stopped by the stimulation therapy, during the $Ther_{en}$ phase. Figure 4.11-D shows the instantaneous heart rate (HR) during the same period. It can be noticed that tachycardia (high HR) events, correlated to the apnea and hypoxia events and provoked by chemo and baroreflex autonomic functions, are observed during the $Ther_{dis}$ phase. These tachycardia episodes are not present during

the $Ther_{en}$ phase, during which a normal and more stable respiratory sinus arrhythmia is observed. Also, the mean HR during the whole $Ther_{dis}$ episode was higher than the mean HR of the $Ther_{en}$ episode. Finally, Figure 4.11-E shows the hypnogram reconstructed from the manual annotations performed by the Core-lab. The patient spent most of the time in this segment in REM and light sleep (LS) stages. A number of micro-arousals (MA) are observed during the segment, particularly at the end of each apnea episode during the $Ther_{dis}$ phase and after most kinesthetic stimulations, during the $Ther_{en}$ phase. One "awake" event was observed during the $Ther_{en}$ phase. A first qualitative analysis of the sleep structure for this patient showed no major differences between the $Ther_{en}$ and $Ther_{dis}$ phases.
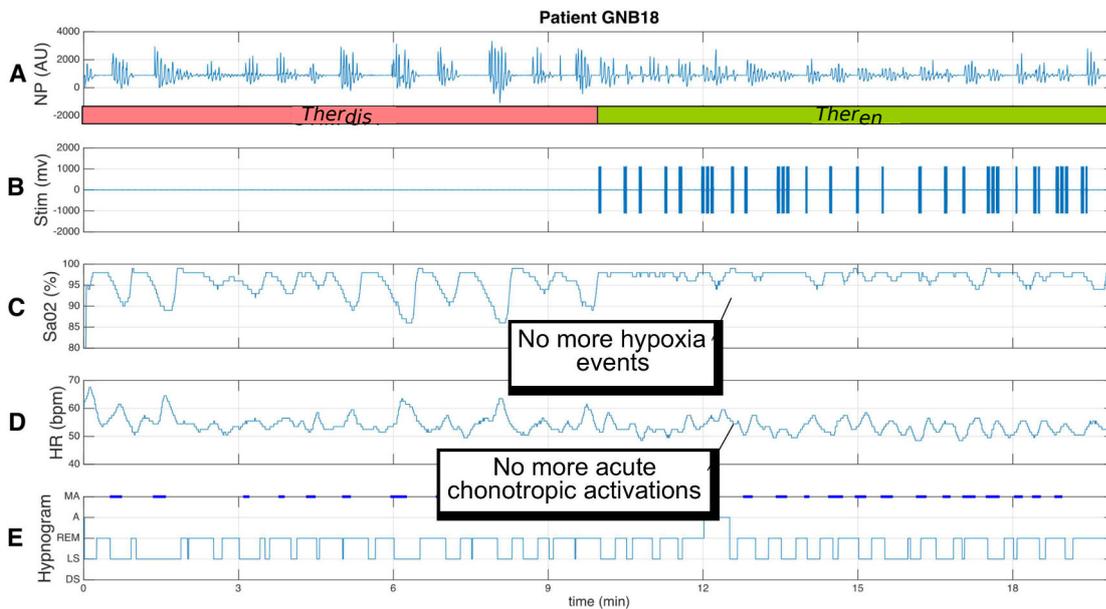
Figure 4.11: Cardiorespiratory response to kinesthetic stimulation of a responder patient. The first 10 minutes correspond to the end of a non-stimulation ($Ther_{dis}$) phase and the next 10 minutes to a phase with triggered stimulation active ($Ther_{en}$). The following signals are displayed: A) nasal pressure (NP), B) signal driving the kinesthetic stimulator (Stim), C) oxygen saturation (SaO $_2$), D) instantaneous heart rate (HR), as detected from the ECG, E) Hypnogram obtained from Core-lab annotations (MA = micro-arousal, A=Awake, REM = Rapid eye movement, LS = light sleep, DS = deep sleep). This response shows extended respiratory episodes accompanied by repeated hypoxia events during the $Ther_{dis}$ phase. Respiratory event durations are reduced and no hypoxia events (SaO$_2$ <90%) are observed during the $Ther_{en}$ phase. The $Ther_{dis}$ phase is also characterized by significant tachycardia events that are related to sympathetic activations due to prolonged apnea and hypoxia. These tachycardia episodes are not observed during the $Ther_{dis}$ phase, which shows a physiological respiratory sinus arrhythmia.

4.4.2.2. Partially responder patient

As previously defined, partially responder patients show a correct response to the therapy during some parts of the night and a lesser or no response in other parts of the night. This loss of response was often associated with changes in posture or sleep stages during the night. Figure 4.12 depicts the same signals shown in Figure 4.11, but for a partially responder patient. A correct response to the therapy is observed during the first minutes. The patient starts moving from a lateral to a dorsal position around minute 5. Once in stable dorsal position (around minute 10), the response to the therapy is strongly reduced, presenting, in particular, three respiratory episodes with the maximum stimulation of 3 burst that failed to restore normal breathing. As a consequence of this non-response, hypoxia episodes and tachycardia, which were not observed during the first 10 minutes, appear after minute 10. This example suggests that i) the actuator should be carefully fixed to the skin of the patient and ii) stimulation parameters should be adjusted over time in order to improve response.
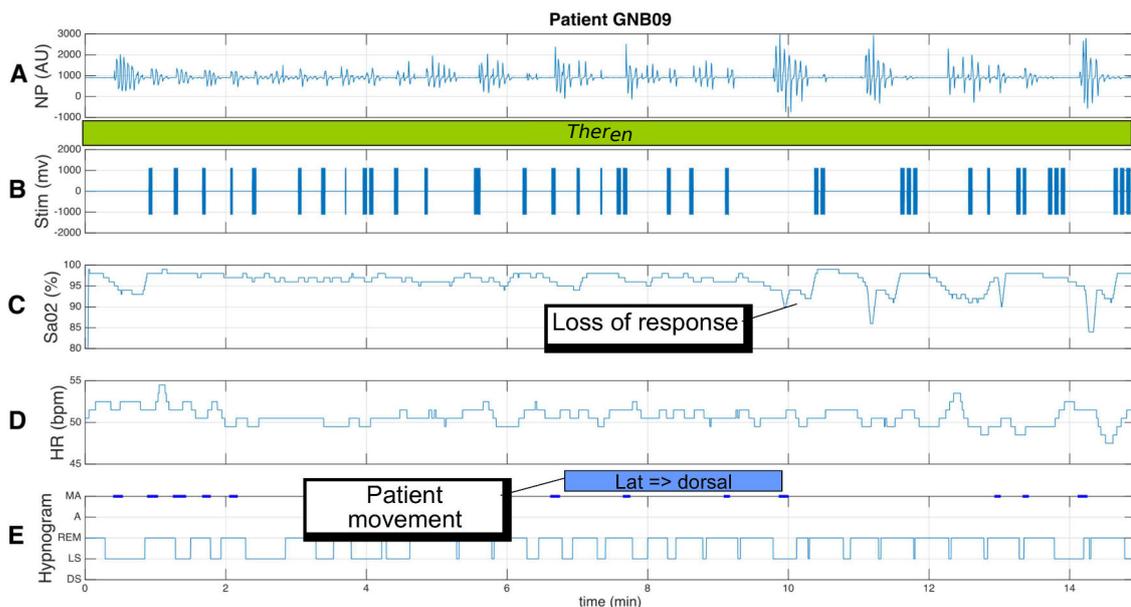
Figure 4.12: Cardiorespiratory response to kinesthetic stimulation of a partially responder patient. The whole segment was acquired during a $Ther_{en}$ phase. The following signals are displayed: A) nasal pressure (NP), B) signal driving the kinesthetic stimulator (Stim), C) oxygen saturation (SaO$_2$), D) instantaneous heart rate (HR), as detected from the ECG, E) Hypnogram obtained from Core-lab annotations (MA = micro-arousal, A=Awake, REM = Rapid eye movement, LS = light sleep, DS = deep sleep). In this example, the patient responds correctly to the therapy during the first 9 minutes. At minute 6 the patient starts moving and changes to dorsal position in minute 10. In this new position (from minute 10), the effect of the therapy is reduced letting appear hypoxia and tachy-bradycardia episodes.

4.4.2.3. Non-responder patient

Figure 4.13 presents an example of a non-responder patient. Most of the respiratory events in this example were treated by the maximum of 3 stimulation bursts and normal respiration was not recovered during or just after the end of the stimulation on each event. Even if the direct contribution of the stimulation therapy in this case is not clear, apnea durations on this segment are rather low, limiting the arrival of hypoxic events. Nevertheless, marked increases in HR and micro-arousals are observed after each major respiratory episode.
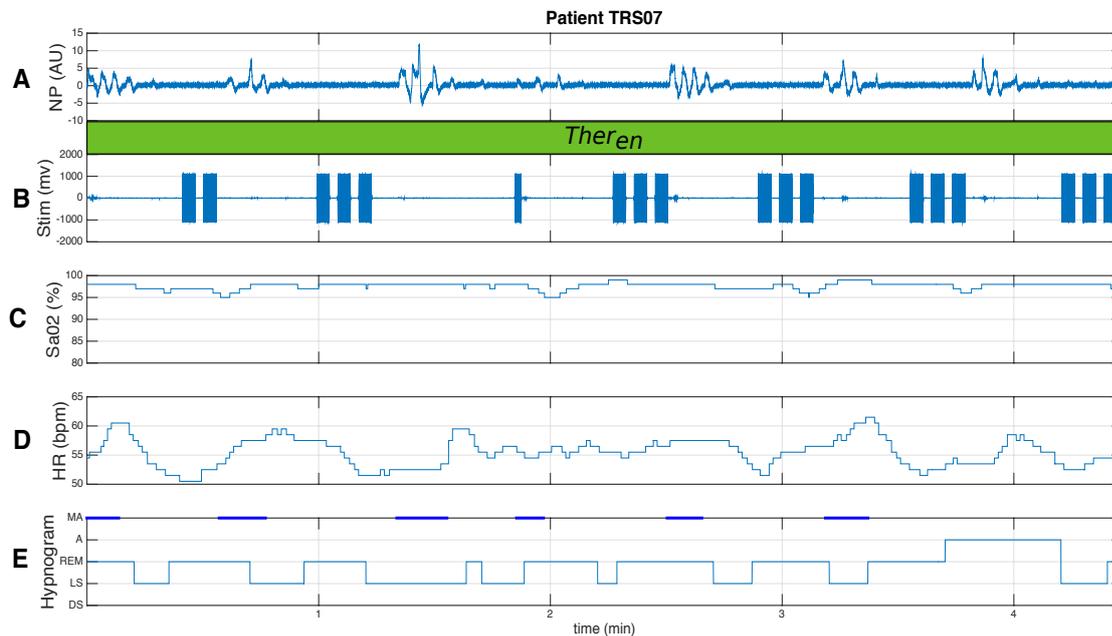
Figure 4.13: Cardiorespiratory response to kinesthetic stimulation of a non-responder patient. The whole segment was acquired during a $Ther_{en}$ phase. The following signals are displayed: A) nasal pressure (NP), B) signal driving the kinesthetic stimulator (Stim), C) oxygen saturation (SaO$_2$), D) instantaneous heart rate (HR), as detected from the ECG, E) Hypnogram obtained from Core-lab annotations (MA = micro-arousal, A=Awake, REM = Rapid eye movement, LS = light sleep, DS = deep sleep). In this example the effect of the therapy is not clear. Although the respiratory events are of limited duration, most events are stimulated with the maximum of 3 stimulation bursts and normal respiration is not recovered just after the stimulation.

4.5. Discussion

The PASITHEA v1 system worked satisfactorily during this first clinical evaluation. Some technical difficulties were observed during the titration phase, including Holter communication loss and the delivery of inappropriate stimulation bursts. These problems were corrected before including the 34 patients of the second study phase. During the

second study phase, the only technical difficulties were related to a loss of continuity in the cable driving the kinesthetic actuator and the physical uncoupling of the actuator from the patient's skin.

Concerning respiratory event detection, the initial method presented in (FEUERSTEIN et al., 2015), was improved and evaluated retrospectively. It should be noticed that the proposed method has been developed for a real-time control application, in order to activate the kinesthetic therapy. This real-time constraint means that the final detection has to be performed during the event (before the event ends and normal breathing resumes), which is not the case of most respiratory event detectors of the literature.

Indeed, Berry et al. reported an overall sensitivity of 58% and specificity of 98% for a detector incorporated into their PAP system (BERRY et al., 2012). Contrary to our detector, they do wait for the end of an event before counting it as an event (post-event detection), which presumably accounts for their better specificity. Using oxygen desaturation and plethysmography as input signals, the detector proposed by Amir et al. showed a global sensitivity of 81% and a PPV of 81.4% (AMIR et al., 2012). Yet again, their detector counted events once terminated, since oxygen desaturation can occur between 5 and 60 seconds after the end of a hypopnea/apnea. Under the real-time constraints imposed by the PASITHEA project, the proposed, improved real-time respiratory event detector provides a satisfactory performance in terms of sensibility, specificity and, in particular, detection delay.

In this chapter is also shown original results concerning triggered kinesthetic stimulation for the treatment of SAS. This first evaluation gave us valuable information on the feasibility of this therapy. Qualitative analysis of the effect of the therapy on responder patients showed how the acute cardiorespiratory consequences of respiratory events observed during the $Ther_{dis}$ period (prolonged apnea, hypoxia events associated with tachy- and bradycardia), which may be deleterious to the patient in the long term, may be stopped or significantly attenuated during the $Ther_{en}$ phase (see for example Fig. 4.11).

However, not all patients responded correctly to the therapy. We hypothesize that most of the non-responses observed on partially-responder patients may be avoided by i) an earlier detection of respiratory episodes (such as that obtained from the improved detector), leading to an earlier therapy; ii) appropriate adaptation and personalization of the stimulation parameters and iii) an improvement and dynamic estimation of the mechanical coupling between the actuator and the skin of the patient. Indeed, the control algorithm used in this first study was a classical (on-off control) and the stimulation parameters (amplitude, burst duration, silent interval, maximum number of bursts) were empirically fixed for all patients using the analysis of the first 12 patients of the clinical study. However, in chapter 5, it is presented a description of why in the context of this therapy, the on-off controller is considered as an optimal control since a bang-bang solution (see section 3.2.3) is needed so that respiratory events can be stopped in the shortest possible time avoiding the deleterious effect associated with SAS.

The objective of the second phase of the PASITHEA project which is presented in

chapter 7 was to develop and evaluate a more advanced auto-adaptive and personalized therapy delivery. The information acquired on this first qualitative analysis and the more specific response quantitative analyses, also explained in chapter 5, are particularly valuable for these developments. Finally, like in any other therapy, it is expected that some patients will not respond to the proposed stimulation approach. Further studies, presented in chapter 6, will address the problem of optimal patient selection for this therapy.

4.6. Conclusion

This chapter presented the functioning and the first qualitative evaluation of our original ambulatory system for real-time detection and triggered therapy delivery, directed to patients suffering from SAS. A first evaluation of this system on 46 severe obstructive SAS patients has been performed, by assessing the ability of the system to correctly detect respiratory events in real-time. This section also presents preliminary results on the effect of the triggered kinesthetic stimulation therapy on these events. The main contributions exposed in this chapter were focused on the development of the kinesthetic stimulator and on the evaluation and analysis of the data obtained from the previously mentioned clinical protocol along with the respiratory events detector that was implemented.

Real-time respiratory event detection is clearly a challenge and the characteristic trade-off between high sensitivity and high PPV is accentuated by the real-time constraints. For the sake of the PASITHEA project, the aim was to detect as many events as possible, and as early as possible, in order to treat them before they can fully develop and result in desaturation or micro-arousal. The improved detector presented in this section was designed for that purpose. The retrospective evaluation, also presented, shows that the improved detector provides a satisfactory performance, approaching the level of performance of some post-event detectors.

Regarding the effects of kinesthetic stimulation on respiratory events, the preliminary results showed in this section were very encouraging and they motivated further analysis in the characterization of the patient's response that will be described in the following chapters. These effects on responder patients were firstly estimated by quantitative and statistical analyses, comparing the duration and frequency of respiratory events during stimulation or non-stimulation periods along with oxygen desaturation and sleep structure analyses (chapter 5).

Concerning non-responder patients, two major improvements of the system were also considered: i) the replacement of the "on-off" control method by a fully-adaptive stimulation approach, based on multi-variate proportional-derivative (PD) controllers and ii) the integration of new sensors to estimate the level of mechanical coupling of the actuator (chapter 7). Also, a better characterization of the patient population that may benefit from the proposed kinesthetic therapy is described in chapter 6.

References

Amblard, A., L. Graindorge, D. Feuerstein, A. Hernández, and J. Pépin (2014a). *Système de traitement d'un trouble respiratoire par stimulation kinesthśique, avec contrôle de stabilisation de la stimulation.* FR Patent App. FR-1462041.

— (2014b). *Systèmeme de traitement d'un trouble respiratoire par stimulation kinesthésiquesique, avec sélection des stratégies de stimulation.* FR Patent App. FR-1462039.

Amir, O., D. Barak-Shinar, A. Henry, and F. Smart (2012). "Photoplethysmography as a single source for analysis of sleep-disordered breathing in patients with severe cardiovascular disease". In: *J. Sleep Res.* 21, pp. 94–100.

Berry, R. M., C. Kushida, M. Kryger, H. Soto-Calderon, B. Staley, and S. Kuna (2012). "Respiratory Event Detection by a Positive Airway Pressure Device". In: *Sleep* 35.3, pp. 361–367.

Feuerstein, D., L. Graindorge, A. Amblard, A. Tatar, G. Guerrero, S. Christophle-Boulard, C. Loiodice, A. I. Hernandez, et al. (2015). "Real- time detection of sleep breathing disorders". In: *2015 Computing in Cardiology Conference (CinC).* IEEE, pp. 317–320.

Hernández, A., J. Cruz, and G. Garrault (2007b). *Device for supervision and stimulation intended to fight sleep apnea.* WO Patent App. PCT/EP2007/055,723.

On-off Kinesthetic Stimulation Therapy for Sleep Apnea Syndrome: Effects in event duration and oxygen saturation levels

This chapter presents quantitative results obtained from the first clinical study of the PASITHEA project (HYPNOS study), presented in detail chapter 4. In particular, the intra-patient effects of the proposed on-off controller for kinesthetic stimulation therapy are evaluated in terms of i) the duration of respiratory episodes, ii) the corresponding oxygen saturation levels and iii) sleep structure, when comparing periods during which the therapy was enabled or disabled. Most of the contents of this chapter have been recently published in an international journal (see appendix A). A new method for the estimation of two markers that reflect acute modifications in SaO_2 levels associated with SAS is also presented in this chapter.

5.1. The proposed On-Off controller

Based on the control theory explained in chapter 3, an on-off controller was proposed for the management of the kinesthetic stimulation for the treatment of SAS. This controller was evaluated in a first clinical protocol (HYPNOS study) described in chapter 4. In section 4.2, an introduction of the functioning of this controller was presented. However, the objective in chapter 4 was to evaluate the performance of the respiratory event detector and to present qualitative results of the response to the therapy implementing this controller. In

this chapter quantitative results of the performance of such controller are presented. Figure 4.6 shows a block diagram of the PASITHEA system integrating the proposed controller.

It is to note that, as previously mentioned, this controller is considered as optimal since a bang-bang solution (see section 3.2.3) is needed so that respiratory events can be stopped in the shortest possible time avoiding the deleterious effect associated with SAS. Indeed, in order to propose an optimal control at least one of two conditions must be fulfilled: the proposal of a cost function to minimize or a performance index to maximize, where this function may include a number of observed variables. In the context of this work, since our plant to control is the patient and its output is the nasal pressure (NP) signal, we proposed a cost function $\delta(NP(t))$ to minimize. This function is proportional to the respiratory event durations $D(i)$, with $i = 1, ..., N$, where N is the total number of respiratory events for one patient during the whole night. Equation 5.1 shows such cost function.

$$\delta(NP(t)) \;\; \alpha \;\; D(i) = t_i^{end} - t_i^{start} \tag{5.1}$$

Where, t_i^{start} and t_i^{end} are the beginning and end of the ith respiratory event.

As in any detector, it is inevitable the presence of a certain amount of detection errors. We decided that instead of relying on the output of the respiratory event detector to determine the time instants t^{start} and t^{end} for the controller evaluation, clinical annotations were taken as our ground truth. The goal in this chapter is thus to present quantitative results of such evaluation.

Respiratory event duration and SaO_2 are closely related since decreases in event durations typically reduce SaO_2 drops. Thus, our controller is also capable of indirectly affected SaO_2. Figure 5.1 shows three different responses to therapy where it can be observed how SaO_2 drops become more severe as durations increase.

The following sections will describe the implemented methodology for the evaluation of the proposed controller. Results from the analyses are also presented in section 5.3.

5.2. Quantitative evaluation of the on-off controller

5.2.1. Recall of study design and participants

In section 4.3.1, we presented the details of the HYPNOS clinical trial, including the procedures followed in this study and the patient population. The analyses described in this chapter have been performed on 24 patients from the HYPNOS trial that were available for the analysis of the effect of the therapy. Each of these patients underwent a full PSG recording where intermittent periods of 30 minutes where applied with the therapy enabled ($Ther_{en}$) or disabled ($Ther_{dis}$), as recalled in Figure 4.10.

A set of physiological markers regarding respiratory event duration, SaO_2 levels and sleep deterioration has been estimated from the acquired signals during the whole night and grouped into one class for $Ther_{en}$ periods and another class for $Ther_{dis}$ periods. The estimation of these markers partly rely on manual clinical annotations performed off-line
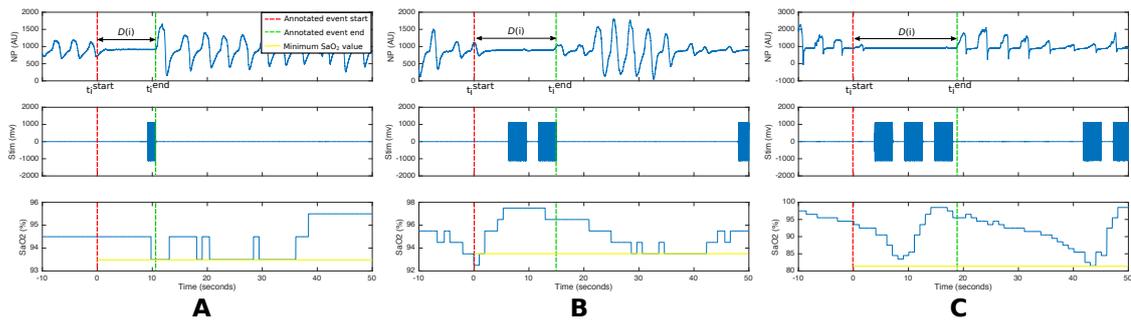
Figure 5.1: Example of how SaO$_2$ drops become more severe as event durations increase. Three physiological signals are displayed: the first panel shows the nasal pressure (NP) signal, the second panel presents the stimulation (Stim) signal delivered by the kinesthetic actuator and the third panel illustrates the oxygen saturation (SAO$_2$) signal. Three different examples are presented: A) a short respiratory event where only one stimulation burst was required in order to stop the episode, B) a respiratory event where two stimulation bursts were required and C) an example of a long respiratory event where three stimulation burst were delivered. Red and green segmented lines represent the start and end of a given respiratory event respectively. Yellow continuous lines represent the minimum level reached in the SaO$_2$ by a given respiratory episode. Indicators t_i^{start} and t_i^{end} represent the start and end of the time instants taken for the controller evaluation where $D = t_i^{end} - t_i^{start}$ is the duration of the given episode.

from PSG recordings. These annotations were performed by a single expert scorer at the core laboratory (CHU Grenoble), with quality assured by an intra-scorer quality control process. Although patients and physicians were aware of the $Ther_{en}$ and $Ther_{dis}$ treatment periods, the PSG core laboratory was blinded to the occurrence of stimulation during a respiratory event. No stimulation artifact on the respiratory or electroencephalogram waveforms was noted on the scored PSG signals.

Once the physiological markers have been extracted and grouped into classes, statistical comparison of the markers in each class, for each patient (intra-patient comparison), is performed, in order to evaluate the effect of the therapy in a given patient. More details on the data processing methods are given below.

5.2.2.   Data processing and statistical analysis

Three signals available from the PSG recording were analyzed in this work (Fig. 4.10): the nasal pressure (NP) signal, the oxygen saturation signal (SaO$_2$) and the signal driving the kinesthetic stimulator ($Stim$). Manual annotations performed by the core-lab for the whole duration of each PSG recording were also used to derive the time instants of beginning and end of each respiratory event and to obtain the information about the sleep stage of the patient. Finally, the PASITHEA system yields a signal with precise time markers representing the beginning and end of each $Ther_{en}$ and $Ther_{dis}$ period (typically 30 minutes each cycle).

Five main variables have been obtained by the processing of the above-mentioned data:

- the duration of each respiratory event (apnea or hypopnea),

- the detection of the presence of at least one kinesthetic stimulation burst during a given respiratory episode,

- the generation and analysis of the hypnogram from sleep stage annotations,

- the detection of micro-arousals and

- an estimation of the level of hypoxia produced by each event, through an original analysis of the SaO2 signal.

Estimation of event duration

Data processing starts by the identification of the beginning, t_i^{start} and end t_i^{end} of each respiratory event $i(i = 1, ..., N)$, where N is the total number of events for one patient during the whole night. These instants were determined from the core-lab annotations. A set containing the classification of each respiratory event C, with $C = \{c_i \in [\text{Apnea}, \text{Hypopnea}]\}$ was also created from these annotations.

The *Stim* signal was processed in order to verify if a given episode i was stimulated or not within the time support $[t_i^{start}, t_i^{end}]$ and the result was recoded in set S, with $S = \{s_i \in [\text{ON}, \text{OFF}]\}$. The duration of each event, classified according to the type of respiratory event and the presence or absence of stimulation was calculated and stored in set D_s^c, $D_{s_i}^{c_i} = t_i^{end} - t_i^{start}$. In figure 5.1 we can observe how the respiratory event duration is calculated for a given stimulated apneic episode.

Characterization of sleep structure

The reconstructed hypnogram signal was analyzed in order to determine the number of micro-arousals and the time spent in each sleep stage for each *Ther* period $j(j = 1, ..., K)$, where K is the total number of complete periods $Ther \in [Ther_{en}, Ther_{diss}]$. The results were recorded in set M and SL, where $M = \{m_j \in Ther\}$ is a set containing the number of micro-arousals for each cycle and $SL_j^{ss} = \{t_{ss} \mid j \in Ther\}$ is a set containing the time spent in each sleep stage t_{ss} with $ss \in [\text{Awake}, \text{REM}, \text{Stage1}, \text{Stage2}, \text{Stage3}]$.

Event-based quantification of hypoxia levels

Most methods in the literature for the evaluation of hypoxia rely on global statistics of the SaO_2 signal. The oxygen desaturation index (ODI) and the time spent in SaO_2 below 90% are the most commonly implemented markers. Several studies such as (CAMPO et al., 2006; GYULAY et al., 1993; TANIGAWA et al., 2004) have used these indicators to assess the severity of hypoxia. Results from (UNAL et al., 2002) and (OEVERLAND et al., 2002) suggest that markers such as the time spent in SaO_2 below 90% and ODI are suitable to estimate the severity of SAS. Concerning ODI, this indicator is calculated as the number

of times per hour of sleep during which the SaO_2 levels drop by a certain degree from the baseline. Common values in the literature for these drop are 3% or 4% for ODI3 or ODI4 respectively. Although these global markers provide valuable information on the overall oxygen saturation levels during the night, they are not applicable to our case, in which acute responses of each event should be measured.

The estimation of acute modifications observed in the SaO_2 signal may be challenging. Besides the noise that is often present in long-term SaO_2 recordings, a first difficulty is related to the fact that, due to hemodynamic and metabolic time constants, the observed variable presents a significant delay with respect to the instant of the beginning of the respiratory event that generated it. These time constants are not known *apriori* and may present intra and inter-patient variations. Another difficulty is encountered when two or more respiratory events occur in a time support which is less than the mean phase delay observed in the SaO_2 signal. In these cases, it is impossible to differentiate the consequences of each of the events on the level of hypoxia. Also, very low frequency variations of the SaO_2 signal are normally observed during the night, making the estimation of a reference SaO_2 level using long-term (minutes or hours) time supports not accurate for our purpose.

In order to cope with these difficulties, we propose a method for the estimation of two markers that reflect the acute modifications of SaO_2, associated to a given respiratory event i and using a local SaO_2 reference estimation (Fig. 5.2).

Local estimation of acute hypoxemia:

Due to the above-mentioned phase delay of the SaO_2 signal with respect to each SAS event, the signal has been analyzed in a time support of $[t_i^{end}, t_i^{end} + t_{ex}]$, where t_i^{end} is the annotated ending instant of a given respiratory event i and t_{ex} a constant time extension. Within this temporal support, the raw SaO_2 signal is filtered with a forward-backwards second order low-pass filter with a cutoff frequency of 0.5 Hz so as to minimize noise with no phase distortion (red signal in figure 5.2 B). Subsequently, a local minimum detection algorithm was used to determine the minimum position p in the filtered signal. Lastly, the minimum hypoxemia value h (yellow line in figure 5.2 B) was obtained from the raw SaO_2 signal, analyzing the signal value in position p. These hypoxemia values were stored in set H_s^c, where $H_{s_i}^{c_i} = \{h_i\}$.

Relative estimation of acute hypoxemia ($\delta SaO2$):

A relative variation of acute hypoxemia $\delta SaO2$ was estimated for each event as the difference between the minimum hypoxemia value h and the mean value of the SaO_2 signal on a reference time support of $[t_i^{start} - t_1, t_i^{start} + t_2]$ as shown in figure 5.2 A. Variables t_1 and t_2 are time constants that define the size of the reference time support. $\delta SaO2$ values were stored in set DS_s^c, where $DS_{s_i}^{c_i} = \{ref_i - h_i\}$.

In order to avoid overlapping between consecutive events, the validation of each event was subject to the compliance to two conditions: i) the standard deviation of the reference
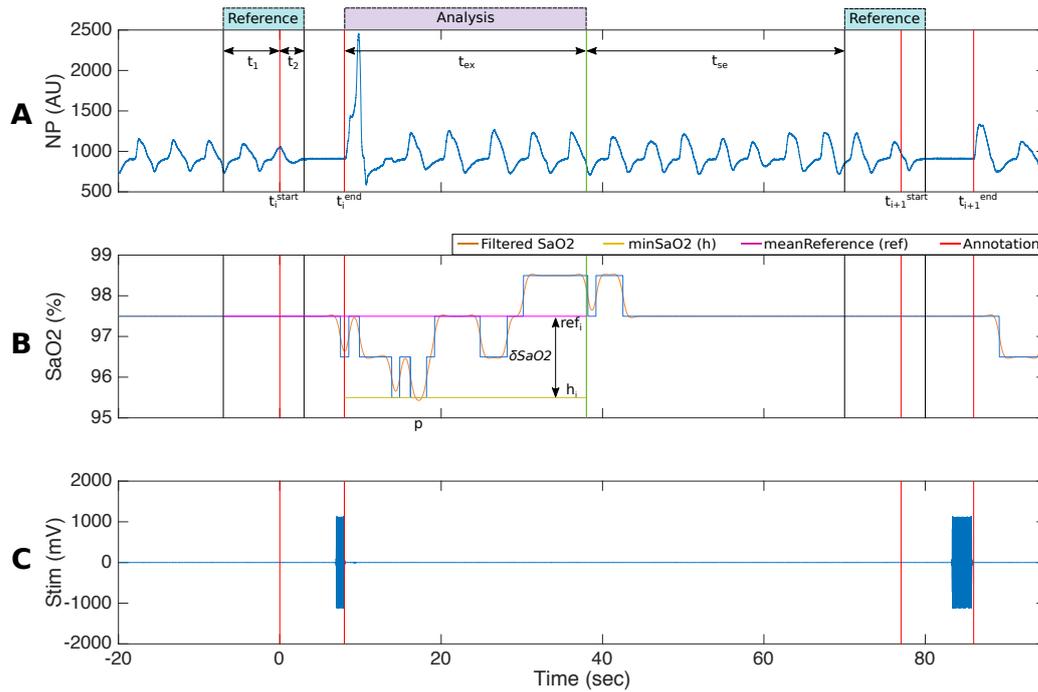
Figure 5.2: Example showing two stimulated apnea events and the notation used in this chapter for the proposed SaO_2 signal processing. The desaturation produced by the first event is estimated from the SaO_2 signal level as described in the text. and the variables used for the calculus of $\delta SaO2$. A) the acquired nasal pressure (NP) signal, B) the SaO_2 and C) signal driving the kinesthetic stimulation (Stim). Red lines represent, the start and end of each event (t^{start}, t^{end}), as taken from the core-lab annotations. The black lines represent the start and end of the reference time support $[t^{start} - t_1, t^{start} + t_2]$ and the green line indicates the end of the analyzed time window ($t_i^{end} + t_{ex}$). The magenta solid line represents the mean SaO_2 value taken from the reference time support (ref) and the mustard solid line represents the minimum SaO_2 value on the analyzed time window (h). Time instant p, indicates the position of the detected minimum of the filtered SaO_2 signal within the analyzed time window.

time support can not exceed a tolerance level tol and ii) the succeeding event ($i + 1$) have to start at least t_{se} seconds after the end of the analyzed time support ($t_i^{end} + t_{ex}$). Clearly, the estimation of $\delta SaO2$ is particularly sensitive to the choice of t_{ex}, t_1 and t_2. Therefore, these constants were heuristically tuned before applying the method.

Statistical analysis

Individual boxplots (per patient) were constructed to show the duration of respiratory events and $\delta SaO2$ (median and interquartile range). Boxplot analysis was also applied for ODI4, mean SaO_2, and time spent at SaO_2 below 90%. Global population results are reported as median and interquartile range (Q3 - Q1). Data were analyzed using the Wilcoxon signed-rank test due to the non-normality distribution of the data. For all tests, a significance level of 0.05 was used. No exclusion of outliers was performed prior statistical

analysis.

5.3. Results

5.3.1. Event duration

Figure 5.3 shows boxplots of individual results for both apnea (Figure 5.3A) and hypopnea (Figure 5.3B) event durations during $Ther_{en}$ and $Ther_{dis}$ periods, respectively. Regarding apnea event duration, 13 patients (56.5%) exhibited a statistically significant decrease in event duration during the $Ther_{en}$ phases when compared to $Ther_{dis}$ phases. Concerning hypopnea events, 11 patients (45.8%) demonstrated a significant decrease in event duration during the $Ther_{en}$ phases compared to $Ther_{dis}$ phases. The average reduction in the duration of stimulated versus non-stimulated events for the patients who presented a significant response was 4.86 seconds (25.48%) for apneas and 6.00 seconds (23.92%) for hypopneas. As shown in Figure 5.3, some patients with a significant reduction in apnea event duration did not necessarily exhibit a similar response for hypopnea event durations and vice-versa. Overall, 75% of the patients showed a statistically significant decrease in apnea or hypopnea event durations. A table with the results from this analysis is presented in Appendix B.

5.3.2. Global oxygen saturation markers

No significant differences were found when comparing $Ther_{dis}$ versus $Ther_{en}$ periods for ODI4 (14.6 (29.3 - 7.3) and 13.9 (23.8 - 6.9)/hour for $Ther_{dis}$ and $Ther_{en}$ periods, respectively), percentage of time spent at SaO2 below 90% (4.0 (27.4 - 1.1)% and 2.5 (24.1 - 0.6)% for $Ther_{dis}$ and $Ther_{en}$ periods, respectively), or mean oxygen SaO2 (94.4 (95.9 - 92.3)% and 94.8 (95.8 - 92.4)% for $Ther_{dis}$ and $Ther_{en}$ periods, respectively). Figure 5.4 shows bloxplots of these findings.

5.3.3. Local, acute SaO2 analysis

Results from the time constants selection showed that the median time between the end of an event (t_i^{end}) and the time instant of its corresponding minimum hypoxemia value h_i is 15.62 (16.81 - 13.33) seconds, with a maximum time of 22.05 seconds. Based on these results, a choice of $t_{ex} = 30s$ was made in order to guarantee that the minimum hypoxemia value due to a given event is within the analyzed time window. This time support of 30 seconds for the analysis of SaO2 signals has already been used in previous works (RAUSCHER et al., 1991)(MORET-BONILLO et al., 2014). Also, based on the results from the heuristic tuning process, the following constants were defined as: $t_1 = 7s$ and $t_2 = 3s$.

Figure 5.5 shows boxplots of individual results for both apnea (figure 4A) and hypopnea (figure 4B) $\delta SaO2$ during $Ther_{en}$ and $Ther_{dis}$ periods respectively. Concerning apnea
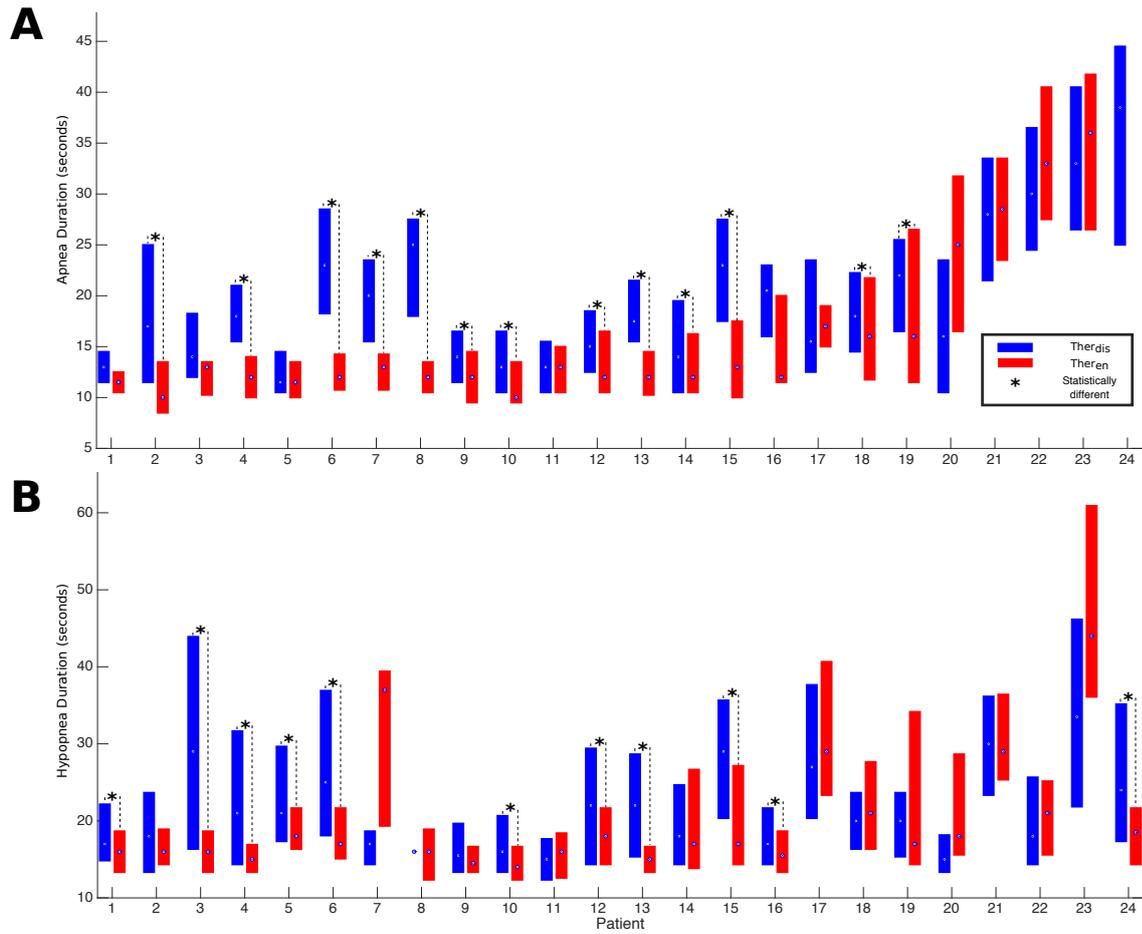
Figure 5.3: Boxplots representing the duration of respiratory events during $Ther_{en}$ and $Ther_{dis}$ periods for each of the 24 patients: A) Apnea duration and B) Hypopnea duration. The box spans the interquartile ranges and the median is indicated by a circle. Statistical difference annotated by * for p<0.05 using a Wilcoxon signed rank test. Patient 24 did not show any apnea event during the $Ther_{en}$ periods.

events, 10 patients (43.5% of the patients who were stimulated) presented a statistically significant decrease on the $\delta SaO2$ between the $Ther_{en}$ and $Ther_{dis}$ phases. Moreover, 5 patients (20.8% of the patients) presented a statistically significant decrease on the $\delta SaO2$ regarding the hypopnea events.

The average reduction of $\delta SaO2$ between events in $Ther_{en}$ versus $Ther_{dis}$ phases for the patients who presented a statistically significant difference was 2.45% on the SaO2 level (55.44% of reduction) for the apnea events and 0.86% (37.61% of reduction) for the case of hypopnea events. In this study, 13 patients (54.2% of the population) presented a statistically significant reduction of $\delta SaO2$ in $Ther_{en}$ phases comparing to $Ther_{dis}$ phases either for apnea or hypopnea events.
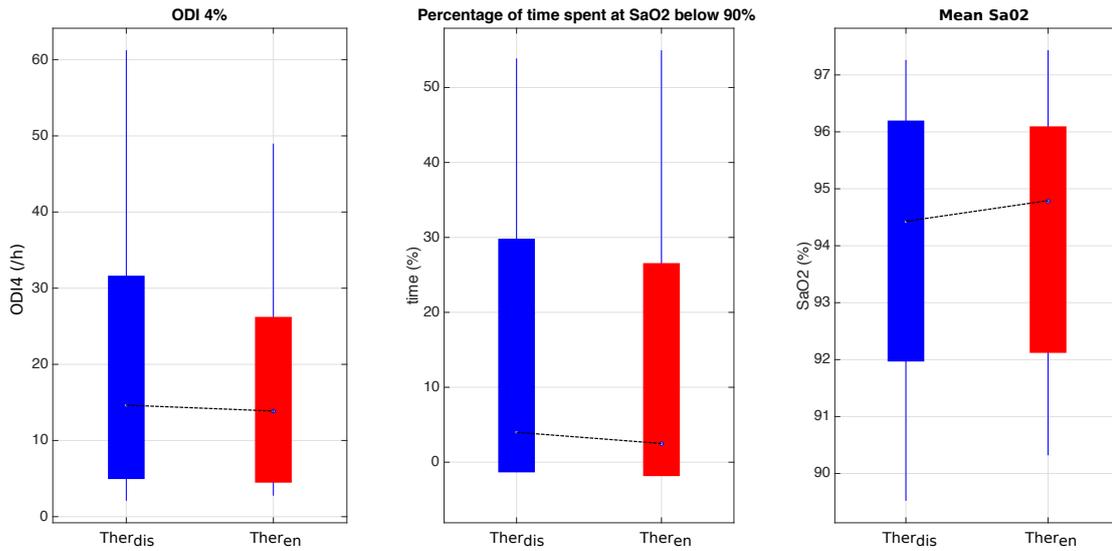
Figure 5.4: Boxplot of ODI4, percentage of time spent at SaO2 below 90% and mean SaO2 calculated for the whole $Ther_{en}$ and $Ther_{dis}$ periods across all patients. Same convention as in Figure 5.3

5.3.4. Sleep analysis

Results for each patient presenting the median, Q1 and Q3 quartiles of the time spent at each sleep stage (Awake, REM, Stage1, Stage2 and Stage3) as well as the micro-arousals indices, during cycles $Ther_{en}$, $Ther_{dis}$ and during the whole night (41 markers in total for each patient) are presented in appendix B. Most of the patients did not show any significant difference between $Ther_{dis}$ and $Ther_{en}$ periods for any sleep stage. Only two patients presented a significant difference in one sleep stage: patient 6 showed significantly larger time spent in awake stage during $Ther_{en}$ comparing to $Ther_{dis}$ whereas patient 12 presented significantly larger time spent in stage 1 during $Ther_{en}$ comparing to $Ther_{dis}$. Concerning the micro-arousal index, no significant differences were found for any patient.

5.3.5. Other outcomes

Based on a patient-rated questionnaire completed the morning after treatment with the PASITHEA device, six patients (25%) complained about the noise from the stimulation. In comparison, thirteen patients (54%) complained about the difficulty to sleep due to the PSG itself. No complications due to the stimulation were observed.

5.4. Discussion

In this chapter we presented the results from the first proof of concept clinical trial testing the ability of kinesthetic stimulation to reduce apnea and hypopnea event duration in patients with OSA and evaluating its effects on SaO_2 levels with the implementation of a novel $\delta SaO2$ method. Overall, 75% of patients included in the analysis demonstrated a
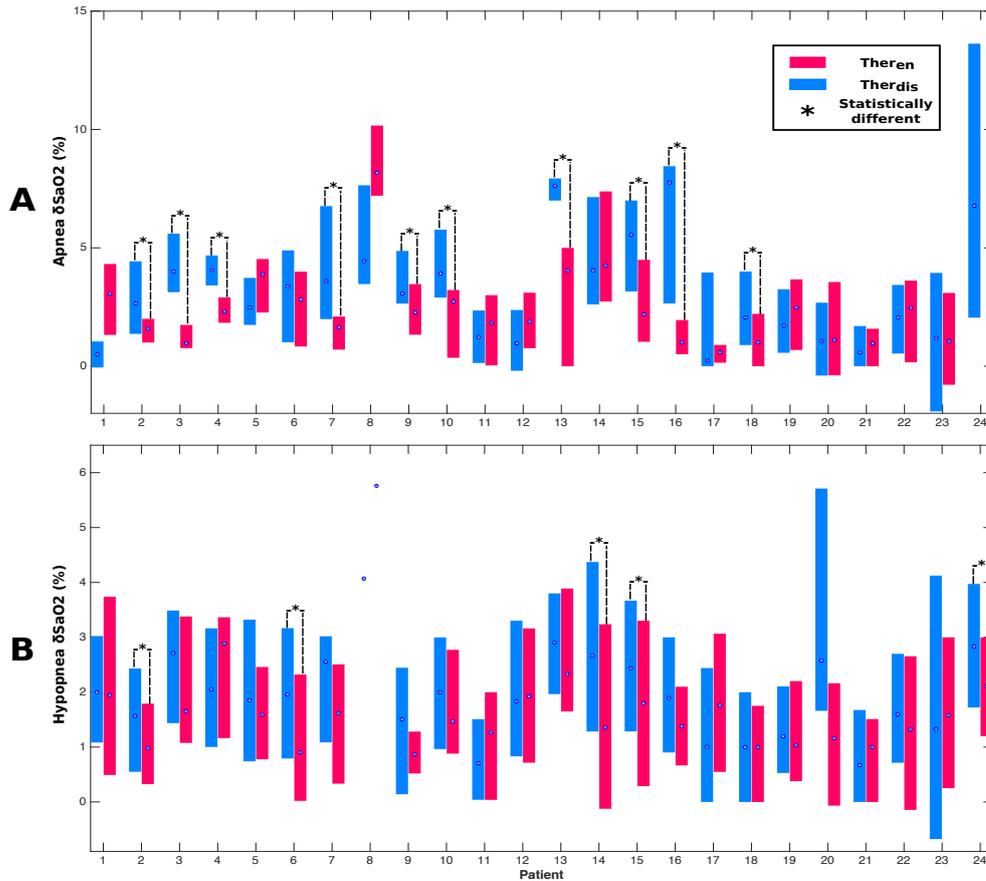
Figure 5.5: Boxplots representing the $\delta SaO2$ of respiratory events during $Ther_{en}$ and $Ther_{dis}$ periods for each of the 24 patients: A) Apnea $\delta SaO2$ and B) Hypopnea $\delta SaO2$. The box spans the interquartile ranges and the median is indicated by a circle. Statistical difference annotated by $*$ for $p < 0.05$ using a Wilcoxon signed rank test. Patient 24 did not show any apnea event during the $Ther_{en}$ periods.

significant reduction (approximately 5 seconds) in the duration of apneas or hypopneas. The study revealed a modest non-significant improvement for the whole group regarding ODI4 and mean SaO_2 when comparing $Ther_{en}$ and $Ther_{dis}$ periods. These findings suggest that kinesthetic stimulation may be an effective treatment for patients with severe OSA.

The overall response to kinesthetic stimulation was significant but clinical relevance of the size effect can be discussed. We believe that the range of improvement shown in this proof of concept study will be increased both by refining the stimulation technique itself and also by a prospective identification of responder's profile as it has been done for hypoglossal stimulation (Strollo Jr et al., 2014; Vanderveken et al., 2017). Indeed, in this study, we retrospectively labelled patients as 'responders' when they presented a statistically significant decrease in terms of event duration for either apnea or hypopnea events. We hypothesize that a better patient selection can be obtained by analyzing the level of autonomic function of each candidate patient, in a preliminary test. Chapter 5 presents encouraging results in this matter.

In order to further reduce event duration, the 6 second time delay required for the validation of events detection, before triggering stimulation bursts, may be reduced by an improvement of the detection algorithm. An additional decrease of event durations is expected with associated reduction in the amount of nocturnal hypoxia. Indeed, as cardiovascular and metabolic consequences of OSA are mainly related to the severity of nocturnal intermittent hypoxia (LÉVY et al., 2014); shortening the mean event duration to less than 8 to 10 seconds will reduce the burden of deleterious consequences. Furthermore, in this study, the stimulation patterns (amplitude, burst duration, frequency) were identical for all patients and kept constant during the evaluation. A closed-loop therapy, which adapts these parameters as a function of patient-specific responses (position and sleep stages) may also improve the effects of kinesthetic stimulation.

New approaches using stimulation therapies in OSA are at different stages of reliability and validation. Hypoglossal nerve stimulation augments the neural output to upper airway dilator muscles; both short and long term studies have demonstrated the efficacy of the technique (STROLLO JR et al., 2014; WOODSON et al., 2016). However, high cost, invasiveness and a complex process of patient selection to identify potential 'responders' all limit the generalization and reimbursement of this treatment. A recently published randomized trial has evaluated transcutaneous electrical stimulation of the upper airway dilator muscles for the treatment of OSA (PENGO et al., 2016). The effect size in this trial was relatively modest and comparable to our results. The delivery of effective transcutaneous electrical stimulation is impacted by skin and soft tissue resistance, and increased intensity of stimulation affects tolerance (PENGO et al., 2016). In our study, problems affecting the coupling interface between the stimulator and the patient's skin were also a significant concern for vibratory kinesthetic stimulation and led us to exclude 12% of our patients from analysis (see Figure 4.9). Furthermore, body position during patient's sleep may also affect the mechanical coupling between the stimulator and the skin of the patient and therefore alter the effectiveness of the kinesthetic stimulation.

In addition, the position of the kinesthetic stimulator on the body may play a role on the response to the therapy. In this work, we have selected the mastoid region because it is rich in mechanoreceptors, it allows for the activation of both a tactile and an auditory startle response and it is particularly interesting from an ergonomic point of view. However, other stimulation areas could also be studied. These different aspects have to be considered when developing the methods in the domiciliary setting.

On the other hand, results obtained from the $\delta SaO2$ analysis show that 54.2% of the patients showed a statistically significant reduction on the $\delta SaO2$ value for apnea or hypopnea events during $Ther_{en}$ periods, when compared to $Ther_{dis}$ periods. In addition, the mean reduction in the $\delta SaO2$ for the patients who presented a significant difference was of 55.44% for apnea events and 37.61% for hypopnea. As expected, the patients who showed a statistically significant reduction on the $\delta SaO2$ also presented a statistically significant reduction in terms of event duration. These findings suggest that when kinesthetic stimulation therapy is applied early during a respiratory event and therefore shortening

breathing pauses; significant drops on the SaO_2 levels may also be avoided. Moreover, the results are also encouraging because as they indicate, the therapy also serves as a treatment to avoid severe changes in SaO_2 levels due to SAS and therefore, it may prevent diseases related to severe variations in those levels.

As it is explained in (IMADOJEMU et al., 2007), hypoxemia resulting from OSA events may provoke intermittent surges of sympathetic activity due to the stimulation of arterial chemoreceptors and also, long-term exposure to intermittent hypoxemia events may increase chemosensitivity (LUSINA et al., 2006). Hence, increases in sympathetic activity to peripheral blood vessels lead to vasoconstriction provoking severe hemodynamic stress (LEUENBERGER et al., 1995), which may act to promote cardiac and vascular diseases (SOMERS et al., 2008) (TRZEBSKI, 1992). It is also important to mention that, in this study, there is still a high rate of patients (45.8%) that did not show any significant differences between $Ther_{en}$ and $Ther_{dis}$ phases in terms of $\delta SaO2$. We presume that the lack of response in this analysis may be due to the same previously mentioned factors: I) inappropriate patient selection (patients presenting an autonomic dysfunction), II) problems on the coupling interface between the actuator and the patient's skin and III) fixed set of values for stimulation parameters (amplitude and burst duration) used during all night and for all patients. In chapter 7 we present a new version of the PASITHEA system that integrates an optimized event detector and an improved control method.

Concerning the characterization of the response to the therapy, this first proof-of-concept study was focused on the duration of respiratory events and the analysis of variations in SaO_2 levels. After the encouraging results reported in this chapter, additional pathophysiological studies should be conducted in order to better characterize this new treatment modality in terms of upper airway collapsibility, arousal thresholds and loop gain. Finally, although preliminary results on sleep architecture are presented in appendix B, we acknowledge that, by design, this first study do not allow a robust assessment of the impact of kinesthetic stimulation on whole night sleep architecture. A randomized trial is currently ongoing that compares two nights with and without stimulation and measures other clinical outcomes including sleep disruption, as well as subjective and objective sleepiness (NCT02789748). Chapter 7 presents a more detailed description of this new randomized trial.

5.5. Conclusion

This chapter describes the effects in terms of the duration of respiratory events and SaO_2 levels of a novel non-invasive neuromodulation SAS therapy, based on triggered kinesthetic stimulation. Results show that the proposed therapy significantly decreases the duration of apneas or hypopneas (approximately 5 seconds) in 75% of patients included in the analysis. Moreover, they show that therapy also decreases the amplitude of drops in SaO_2 levels in 54.2% of the studied patients with an average reduction on the $\delta SaO2$ of 55.44% for apnea and 37.61% for hypopnea events.

Despite the fact that an acute analysis of the signals obtained from PSG records is clearly a challenge since noise and artifacts from patient movement during sleep are normally present, in this chapter, new methodologies in combination with classic markers for the evaluation of the performance of this therapy were proposed and applied to a population of 24 patients. Therefore, it is important to note that the main contribution described in this chapter was to quantitatively demonstrate the effects of kinesthetic therapy on patients suffering from SAS.

Although the results are encouraging for the feasibility of this therapy, some improvements are needed in order to reduce the lack of response rate. For this reason, chapter 7 presents the current work directed towards the evaluation of an improved system through a new clinical protocol. This improved system replaces the "on-off" control method used in this work by a fully-adaptive, closed-loop stimulation approach, based on concurrent, coupled proportional-derivative (PD) controllers in order to adapt the stimulation properties as a function of the physiological response of the patient (PÉREZ et al., 2016). In addition, characterization of the patient population who may benefit from the proposed kinesthetic therapy has being performed in order to identify criteria for patient selection (see chapter 6).

References

CAMPO, F. DEL, R. HORNERO, C. ZAMARRÓN, D. E. ABASOLO, and D. ÁLVAREZ (2006). "Oxygen saturation regularity analysis in the diagnosis of obstructive sleep apnea". In: *Artificial intelligence in medicine* 37.2, pp. 111–118.

GYULAY, S., L. OLSON, M. HENSLEY, M. KING, K. M. ALLEN, and N. SAUNDERS (1993). "A Comparison of Clinical Assessment in the Diagnosis of Obstructive Sleep". In: *Am Rev Respir Dis* 147, pp. 50–53.

IMADOJEMU, V. A., Z. MAWJI, A. KUNSELMAN, K. S. GRAY, C. S. HOGEMAN, and U. A. LEUENBERGER (2007). "Sympathetic chemoreflex responses in obstructive sleep apnea and effects of continuous positive airway pressure therapy". In: *American College of Chest Physicians* 131.5, pp. 1406–1413.

LEUENBERGER, U., E. JACOB, L. SWEER, N. WARAVDEKAR, C. ZWILLICH, and L. SINOWAY (1995). "Surges of muscle sympathetic nerve activity during obstructive apnea are linked to hypoxemia". In: *Journal of Applied Physiology* 79.2, pp. 581–588.

LÉVY, P., M. KOHLER, W. T. MCNICHOLAS, F. BARBÉ, R. D. MCEVOY, V. K. SOMERS, L. LAVIE, and J.-L. PEPIN (2014). "Obstructive sleep apnoea syndrome." In: *Nature reviews. Disease primers* 1, pp. 15015–15015.

LUSINA, S.-J. C., P. M. KENNEDY, J. T. INGLIS, D. C. MCKENZIE, N. T. AYAS, and A. W. SHEEL (2006). "Long-term intermittent hypoxia increases sympathetic activity and chemosensitivity during acute hypoxia in humans". In: *The Journal of physiology* 575.3, pp. 961–970.

Moret-Bonillo, V., D. Alvarez-Estévez, A. Fernández-Leal, and E. Hernández-Pereira (2014). "Intelligent approach for analysis of respiratory signals and oxygen saturation in the sleep apnea/hypopnea syndrome". In: *The open medical informatics journal* 8, p. 1.

Oeverland, B., O. Skatvedt, K. J. Kværner, and H. Akre (2002). "Pulseoximetry: sufficient to diagnose severe sleep apnea". In: *Sleep medicine* 3.2, pp. 133–138.

Pengo, M. F., S. Xiao, C. Ratneswaran, K. Reed, N. Shah, T. Chen, A. Douiri, N. Hart, Y. Luo, G. F. Rafferty, et al. (2016). "Randomised sham-controlled trial of transcutaneous electrical stimulation in obstructive sleep apnoea". In: *Thorax*, thoraxjnl–2016.

Pérez, D., G. Guerrero, D. Feuerstein, L. Graindorge, A. Amblard, J.-L. Pépin, L. Senhadji, and A. Hernández (2016). "Closed-loop kinesthetic stimulation for the treatment of sleep apnea syndromes". In: *Computing in Cardiology Conference (CinC), 2016*. IEEE, pp. 841–844.

Rauscher, H., W. Popp, and H. Zwick (1991). "Computerized detection of respiratory events during sleep from rapid increases in oxyhemoglobin saturation". In: *Lung* 169.1, pp. 335–342.

Somers, V. K., D. P. White, R. Amin, W. T. Abraham, F. Costa, A. Culebras, S. Daniels, J. S. Floras, C. E. Hunt, L. J. Olson, et al. (2008). "Sleep apnea and cardiovascular disease: An American heart association/American college of cardiology foundation scientific statement from the American heart association council for high blood pressure research professional education committee, council on clinical cardiology, stroke council, and council on cardiovascular nursing in collaboration with the national heart, lung, and blood institute national center on sleep disorders research (national institutes of health)". In: *Journal of the American College of Cardiology* 52.8, pp. 686–717.

Strollo Jr, P. J., R. J. Soose, J. T. Maurer, N. De Vries, J. Cornelius, O. Froymovich, R. D. Hanson, T. A. Padhya, D. L. Steward, M. B. Gillespie, et al. (2014). "Upper-airway stimulation for obstructive sleep apnea". In: *New England Journal of Medicine* 370.2, pp. 139–149.

Tanigawa, T., N. Tachibana, K. Yamagishi, I. Muraki, M. Umesawa, T. Shimamoto, and H. Iso (2004). "Usual alcohol consumption and arterial oxygen desaturation during sleep". In: *Jama* 292.8, pp. 923–925.

Trzebski, A. (1992). "Arterial chemoreceptor reflex and hypertension". In: *Hypertension* 19.3 pt 1, pp. 562–566.

Unal, M., L. Ozturk, and A. Kanik (2002). "The role of oxygen saturation measurement and body mass index in distinguishing between non-apnoeic snorers and patients with obstructive sleep apnoea syndrome". In: *Clinical otolaryngology and allied sciences* 27.5, pp. 344–346.

Vanderveken, O. M., J. Beyers, S. Op de Beeck, M. Dieltjens, M. Willemen, J. A. Verbraecken, W. A. De Backer, and P. H. Van de Heyning (2017). "Development

of a Clinical Pathway and Technical Aspects of Upper Airway Stimulation Therapy for Obstructive Sleep Apnea". In: *Frontiers in neuroscience* 11, p. 523.

WOODSON, B. T., R. J. SOOSE, M. B. GILLESPIE, K. P. STROHL, J. T. MAURER, N. DE VRIES, D. L. STEWARD, J. Z. BASKIN, M. S. BADR, H.-S. LIN, et al. (2016). "Three-year outcomes of cranial nerve stimulation for obstructive sleep apnea: the STAR trial". In: *Otolaryngology–Head and Neck Surgery* 154.1, pp. 181–188.

Autonomic differences based on the response to kinesthetic stimulation therapy in sleep apnea patients

In previous chapters, we have shown that the proposed kinesthetic stimulation therapy is capable of reducing the respiratory event duration, therefore preventing severe exposures to hypoxemia. However, approximatively 25% of the patients did not present any significant amelioration when therapy is applied. In this chapter, we present a method to reduce the non-responder rate, optimizing this therapy by improving patient selection. In the first section, we present a brief introduction along with the underlying hypothesis of the proposed method. Then, the methodology and the description of the algorithm implemented are described. Results from a retrospective analysis based on the HYPNOS database are shown and the chapter concludes with a discussion on the potential application of this method.

6.1. Introduction and hypothesis

In chapter 5, we have shown that in the HYPNOS trial, first proof of concept study of the PASITHEA system, 75% of patients included in the analysis presented a statistically significant reduction in the duration of SAS episodes. Despite the encouraging results obtained, there is still a high rate of "no-responder" patients to the proposed kinesthetic stimulation therapy (5.4). Our hypothesis is thus, that one of the key mechanisms underlying the effectiveness of this therapy is that eligible patients should have a functional peripheral nervous system, in particular the autonomic nervous system (ANS). This hypothesis is related to the fact that the main physiological mechanism involved in the response to the kinesthetic stimulation is mediated by the startle reflex (presented in section 3.1.2), which

relies on functional pathways of the peripheral and autonomic responses. Therefore, in
this chapter, we investigate retrospectively the ANS function of all the patients in the
HYPNOS database, based on widely used heart rate variability (HRV) and heart rate
complexity (HRC) parameters and correlate these ANS markers with a maker of response
to the kinesthetic stimulation therapy. The results may prove the relevance of the ANS
function for a more accurate selection of patients to whom the proposed therapy should be
applied.

6.2.   Methodology

6.2.1.   Study design

As previously mentioned, in chapter 5 we demonstrated in the HYPNOS study, the
ability of the kinesthetic stimulation therapy to reduce the duration of apnea and hypopnea
episodes in patients with SAS. Therein we compare intermittent 30-minute periods during
which the stimulator was active ($Ther_{en}$) in relation to 30-minute inactive stimulation
periods ($Ther_{dis}$). Based on differences between $Ther_{en}$ and $Ther_{dis}$ intervals, we defined
responder patients such as those presenting a statistically significant reduction in the
duration of episodes during $Ther_{en}$ when compared to $Ther_{dis}$ periods. According to this
criterion, four groups of patients were defined: i) only responding to apnea episodes (AR),
ii) only responding to hypopnea episodes (HR), iii) responding to apnea or hypopnea
episodes (AHR) and iv) not responding to any SAS episode (NR). However, given that
frequent premature ventricular contractions (PVC) may confound HRV analysis, an apnea
responder patient was excluded from the study.

6.2.2.   General data analysis approach

Figure 6.1 illustrates the global methodology implemented for the extraction of HRV
and HRC parameters for each patient. A detailed description of each step of the proposed
method is provided in the following sections.

6.2.2.1.   Sleep onset period detection

A reconstructed hypnogram from core-lab sleep annotations was implemented in order
to detect the sleep-onset period (SOP), which is defined as the transition period from
wakefulness to sleep (Ogilvie et al., 1989; Sleep Disorders Centers et al., 1979).
Starting from the SOP detections, 15-minutes windows of a single-lead ECG recorded at a
sampling frequency of 1024 Hz by the polysomnogram (PSG) system were identified in order
to extract the RR series for each patient. Among these time windows, the final segment to
analyze was selected as the first 15-minutes window with at least 85% of the time in any
sleep stage, along with a respiratory frequency always within the classic HF band. The
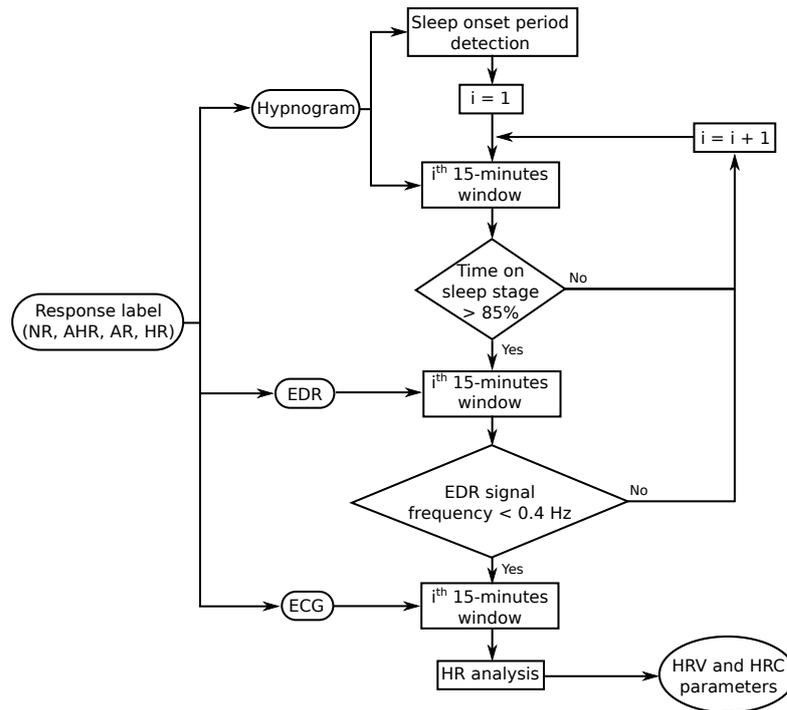
Figure 6.1: Block diagram for the global methodology implementation.

latter criterion was validated based on the approach described in (CALVO GONŹALEZ, 2017; CALVO et al., 2017).

6.2.2.2. RR series extraction

For each patient, the RR series extraction was performed by using a noise-robust wavelet-based method for R-wave peak location previously proposed in our laboratory (DUMONT et al., 2010). Figure 6.2 illustrates this RR series extraction from the location of R-wave peak in the ECG signal. After performing manual corrections when necessary, different parameters capturing heart rate variability (HRV) and heart rate complexity (HRC) were calculated. For spectral analysis, since RR series were not regularly sampled with respect to time, a cubic splines interpolation was applied to obtain uniformly-sampled data at a rate of 4 Hz.

6.2.2.3. ECG-Derived Respiration signal processing

Since the nasal pressure of some patients was not properly recorded, for this analysis, respiration activity was captured by an ECG-Derived Respiration (EDR) method, described in (MOODY et al., 1986), that estimates respiratory information from the amplitude modulation of R-wave peaks.

The estimated EDR signal was uniformly resampled at a rate of 10 Hz and band-pass filtered by a 4th order Butterworth filter between 0.15 and 0.7 Hz, applied in both forward and backward directions, so as to remove frequencies out of the respiratory range. Then,
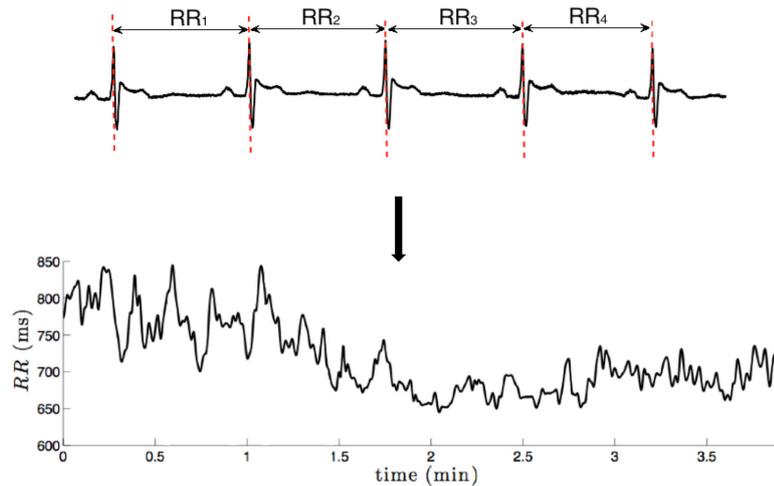
Figure 6.2: R-wave peak detections and RR series extraction from a representative ECG signal. Figure adapted from (CALVO et al., 2018).

instantaneous respiratory frequency was estimated by applying a time-frequency (TF) approach based on the smoothed pseudo Wigner-Ville distribution (SPWVD) transform.

The Wigner Ville distribution is a quadratic TF method defined as the Fourier transform of the instantaneous autocorrelation function (HLAWATSCH et al., 1992). However, since it is affected by interference terms, (COSTA et al., 1995) introduced a smoothing kernel function, $\Omega(\tau, \upsilon)$, that attenuates interferences while maintaining an acceptable TF resolution. Being $A_{EDR}(\tau, \upsilon)$ the Ambiguity Function of EDR series, $x_{EDR}(t)$, the SPWVD is defined as:

$$A_{EDR}(\tau, \upsilon) = \int\limits_{-\infty}^{\infty} x_{EDR}\left(t + \frac{\tau}{2}\right) x_{EDR}^*\left(t - \frac{\tau}{2}\right) e^{-j2\pi\upsilon t} dt \tag{6.1}$$

$$\Omega(\tau, \upsilon) = exp\left\{-\pi\left[\left(\frac{\upsilon}{\upsilon_o}\right)^2 + \left(\frac{\tau}{\tau_o}\right)^2\right]^{2\lambda}\right\} \tag{6.2}$$

$$SPWVD_{EDR}(t, f) = \int\int \Omega(\tau, \upsilon) A_{EDR}(\tau, \upsilon) e^{j2\pi(t\upsilon - \tau f)} d\upsilon d\tau \tag{6.3}$$

Based on (CALVO GONZÁLEZ, 2017), the most efficient interference terms cancellation for the lowest TF filtering was found when kernel parameters were adjusted to $\upsilon_0 = 0.06$ and $\tau_0 = 0.03$.

The simplest method to estimate instantaneous respiratory frequency consists in finding frequencies presenting the largest peaks in the spectrum at each time instant $\hat{f}(t)$. However, in order to avoid erroneous peak detections, for each time instant t_j, the search interval was restricted to frequencies between 2δ Hz, centered around a reference frequency $f_r(t_j)$: $[f_r(t_j) - \delta, f_r(t_j) + \delta]$; defined as the exponential average of previous estimates:

$$f_r(t_j) = \beta f_r(t_{j-1}) + (1 - \beta)\hat{f}(t_{j-1}), \tag{6.4}$$

where β is the forgetting factor. As in (BAILÓN et al., 2006), these parameters were fixed to $\beta=0.7$ and $\delta=0.01$, since, based on real respiratory patterns, respiratory frequency variations should not be faster than 0.01 Hz per 0.25 seconds. Figure 6.3 displays the SPWVD of an exemplifying EDR, together with its estimated, $\hat{f}(t)$, and corrected, $f_r(t)$, instantaneous respiratory frequency.
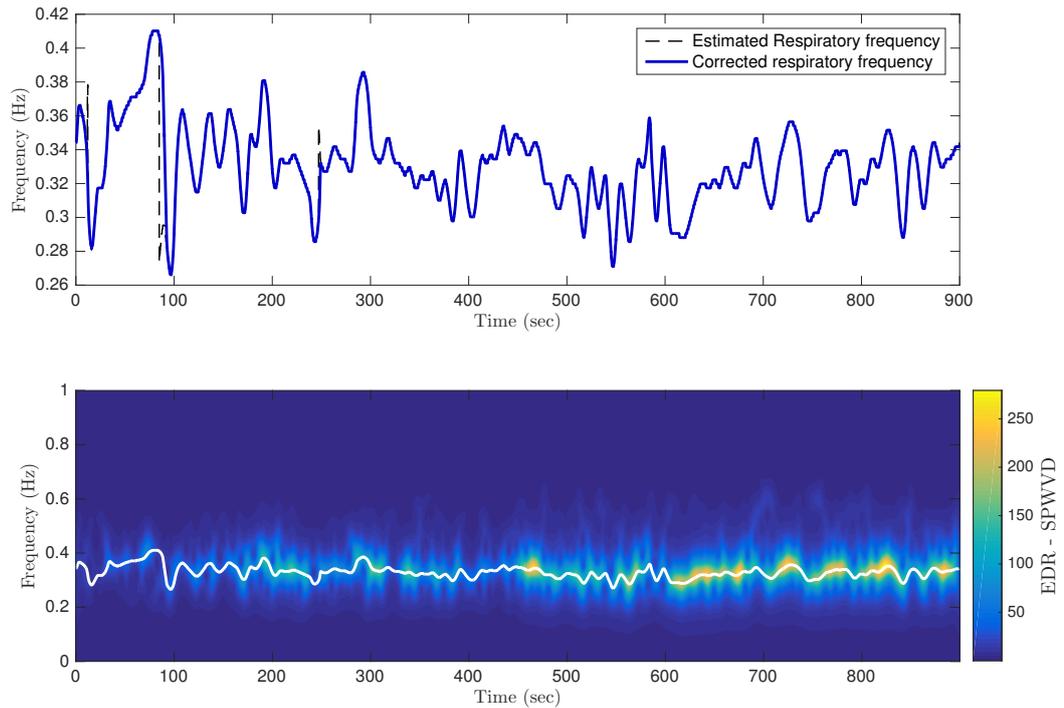
Figure 6.3: Top: example of estimated $\hat{f}(t)$ and corrected $f_r(t)$ instantaneous respiratory frequencies represented in dashed black line and blue solid line respectively. Bottom: SP-WVD spectral power of an estimated EDR series, together with its corrected instantaneous respiratory frequency, $f_r(t)$, (white solid line).

6.2.2.4. Spectral heart rate variability analysis

Classical spectral HRV parameters were estimated for each patient by an autoregressive model based on the Burg method (BURG, 1975) and the Broersen's combined information criterion (BROERSEN, 2000) to optimize model orders.

Total power (*TP*) was calculated as the sum of the four spectral bands: ultra-low frequency (*ULF*: 0-0.003 Hz), very-low frequency (*VLF*: 0.003-0.04 Hz), low frequency (*LF*: 0.04-0.15 Hz) and high frequency (*HF*: 0.15-0.4 Hz). The *HF* component reflects the parasympathetic activity, whereas the *LF* component is modulated by both sympathetic and parasympathetic autonomic contributions (CAMM et al., 1996; ECKBERG, 1997; MALLIANI et al., 1994, 1991; ORI et al., 1992). They were calculated as the average of 5-minute

intervals and normalized by subtracting the *VLF* component from the TP in order to
reduce the effect of noise artifacts:

$$LF_{nu} = \frac{LF}{VLF - TP} \tag{6.5}$$

$$HF_{nu} = \frac{HF}{VLF - TP} \tag{6.6}$$

Moreover, the *LF/HF* ratio was calculated to account for global sympathovagal balance.

6.2.2.5.   Detrended fluctuation analysis

A number of non-linear HRV parameters have been proposed in the literature to
characterize heart rate dynamics that may not be captured by classical linear methods.
Detrended fluctuation analysis (DFA) describes the fractal or self-similarity properties of
RR series by calculating their mean fluctuations for each time scale (Goldberger et al.,
2002; Iyengar et al., 1996; Peng et al., 1995).

When a fractal scaling exponent (α) is close to 0.5 it corresponds to a randomly
changing signal across time scales, whereas an exponent of around 1.5 is related to a
strongly correlated time series. Thus, a signal neither strictly regular nor completely
random would have a scaling exponent of 1, displaying intrinsic fractal-like dynamics.
Short- and long-term scaling exponents (α_1 and α_2) were calculated by analyzing 4-11 and
12-20 beats, respectively, as in (Stein et al., 2005).

6.2.2.6.   Sample entropy

In order to quantify RR series complexity or irregularity, the sample entropy ($SampEn$)
approach was applied. It is a refined version of the traditionally used irregularity measure
Approximate Entropy ($ApEn$) (Richman JS, 2000) and it is defined as the conditional
probability that two sequences of m consecutive data points which are similar to each
other (with a tolerance r) will remain similar when one more consecutive point is included.
Large values of $SampEn$ indicate high irregularity and great complexity, whereas smaller
values refer to a more regular and predictable signal, commonly associated with disease
(Khandoker AH, 2009; M et al., 2008; V et al., 8). Based on (DE et al., 2002), the
embedding dimension was chosen as $m = 3$ and the tolerance distance as $r = 0.2 \cdot SD$.

Highuchi's fractal dimension

Similarly, the Higuchi's fractal dimension (HFD) algorithm (Higuchi, 1988) quantifies
RR series complexity by measuring the mean length of the curve $L(k)$.

From a given time series of N points, $X = x(1), x(2), \ldots, x(N)$, k new time series are
constructed as follows:

$$X_m^k = \left\{ x(m), x(m + k), x(m + 2k), \ldots, x\left(m + int\left[\frac{N - m}{k}\right] k\right) \right\}, \tag{6.7}$$

where $m = 1, 2, \ldots, k$ is the initial time value and k is the discrete time interval between points.

Then, the length $L_m(k)$ of the new sequences is computed as:

$$L_m(k) = \frac{\left\{ \left(\sum_{i=1}^{int[(N-m)/k]} |x(m+ik) - x(m + [i-1]k)| \right) \frac{N-1}{int[(N-m)/k]k} \right\}}{k} \tag{6.8}$$

The length of the curve for the time interval k, $L(k)$, is an average over k sets of $L_m(k)$:

$$L(k) = \frac{1}{k} \sum_{m=1}^{k} L_m(k), k = 1, 2, \ldots, k_{max} \tag{6.9}$$

Finally, the curve is fractal-like with dimension D if $L(k)$ is proportional to k^{-D}. Thus, by means of a least-squares linear best-fitting procedure applied to the graph $L(k)$ vs. k on a bi-logarithmic scale, D is computed as the slope of the line fitting $\{ln(1/k); ln(L(k))\}$. As in (MAGRANS et al., 2013), HFD was calculated as the average of the D values obtained in the range of $25 \leq k_{max} \leq 70$.

6.2.3. Statistical analysis

Comparisons between responders and non-responders for each autonomic parameter were evaluated by Mann-Whitney U non-parametric tests. The level of significance was set at $p < 0.05$.

A leave-one-out cross-validation was applied in order to overcome the limited sample of patients and avoid overfitting. This method selects one subject as validation data and the remaining 22 patients as training data. The process is repeated 23 times and the performance of each parameter, in order to distinguish between responders and non-responders, is quantified as the mean AUC (Area Under the ROC Curve) of the 23 evaluations.

6.3. Results

6.3.1. Heart rate variability

Figure 6.4 A, B and C, show quantitative results for the classical spectral HRV parameters. Statistically significant increases were observed in HF_{nu} from two different responder groups (apnea-hypopnea, AHR, and hypopnea, HR) vs non-responders (NR), whereas the apnea responder (AR) group did not show any significant difference when compared to non-responders (NR). Moreover, no statistically significant differences were observed when comparing any group of responders with respect to non-responders for both LF_{nu} and LF/HF.

Since the HF band contains the respiration effect modulated by the vagal tone, HF_{nu} captures both the contribution of the ANS itself and respiration, not allowing to distinguish

variations coming from each factor separately. However, since mean respiratory frequency did not show statistically significant differences among the analyzed groups (see table 6.1), HRV results suggest that differences found in the HF_{nu} of responder and non-responder patients may be mainly due to alterations in the underlying ANS function of non-responders.

Table 6.1: Mean $\pm$ standard deviation [Hz] of the mean respiratory frequency for all groups: Non-responders (NR), apnea responders (AR), hypopnea responders (HR) and all responders (AHR). Statistical analysis was performed by a Mann-Whitney U test comparing each responder group with non-responders.

	NR	AR	HR	AHR
Mean respiratory frequency (Hz)	0.32 ± 0.03	0.31 ± 0.03	0.30 ± 0.05	0.32 ± 0.04
p-value	$-$	0.3939	0.4286	0.8182

6.3.2. Heart rate complexity

Figure 6.4 D, E and F, display the statistically significant differences found in HRC parameters when comparing responder groups with non-responders. Concerning α_1, non-responders presented higher values related to a more correlated pattern of RR series with respect to responder patients; whereas $SampEn$ and HFD showed a statistically significant increase in complexity for responders with respect to non-responders.

6.3.3. Leave-one-out cross-validation

Table 6.2 summarizes the mean and standard deviation of the AUC obtained for each parameter and group. Moreover, Figure 6.5 shows the resulting ROC curves for the results obtained in HRV and HRC analysis for each responder group.

Table 6.2: Mean $\pm$ standard deviation of the AUC resulting from leave-one-out analysis for each statistically significant responder group with respect to non-responders

	HF_{nu}	α_1	$SampEn$	HFD
All Responders	0.80 ± 0.03	0.78 ± 0.04	0.92 ± 0.01	0.83 ± 0.03
Apnea Responders	0.76 ± 0.03	0.75 ± 0.04	0.89 ± 0.02	0.81 ± 0.04
Hypopnea Responders	0.83 ± 0.03	0.83 ± 0.04	1.00 ± 0.00	0.88 ± 0.03

6.4.   Discussion

In this chapter we retrospectively analyzed data from the HYPNOS trial to investigate if there were differences in the ANS function between SAS patients classified as responders and non-responders to kinesthetic stimulation therapy in terms of reduction in apnea/hypopnea event durations.
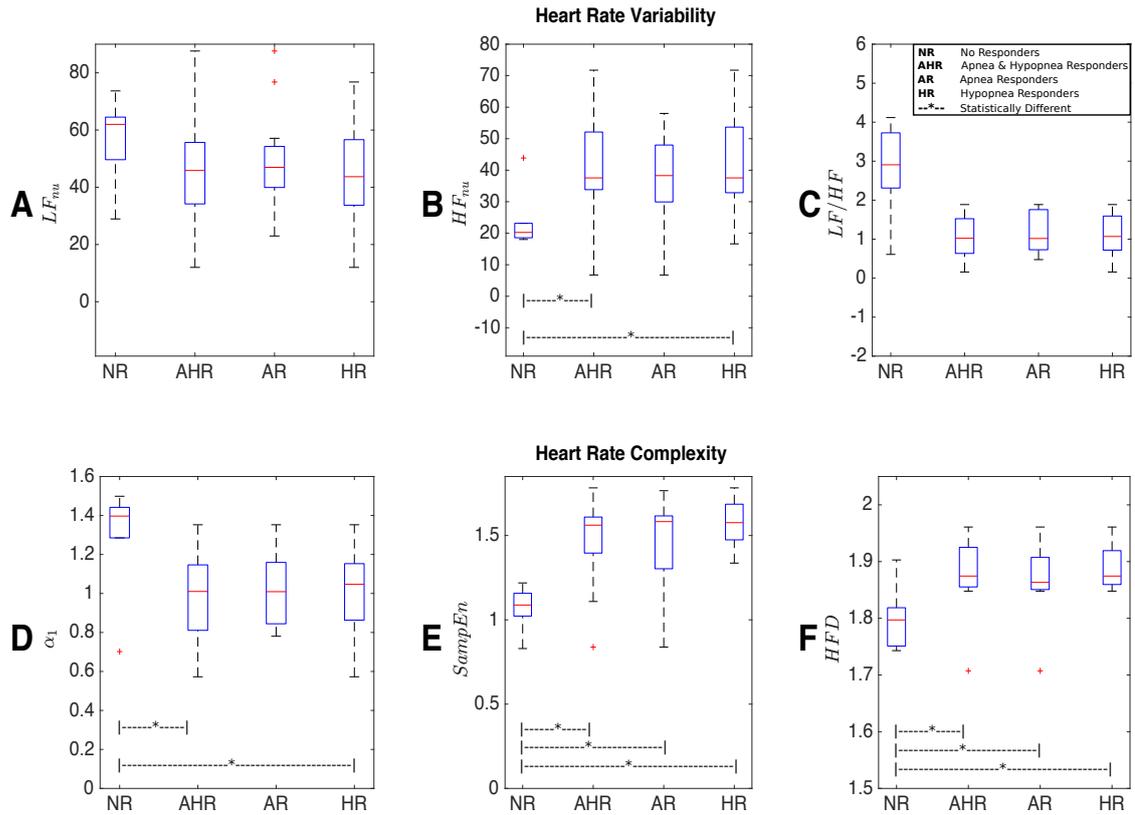
Figure 6.4: Boxplots resulting from heart rate variability and heart rate complexity analysis: A) Normalized LF (LF_{nu}), B) Normalized HF (HF_{nu}), C) LF/HF ratio, D) Short-term fractal scaling exponent (α_1), E) Sample Entropy ($SampEn$) and F) Higuchi's Fractal Dimension (HFD). Analyzed groups are divided as non-responders (NR), apnea & hypopnea responders (AHR), apnea responders (AH) and hypopnea responders (HR). Statistically significant differences are represented by black dashed lines.

Regarding HRV results, a statistically significant reduction in HF_{nu} was noted in non-responder patients in relation to most responder groups. Since the analyzed time window included the first 15 minutes after sleep onset, this greater vagal modulation, according to HF_{nu}, found in responder patients may be related to a healthier ANS condition (TRINDER et al., 2001), suggesting an increased autonomic sensitivity during vagal predominance in those patients responding to therapy.

Concerning HRC results, a statistically significant increase in α_1 was noted in non-responder patients with respect to most responder groups, indicating that non-responders present a more correlated RR series than the fractal-like dynamics associated with healthy subjects. Moreover, non-responder patients showed a statistically significant reduction in cardiac complexity, according to $SampEn$ and HFD, when compared to any responder group.

Given that the ANS is controlled by complex interactions that allow the organism to adapt to certain physiological conditions, such as metabolic variations or disease(GOLDBERGER et al., 2002), a complexity reduction in biological controlling systems
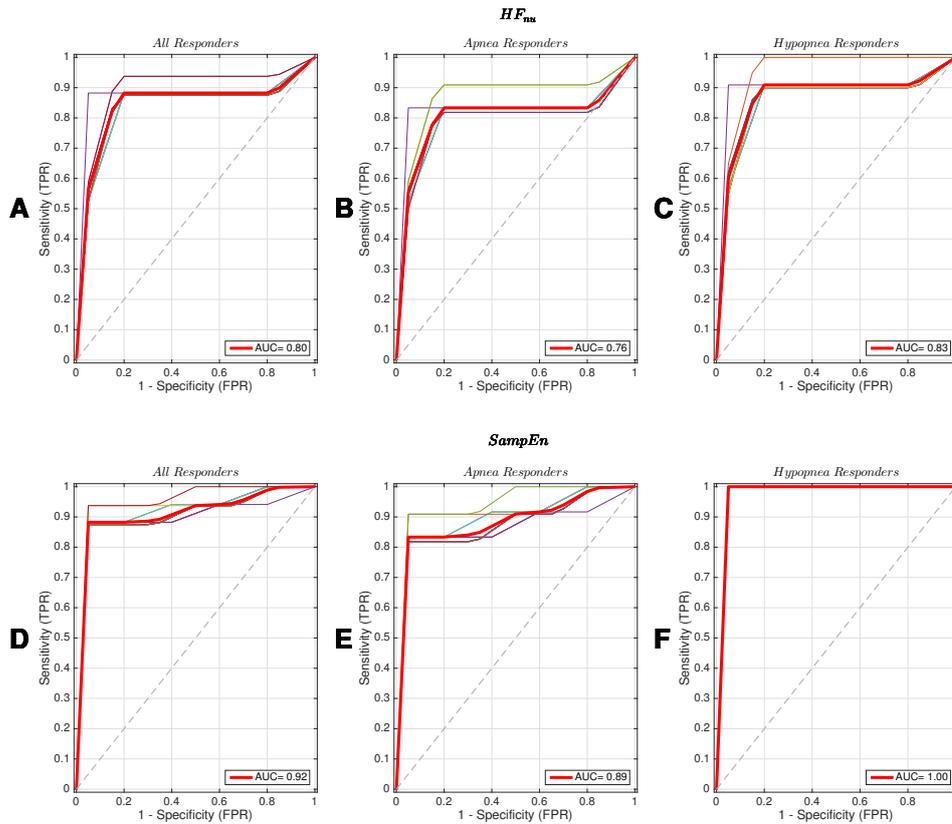
Figure 6.5: Mean ROC curves of HF_{nu} and $SampEn$. These parameters led to the highest mean AUC values among the analyzed HRV and HRC markers. A and D present the results from the all responders group, B and E show results for the apnea responders group and C and F illustrate the results from hypopnea responders group.

reflects the decrease of the organism adaptability that is generally associated with age and/or diseases. Thus, the results suggest an autonomic adaptability reduction in non-responders that may be influenced by deleterious consequences associated with the repeated acute cardiorespiratory responses induced by apnea or hypopnea events in the long term (Somers et al., 2008; Stansbury et al., 2015).

Although it is well known that the total power in the HF band is closely related to respiratory sinus arrhythmia, according to the results presented in section 6.3.1, HF_{nu} results suggest that differences found between responder and non-responder patients are predominantly due to alterations in parasympathetic activity.

Overall, the obtained results suggest that a key mechanism underlying the effectiveness of this novel therapy is the presence of a functional ANS. Therefore, the lack of response to therapy described in chapter 5 may be due to an inappropriate patient selection that should have included a complete HRV and HRC analysis.

Regarding leave-one-out cross-validation findings, HFD and $SampEn$ turned out to be the best performing parameters for distinguishing between non-responders and any

responder group of patients, with a mean AUC for the three performed comparisons of 0.84 and 0.94, respectively. Therefore, future developments should be focused on the description of predictive models based on the combination of HRV and HRC parameters, in order to identify appropriate candidates that may benefit from kinesthetic stimulation therapy.

6.5. Conclusion

In this study, we analyzed several HRV and HRC parameters on a group of SAS patients, classified as responders and non-responders to kinesthetic stimulation therapy, in order to compare their autonomic response during sleep onset. Statistically significant differences were found in HF_{nu}, α_1, $SampEn$ and HFD, suggesting a decreased vagal modulation and cardiac adaptability in those patients not responding to therapy. Although the present work is based on a small population of 23 SAS patients and, thus, conclusions on predictors of therapeutic effectiveness cannot be extracted, the results indicate important trends that could improve the identification of patients eligible for kinesthetic stimulation therapy which represents a major contribution for the implementation of this therapy in a clinical context.

References

BAILÓN, R., L. SORNMO, and P. LAGUNA (2006). "A robust method for ECG-based estimation of the respiratory frequency during stress testing". In: *IEEE transactions on biomedical engineering* 53.7, pp. 1273–1285.

BROERSEN, P. (2000). "Finite sample criteria for autoregressive order selection". In: *Signal Processing, IEEE Transactions on* 48.12, pp. 3550–3558. ISSN: 1053-587X. DOI: `10.1109/78.887047`.

BURG, J. P. (1975). "Maximum Entropy Spectral Analysis". PhD thesis. Stanford, CA 94305: Stanford University.

CALVO GONZÁLEZ, M. (2017). "Analysis of the cardiovascular response to autonomic nervous system modulation in Brugada syndrome patients". PhD thesis. Rennes 1.

CALVO, M., V. LE ROLLE, D. ROMERO, N. BÉHAR, P. GOMIS, P. MABO, and A. HERNÁNDEZ (2017). "Time-frequency analysis of the autonomic response to head-up tilt testing in Brugada syndrome". In: *Computing in Cardiology Conference (CinC), 2017*. IEEE.

— (2018). "Sex-specific analysis of the cardiovascular function". In: ed. by P. KERKHOF and V. MILLER. 1st. Springer International Publishing. Chap. 7b. Gender differences in the autonimic response to exercise testing in Brugada syndrome.

CAMM, A., M. MALIK, J. BIGGER, G. BREITHARDT, S. CERUTTI, R. COHEN, P. COUMEL, E. FALLEN, H. KENNEDY, R. KLEIGER, et al. (1996). "Heart rate variability: standards of measurement, physiological interpretation and clinical use. Task Force of the European

Society of Cardiology and the North American Society of Pacing and Electrophysiology". In: *Circulation* 93.5, pp. 1043–1065.

Costa, A. H. and G. Boudreau-Bartels (1995). "Design of time-frequency representations using a multiform, tiltable exponential kernel". In: *IEEE Transactions on Signal Processing* 43.10, pp. 2283–2301.

DE, L., R. JS, G. MP, and M. JR (2002). "Sample entropy analysis of neonatal heart rate variability". In: *American Journal of Physiology - Regulatory, Integrative and Comparative Physiology* 283.3, R789–R797.

Dumont, J., A. I. Hernandez, and G. Carrault (2010). "Improving ECG beats delineation with an evolutionary optimization process". In: *IEEE Transactions on Biomedical Engineering* 57.3, pp. 607–615.

Eckberg, D. L. (1997). "Sympathovagal Balance: A Critical Appraisal". In: *Circulation* 96.9, pp. 3224–3232. DOI: `10.1161/01.CIR.96.9.3224`.

Goldberger, A. L., L. A. Amaral, J. M. Hausdorff, P. C. Ivanov, C.-K. Peng, and H. E. Stanley (2002). "Fractal dynamics in physiology: alterations with disease and aging". In: *Proceedings of the National Academy of Sciences* 99.suppl 1, pp. 2466–2472.

Higuchi, T. (1988). "Approach to an irregular time series on the basis of the fractal theory". In: *Physica D: Nonlinear Phenomena* 31.2, pp. 277–283.

Hlawatsch, F. and G. F. Boudreaux-Bartels (1992). "Linear and quadratic time-frequency signal representations". In: *IEEE signal processing magazine* 9.2, pp. 21–67.

Iyengar, N., C. Peng, R. Morin, A. L. Goldberger, and L. A. Lipsitz (1996). "Age-related alterations in the fractal scaling of cardiac interbeat interval dynamics". In: *American Journal of Physiology-Regulatory Integrative and Comparative Physiology* 40.4, R1078.

Khandoker AH Jelinek HF, P. M. (2009). "dentifying diabetic patients with cardiac autonomic neuropathy by heart rate complexity analysis". In: *BioMedical Engineering OnLine* 8.1, p. 3.

M, J., T. Z, T. I, J. J, J. K, and B. M (2008). "Short-term heart rate complexity is reduced in patients with type 1 diabetes mellitus". In: *Clinical Neurophysiology* 119.5, pp. 1071–1081.

Magrans, R., P. Gomis, P. Caminal, and A. Voss (2013). "Higuchi's fractal complexity of RR and QT interval series during transient myocardial ischemia". In: *Computing in Cardiology Conference (CinC), 2013*. IEEE, pp. 421–424.

Malliani, A., F. Lombardi, and M. Pagani (1994). "Power spectrum analysis of heart rate variability: a tool to explore neural regulatory mechanisms." In: *British Heart Journal* 71.1, pp. 1–2.

Malliani, A., M. Pagani, F. Lombardi, and S. Cerutti (1991). "Cardiovascular neural regulation explored in the frequency domain." In: *Circulation* 84.2, pp. 482–92. DOI: `10.1161/01.CIR.84.2.482`. eprint: `http://circ.ahajournals.org/content/84/2/482.full.pdf+html`.

Moody, G. B., R. G. Mark, M. A. Bump, J. S. Weinstein, A. D. Berman, J. E. Mietus, and A. L. Goldberger (1986). "Clinical validation of the ECG-derived respiration (EDR) technique". In: *Group* 1.3.

Ogilvie, R. D., R. T. Wilkinson, and S. Allison (1989). "The detection of sleep onset: behavioral, physiological, and subjective convergence." In: *Sleep: Journal of Sleep Research & Sleep Medicine.*

Ori, Z., G. Monir, J. Weiss, X. Sayhouni, and D. Singer (1992). "Heart rate variability. Frequency domain analysis." In: *Cardiology clinics* 10.3, pp. 499–537.

Peng, C.-K., S. Havlin, H. E. Stanley, and A. L. Goldberger (1995). "Quantification of scaling exponents and crossover phenomena in nonstationary heartbeat time series". In: *Chaos: An Interdisciplinary Journal of Nonlinear Science* 5.1, pp. 82–87.

Richman JS, M. J. (2000). "Physiological time-series analysis using approximate entropy and sample entropy". In: *American Journal of Physiology - Heart and Circulatory Physiology* 278.6, H2039–H2049.

Sleep Disorders Centers, A. of and A. for Psycho- physiological Study of Sleep (1979). "Glossary of terms used in the sleep disorder classification". In: *Sleep* 2, pp. 123–129.

Somers, V. K., D. P. White, R. Amin, W. T. Abraham, F. Costa, A. Culebras, S. Daniels, J. S. Floras, C. E. Hunt, L. J. Olson, et al. (2008). "Sleep apnea and cardiovascular disease: An American heart association/American college of cardiology foundation scientific statement from the American heart association council for high blood pressure research professional education committee, council on clinical cardiology, stroke council, and council on cardiovascular nursing in collaboration with the national heart, lung, and blood institute national center on sleep disorders research (national institutes of health)". In: *Journal of the American College of Cardiology* 52.8, pp. 686–717.

Stansbury, R. C. and P. J. Strollo (2015). "Clinical manifestations of sleep apnea". In: *Journal of thoracic disease* 7.9, E298.

Stein, P. K., P. P. Domitrovich, N. Hui, P. Rautaharju, and J. Gottdiener (2005). "Sometimes higher heart rate variability is not better heart rate variability: results of graphical and nonlinear analyses". In: *Journal of cardiovascular electrophysiology* 16.9, pp. 954–959.

Trinder, J., J. Kleiman, M. Carrington, S. Smith, S. Breen, N. Tan, and Y. Kim (2001). "Autonomic activity during human sleep as a function of time and sleep stage". In: *Journal of sleep research* 10.4, pp. 253–264.

V, T., N. S, B. T, and U. A (8). "Decrease in the heart rate complexity prior to the onset of atrial fibrillation". In: *Europace* 6.398–402.

Closed-loop Kinesthetic Stimulation for the Treatment of Sleep Apnea Syndromes

This chapter presents the preliminary results obtained from the second study phase of the PASITHEA project (EKINOX study), regarding the validation of a novel closed-loop control algorithm for adaptive patient-specific kinesthetic stimulation therapy for the treatment of sleep apnea syndromes. In the first part, we will present a brief introduction and the methods that have been developed for the validation of the previously mentioned controller. In section 7.3, we describe the results obtained from the analyses, and in sections 7.4 and 7.5, a discussion of the outcomes and a conclusion is presented. The content of this chapter is based on the related publication (PÉREZ et al., 2016).

7.1. Introduction and hypothesis

In previous chapters, we presented our novel system (PASITHEA) for real-time monitoring and treatment of SAS, based on an adaptive kinesthetic stimulation integrating an on-off controller. This system triggers a mechanical stimulation applied to the skin of the patient when apnea or hypopnea events are detected by an automatic, real-time respiratory detector. In chapter 4, we described the three elements that compose the system: i) a modified cardiorespiratory ambulatory recorder (Holter) for real-time acquisition, recording and wireless transmission of two electrocardiogram (ECG) channels, nasal pressure (NP) and blood oxygen saturation (SaO_2) during a whole night; ii) a kinesthetic stimulation system and iii) a real-time control application for triggering kinesthetic stimulation, running into a standard computer. Chapter 4 and 5 also described that the first evaluation (HYPNOS study) was based on an "on-off" control algorithm, which triggers the kinesthetic stimulation as a function of respiratory event detections. Moreover, the

stimulation parameters (amplitude, burst duration, silent interval, maximum number of bursts) were empirically fixed for all patients. Results in chapter 5, showed that the patients who responded to therapy presented a reduced duration of respiratory events and an attenuation of the consequent hypoxia events and acute cardiorespiratory responses during the periods in which the therapy was active. However, not all patients responded correctly to the therapy. One approach to minimize this non-responder rate is to optimize patient selection to the therapy, which was the objective of chapter 6. Another, complementary approach is to optimize therapy delivery. Indeed, as previously mentioned, part of the lack of response may be imputed to the dynamic properties of the mechanical coupling of the actuator, movement of the patient and the fact that different stimulation amplitudes may be necessary for different patients, and even for the same patient, during the night. Therefore, we hypothesize that we can optimize therapy delivery by the integration of a closed-loop control, capable to adapt and personalize stimulation parameters. In this section, we propose the integration of such real-time closed-loop control method, as an improvement of the original system. Description of the improvements developed for the elements of the PASITHEA system, along with preliminary results based on data acquired from a new clinical evaluation protocol (EKINOx protocol), specifically designed for the new version of the system are also presented.

7.2. Methodology

7.2.1. Methodological and technical improvements of the PASITHEA system

As previously described in chapter 4, we implemented a real time apnea/hypopnea detector which takes as input the raw signal from a nasal pressure transducer embedded into a cardiorespiratory Holter (Spider SAS, Sorin CRM, France). After conclusion of the first clinical evaluation of the PASITHEA project (HYPNOS study), one of our main hypothesis for the improvement of the patient responsiveness rate to therapy, was to implement a new optimized version of the respiratory event detector capable of detect even more precociously the respiratory events in order to avoid the physiological consequences related to long exposure to a respiratory events (see chapter 5). Section 7.2.1.1 describes the improvements performed on the detector.

Another possibility for optimization concerns the closed-loop control method. Although the on-off method presented in previous chapters have shown interesting and promising results, we believe that an improvement of patients response could be obtained by a fully adaptive closed-loop method. This new closed-loop method is described in section 7.2.2.

The above mentioned improvements on the system required new developments on the actuator hardware, on the real-time control application (for the integration of the new detector and the new control method) and on the firmware of the stimulator. These technological improvements are presented in sections 7.2.1.2 and 7.2.1.3.

7.2.1.1. Apnea/hypopnea detector optimization

We propose two significant improvements to the detector: i) an inclusion of a new algorithm for noise detection and ii) an optimization of the detector's parameters with evolutionary optimization algorithms (EA) in order to reduce the detection delay while maximizing the general performance.

In this sense, a detection of noise or absence of signal is performed on a smoothed low-pass filtered nasal pressure (NP) signal after certain user-configured initialization time. If there is no signal (for example, cannula is not connected to the patient or the patient is breathing from the mouth) then the signal energy will be low for a prolonged period of time. The absence of signal is detected if the signal is flat (i.e. below the positive cycle detection threshold) for too long. Note that this verification can only be done on the pre-processed signal which is smoothed and centered. Therefore this detector of signal absence has one data point delay. If a flat signal is confirmed, any on-going apnea is ended, calculations of thresholds are postponed and there is no further cycle detection or apnea/hypopnea detection. Figure 7.1 shows a diagram of the previously mentioned cycle detection function. A complete description of the first version of this respiratory detector including this cycle detector can be found in (FEUERSTEIN et al., 2015).

Alternatively, if there are abnormal shifts in the baseline of the signal, they may cause erroneous detection of the respiratory cycles and of the thresholds for inhalation and exhalation. This baseline shift detector is not active when the respiration state is in apnea. When active, the detector assesses the baseline of a short portion of signal and compares the spread of the current short term baseline to a long portion of the signal that represents the correct signal baseline. If the spread is too high, then it is likely to be due to abnormal baseline shifts and it is thus declared as noise. Accordingly, if noise is declared, the current data point is not taken into account neither for the long-term baseline calculation nor in the reference signal for centering the signal around zero. In addition, any on-going hypopnea is ended, calculations of thresholds are postponed and there is no further cycle detection or apnea/hypopnea detection.

On the other hand, an optimization of the detector's parameters implementing evolutionary algorithms (EA) in order to reduce the detection delay and the general performance was also performed. Based on a sensitivity analysis of the first version of the respiratory detector (FEUERSTEIN et al., 2015), a reduced group of parameters were selected for optimization:

1. DurationFlatMin: Minimum duration of flat signal to confirm the duration of an apnea.

2. DurationFlatMax: Maximum duration of flat signal to confirm the duration of an apnea.

3. Earlytime: Early time point for the detection of apnea since the last inspiration (before the usual 10 seconds)
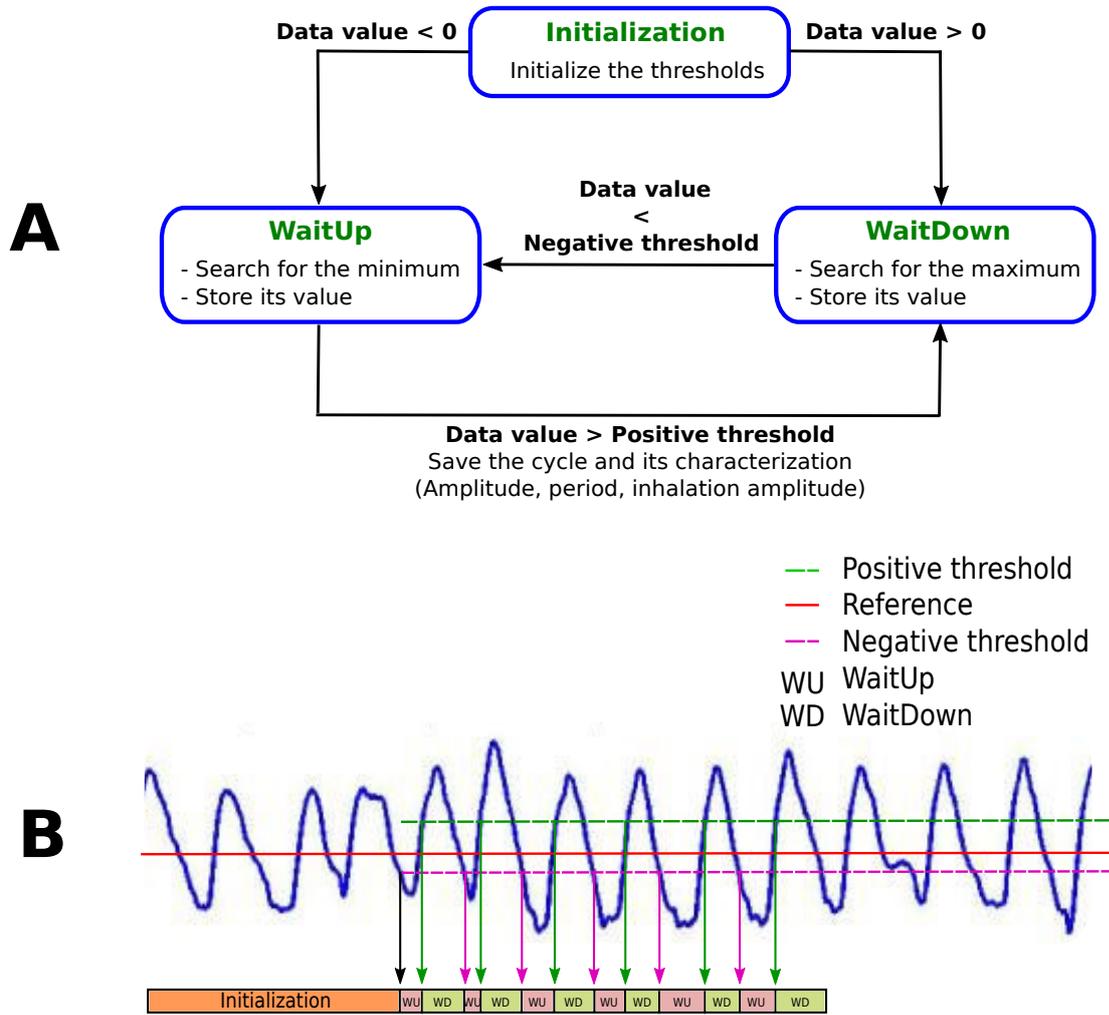
Figure 7.1: Functioning diagram of the cycle detector. A) Machine state for the cycle detection function and B) example of cycle detection.

4. Hypduration: The early time point for the detection of hypopnea since the drop of inhalation amplitude (before the usual 10 seconds).

The EA process was computed by comparing detection signals with respect to the experimental detection signal reconstructed from clinical annotations acquired during the HYPNOS study, through the minimization of the error function ϵ, defined as:

$$\epsilon(\theta) = \sum_{i=1}^{N} \left| \frac{Y_{det,\theta}(i) - Y_{exp}(i)}{max(Y_{exp}(i))} \right|^2 \tag{7.1}$$

$Y_{exp}(i)$ and $Y_{det,\theta}(i)$ are the ith experimental value and the ith detection output sample for the detection of Y when using the set of parameters θ, respectively. Moreover, N indicates the number of samples for each output being compared and Y refers to respiratory event detection signal for the whole night.

As in previous works of our team (LE ROLLE et al., 2015, 2011; OJEDA et al., 2014), the best set of parameters for each subject were identified through an approach based on evolutionary algorithms (EA). These stochastic search methods are founded on theories of natural evolution, such as selection, crossover and mutation (GOLDBERG et al., 1988). Being an individual an optimization solution (a parameter value set), the algorithm started with the initialization of 30 random individuals, each parameter value of the individual being randomly selected from a specified parameter space. By quantifying each individual fitness through the error function ϵ, the population was continuously evolved for at least 20 generations, following four main steps:

1. Selection of parent individuals for combination, biased towards those having the best errors.

2. According to a probability p_c, combination of parent individuals through crossover to generate new children. Then, with a probability p_m, modification of these individuals by mutations.

3. Fitness assessment in new individuals.

4. Replacement of individuals having the lowest fitness.

Figure 7.2 shows a flow diagram of a simple EA following the above mentioned steps.
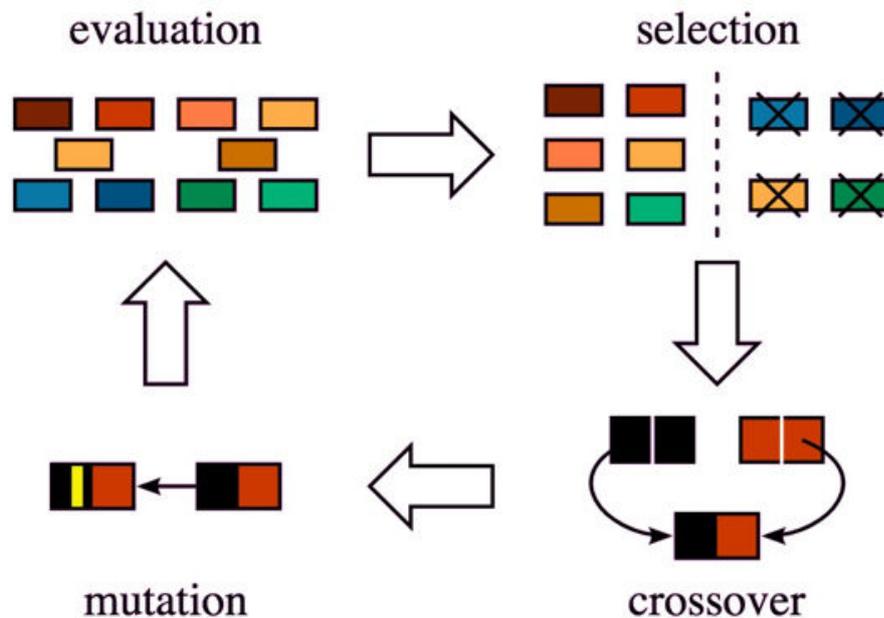
Figure 7.2: Flow diagram of a simple evolutionary algorithm in one generation. Adapted figure from (CHENG et al., 2015).

7.2.1.2. Kinesthetic stimulation device

In the context of this therapy, another sensitive aspect to be taken into account for patient responsiveness is the fact that problems affecting the coupling interface between the stimulator and the skin of the patient are of significant concern for vibratory kinesthetic stimulation. Furthermore, body position during sleep may also affect the mechanical coupling between the stimulator and the skin of the patient and therefore alter the effectiveness of the kinesthetic stimulation. For this reason, a modification of the PASITHEA's kinesthetic stimulation device was also made in order to allow future estimation of the mechanical coupling with the inclusion of a 3-axis accelerometer (Analog devices, ADXL335) attached to the actuator.

In addition, the firmware on the device was also modified in order to alter the behavior of the buttons and adding a new feature that allow the patient to stop the therapy for a certain period of time, letting a time window without stimulation that let the patient sleep.

7.2.1.3. Real-time control application

The new control application, illustrated in figure 7.3, is based on the first version developed for the HYPNOS study. This new version, like the previous one, is in charge of: i) establishing wireless communication links with the cardiorespiratory Holter and the stimulator, ii) receiving data from the holter, iii) performing real-time signal processing on the received signals for the detection of apnea or hypopnea episodes and iv) according to the detector's output, apply the proposed controller and send the appropriate command to the kinesthetic stimulator through a BT link.

The main differences between versions are: the adaptation of the new application to be used with the new controller described in the next section 7.2.2, the inclusion of the optimized version of the respiratory event detector (see 7.2.1.1), the inclusion of a real-time QRS detector developed by our team (DOYEN, 2018), new real-time signal processing features for the input signals (acquired from the Holter) and several performance, behavior and appearance modifications.

7.2.2. Coupled PD controller for adaptive kinesthetic stimulation

As described in chapter 3, concerning SAS, several structural and functional determinants of an anatomical predisposition for airway closure differ among patients. Therefore, patient-specific therapies are needed. In chapter 4, a novel therapy for the treatment of SAS with the inclusion of an optimal on-off controller, where the stimulation parameters were fixed, was introduced. Although it showed encouraging results, a 25% rate of non-response was observed (see chapter 5). We hypothesized that the therapy could be optimized by adapting the stimulation parameters in order to personalize the stimulation for each patient. Moreover, the inclusion of additional control variables could provide more information regarding the response of the patient to therapy, allowing a better estimation of the optimal
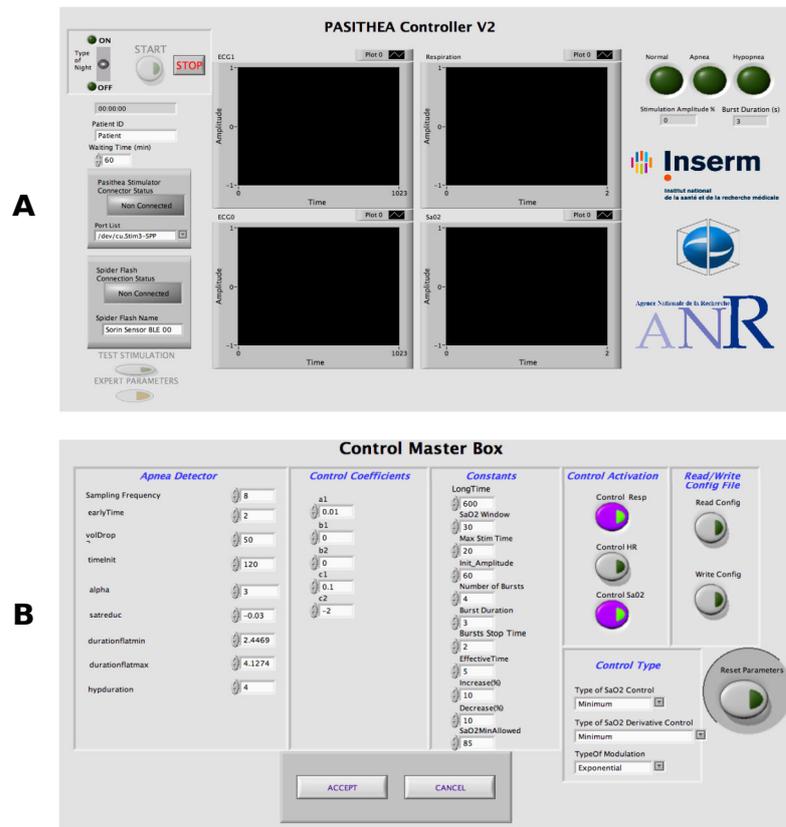
Figure 7.3: Second version of the real-time application for data acquisition, processing and control. A) Left side of the screen of the application: user-defined configuration parameters and BT connection with the Holter and the stimulator along with configuration and test buttons. Central part of the screen of the application: 4 screens showing real-time acquired data: 2 ECG channels (top), nasal pressure (bottom left), SaO_2 (bottom right). Right side of the screen of the application: Output of the real-time respiratory event detector (normal, apnea or hypopnea) and characteristics of the stimulation. B) Configuration window view for customize all the different set of parameters to be used by the adaptive controller and the respiratory event detector.

stimulation to be delivered by the system. Based on the analyses performed during this PhD research, SaO_2 and HR seem to be suitable markers for the characterization of patient response. Thus, these markers were incorporated in a novel closed-loop control system, integrating concurrent, coupled proportional-derivative (PD) controllers in order to manage the kinesthetic stimulation amplitude delivered to the patient by the therapeutic system. The control system is composed of three main modules operating in real-time: i) a signal processing module, ii) control activation and iii) the coupled PD controller.

The signal processing module performs data processing on input signals which are: i) the NP signal, ii) one ECG lead and iii) the SaO_2 signal. QRS detection is performed on the ECG signal and the instantaneous heart rate (HR), as well as the ΔHR signal are derived. The SaO_2 signal is delayed and low-pass filtered ($FSaO_2$), to then calculate its derivative. This pre-processing is applied in order to compensate for the fact that

the consequences of respiratory events on the SaO_2 signal are observed after a certain physiological delay (see chapter 5). The NP signal is processed by an optimized version of the real-time apnea/hypopnea detector presented in section 7.2.1.1 which has three possible outputs: no apnea/hypopnea detected, apnea detected and hypopnea detected.

The control activation module enables the coupled PD controller module when it receives as input an apnea or hypopnea detection and will disable it in case of a return to normal respiration. In this sense, the new controller proposed in this chapter is an improvement of an on-off controller, allowing for more complex, adaptive adjustment of the stimulation amplitude with respect to the acute physiological responses of the patient.

Five control variables are presented as input to the coupled PD controller: i) the event duration signal (TResp) which represents the time spent from the detection instant of the current event to the current time instant, ii) ΔHR, iii) $\dfrac{\partial \Delta HR}{\partial t}$, iv) $FSaO_2$ signal and v) $\dfrac{\partial FSaO_2}{\partial t}$.

The coupled PD controller module synthesizes a signal, with an amplitude modulated by the controller's output, that will be used to drive the kinesthetic actuator. This modulated amplitude has a percentage range between 0% and 100%, which is translated by the system to the specific input signal value to generate the equivalent acceleration delivered by the actuator (100% amplitude (2V RMS) typically corresponds to a normalized acceleration of 13.7 m/s^2). In addition, the synthesized signal is delivered in a burst sequence of 4 bursts with a fixed stimulation duration of 3 seconds followed by a silent period of 2 seconds. Figure 7.4 shows an example of a stimulated event, implementing this control algorithm.

7.2.3.   Closed-loop algorithm

Figure 7.5 shows a diagram of the closed-loop control algorithm. The loop is executed in real-time and all the variables are constantly calculated. The time passed since the beginning of the application is stored in variable t while the event number for each detection is stored in $e(e = 1, 2, ..., N)$, where N is the total number of respiratory events during the whole night. The beginning, t_e^{start} and end t_e^{end} of each respiratory event e are also available variables. When an event detection e arrives, the amplitude of the stimulation burst at each time instant ($A(t, e)$) is obtained by the following equations:

$$A(t + 1, e) = A(t, e) + a_1 TResp(t, e) + b_1 \Delta HR(t, e) + b_2 \frac{\partial \Delta HR(t, e)}{\partial t}$$
$$+ c_1 (100 - FSa0_2(t, e)) + c_2 \frac{\partial FSa0_2(t, e)}{\partial (t)} \quad (7.2)$$

$$A(t_{e+1}^{start}) \quad = \quad f_1 \quad = \quad \begin{cases} A(t_e^{end}) - A(t_e^{end}) * 0.1 & \text{if } TResp(t_e^{end}) < 9 \\ A(t_e^{end}) + A(t_e^{end}) * 0.1 & \text{if } TResp(t_e^{end}) \geq 9 \end{cases} \quad (7.3)$$
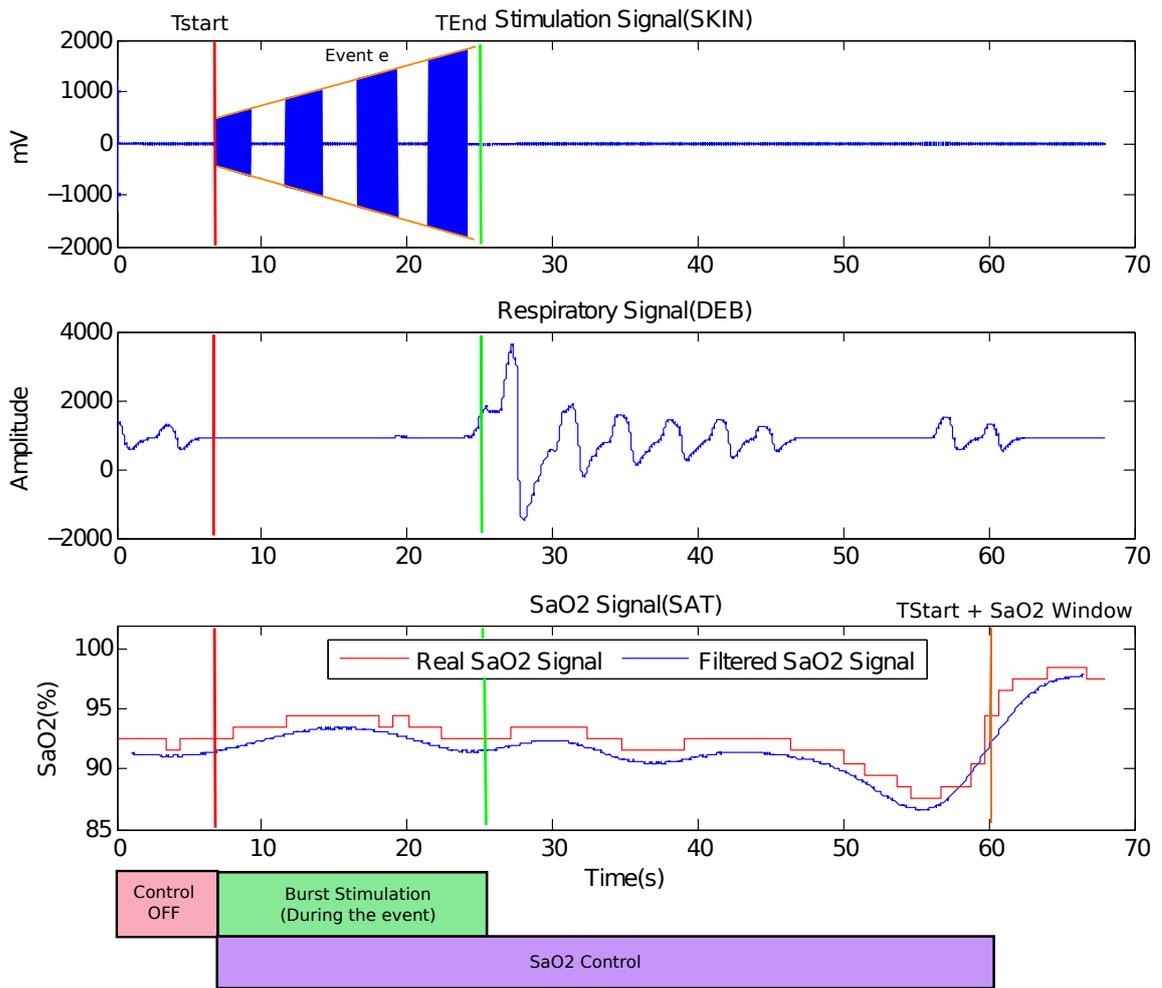
Figure 7.4: Example of the adaptive kinesthetic stimulation therapy for a given apnea event. The first upper panel shows the stimulation signal delivered by the system for a given event, e. The second panel presents the respiratory signal of the patient. The third panel illustrates the SaO_2 signal, where the orange signal is the real signal acquired by the system and the blue signal is its processed and filtered version. The boxes below the figure represent the state of the controller during a given respiratory events. Note the linear increase in the stimulation amplitude due to the fact that the event duration (Tresp) is increasing. The red and green lines represent the start and end of the respiratory event as detected by the system. The orange line represents the end of the SaO_2 analysis window.

$$TResp = f2 = t - t_e^{start} \qquad (7.4)$$

$$A(t+1, e) = max(20, A(t+1, e)) \qquad (7.5)$$

$$A(t+1, e) = min(100, A(t+1, e)) \qquad (7.6)$$

where a_1, b_1, b_2, c_1, c_2 are the control coefficients, to be optimized.
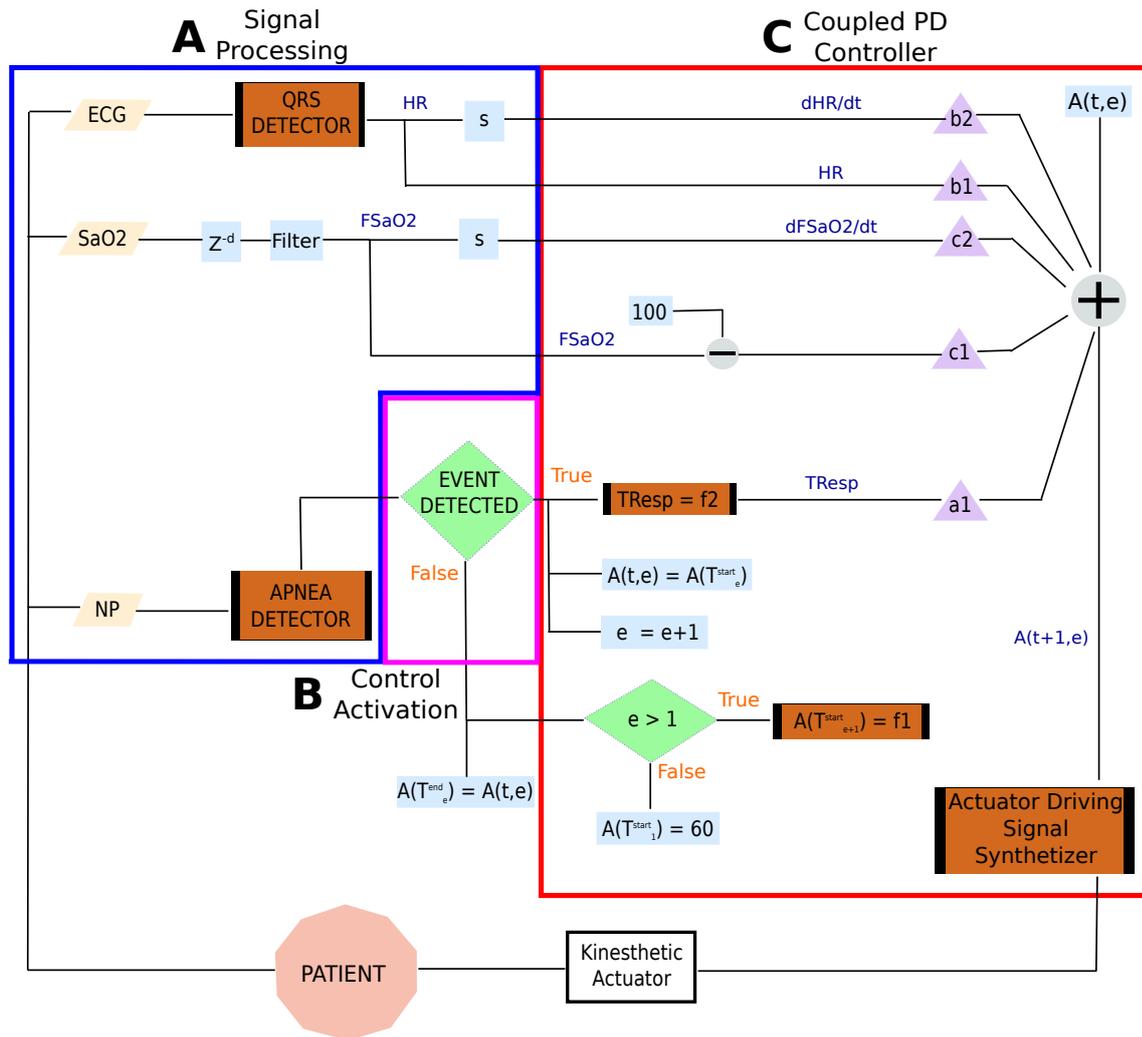
Figure 7.5: Diagram of the proposed closed-loop control. Signals presented as inputs to the control loop are: nasal pressure (NP), oxygen saturation (SaO$_2$) and electrocardiogram (ECG). ECG and NP signals pass through a QRS and a respiratory event detector, respectively, in order to determine the heart rate signal (HR) and the TResp signal which corresponds to the time passed into an apnea/hypopnea event. The control coefficients are represented as a_1, b_1, b_2, c_1, c_2. T_e^{start} and T_e^{end} are the beginning and the end of each detected respiratory event e. Finally, A represents the amplitude value to be delivered by the controller.

7.2.4.   Acceleration signal inclusion

In chapter 5 we discussed that body position during the sleep of the patient may also affect the mechanical coupling between the stimulator and the skin of the patient and therefore alter the effectiveness of the kinesthetic stimulation. In this study, we attached an accelerometer to the actuator (see section 7.2.1.2) in order test our hypothesis through a complete recording night. Each of the 3 axis of the accelerometer were conditioned to be used as input to the PSG recording. Real-time acceleration signals were obtained for each patient, providing information of the position of the patient and the stimulation energy

delivered by the actuator. Indicators of the quality of the mechanical coupling between the actuator and the skin of the patient were estimated from those signals. Analyses of the acceleration signal are currently ongoing in the context of another thesis of our team. However, section 7.3.3 presents preliminary results of the development of a new mechanical coupling index for one patient.

7.2.5.   Study design (EKINOX study)

The second version of the PASITHEA kinesthetic stimulation therapy has started within the framework of another clinical protocol approved by the ethics committee of the Grenoble University Hospital (Comité de Protection des Personnes, Grenoble, France, EKINOX study). The study was conducted with the same applicable good clinical practice requirements and ethical principles described in chapter 4 for the HYPNOS study. In this second protocol, four centers were involved: the University Hospitals of Grenoble, Tours, Bézieres and Rennes. The main objective of this study was to validate the novel fully adaptive closed-loop control stimulation algorithm for the detection and characterization of apnea and hypopnea during sleep, taking, as in the HYPNOS study, the PSG recordings as a gold standard.

The principal differences (described in detail in the following sections) between the first (HYPNOS) and the second (EKINOX) version of the PASITHEA therapy are:

1. Earlier detection of respiratory events

2. Stimulation energy variations by a closed-loop control algorithm.

3. Stimulator encapsulated with an accelerometer to assess coupling to the patient.

4. Two complete experimental nights for each patient (1 night with stimulation and 1 night without it)

This study was divided into two phases: a first stabilization phase with the inclusion of 10 patients, directed to the selection and adjustment of the parameters of the stimulation control and a second randomized phase, with the inclusion of 30 patients, dedicated to the characterization of the patient response to therapy with the inclusion of the control algorithm. Figure 7.6 shows a diagram of the development of this study.

Patients were eligible for this acute study if they previously provided informed consent and had a history of severe obstructive sleep apnea assessed by PSG testing within the past 6 months (Apnea-hypopnea index (AHI) > 30 episodes/h and 80% obstructive events).

Results on this chapter will be focused on the first phase of the EKINOx study, which was finalized before the end of this thesis. Phase 2 is still ongoing. In particular, one of the objectives of phase 1 was to optimize the coefficients of the control method. These control coefficients were tested on the first 10 patients with borderline values, in order to estimate their impact on the controller and a qualitative analysis was performed in
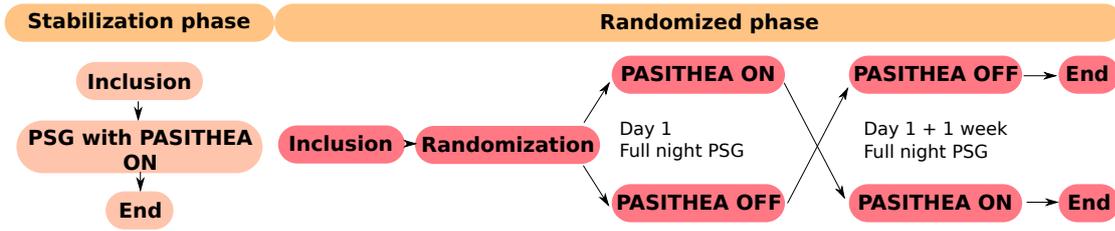
Figure 7.6: Diagram of the two phases of the EKINOX study. Two types of recording nights were proposed in which the system was active (PASITHEA ON) or inactive (PASITHEA OFF). First, a stabilization phase where only one night with the system activated was performed for each patient. Then, a randomized phase where two nights of recording were performed for each patient. The first night was randomly selected as PASITHEA ON or PASITHEA OFF to then be changed for the next night.

order to characterize the patients response to the therapy. The analysis was based on the observation of respiratory event duration, SaO$_2$ level and the cardiorespiratory response, along with a second analysis of the behavior of the controller.

7.3.   Results

7.3.1.   Detector optimization

Results from the optimization of the detector's parameters implementing evolutionary algorithms showed an improvement in performance of 10.3% and 10.2% in terms of sensitivity for apneas and hypopneas respectively. Regarding specificity, an increase of 10.1% for hypopneas along with a decrease of 0.7% for apneas were also obtained from the analysis. Table 7.1 presents the results from the performance analysis.

Table 7.1: Respiratory detector performance results (All the indicators are represented as percentage (%)).

Respiratory event detector	Apnea				Hypopnea			
	Se	PPV	Sp	NPV	Se	PPV	Sp	NPV
First version	66.9	80.7	97.1	94.3	47.1	25.0	84.3	93.5
Optimized version	77.2	76.4	96.4	96.2	57.3	31.8	94.4	85.4

After varying the previously mentioned set of parameters for about fourteen generations, the minimum error between the detector output and the clinical annotations converged to a stable value of -0.6568 as figure 7.7 shows.

The set of parameters θ selected from the optimization are presented in table 7.2.

7.3.2.   Controller evaluation

Qualitative analysis of the physiological response of a representative patient to the proposed adaptive kinesthetic stimulation therapy is presented in figure 7.8, where the
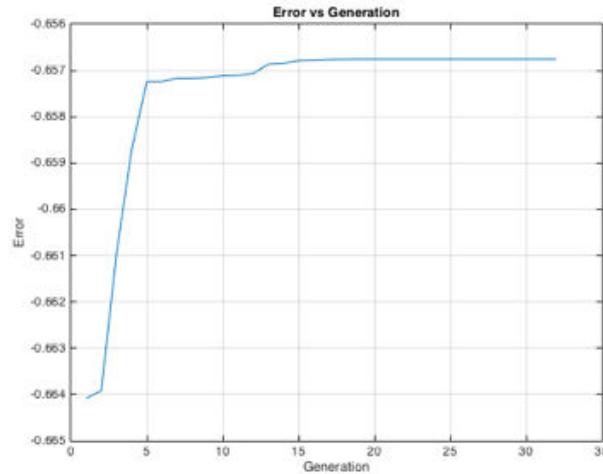
Figure 7.7: Resulting error of the optimized respiratory event detector. It can be observed how the minimum error converges to a stable value of -0.6568 after the 14th generation.

Table 7.2: Optimized set of parameters for the respiratory event detector

Parameter	
DurationFlatMin	2.45 s
DurationFlatMax	4.13 s
Earlytime	2.98 s
Hypduration	4.00 s

acquired data was obtained from the implementation of the following control parameters: $(a_1 = 0.03, c_1 = 0.1, c_2 = -2)$. The nasal pressure signal (Figure 7.8-A) is applied as input to the respiratory event detector. The output of the event detector is shown in Figure 7.8-B (red line). We observe in this example, the detection of a set of apnea events (marked with an "A"), and a set of hypopnea events ("H"). The stimulation signal, synthesized at the output of the controller and used to drive the kinesthetic actuator is shown in Figure 7.8-B, blue line. Note that the stimulation is only delivered when a respiratory event is detected and that the amplitude of the Stim signal changes over time, as a function of the physiological response of the patient. The number of bursts delivered depends on the event duration. In this case, the stimulation was able to stop all the respiratory events within the 6.1 seconds, and in most cases, with a limited number of bursts (one or two bursts). It is also important to highlight that the stimulation amplitude converges to a relatively low, stable value around 50%, showing that the controller tends to minimize the delivered stimulation amplitude, while eliciting the desired physiological response. Another effect of the therapy is shown in figure 7.8-C, where SaO_2 signal remains around 95%, showing no hypoxia events (SaO_2 level below 90%) due to the reduced duration of the respiratory episodes. Finally, figure 7.8-D shows the instantaneous heart rate (HR) signal, as detected from the ECG. It can be observed that there are no significant tachycardia events and the

mean HR is low despite the number of respiratory events.
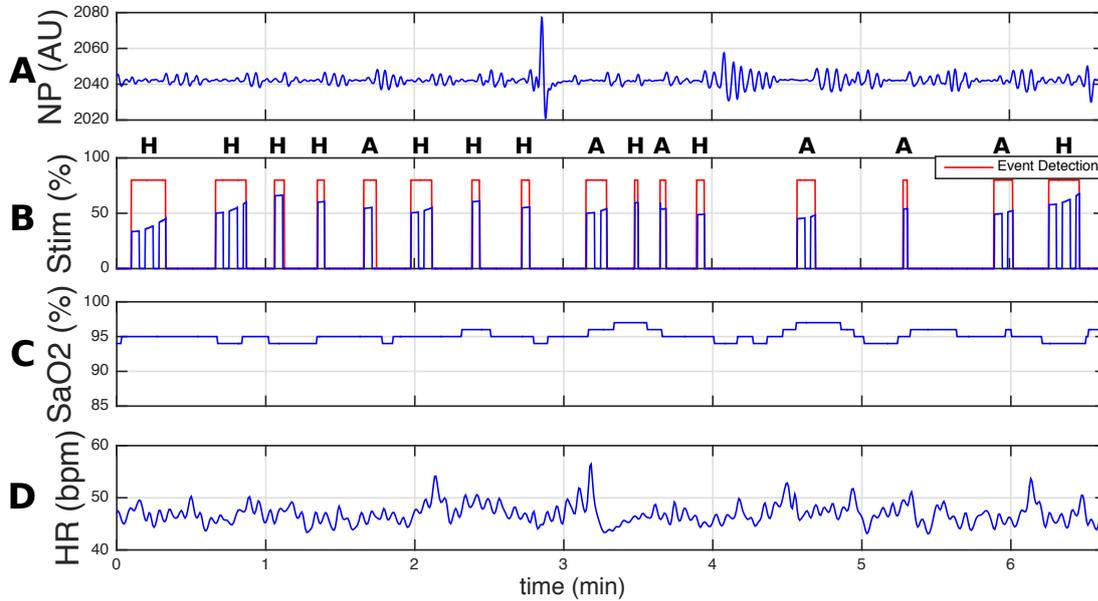
Figure 7.8: Cardiorespiratory response to adaptive kinesthetic stimulation. A) nasal pressure (NP), B) output of the respiratory event detector (red line detections: apnea and hypopnea) along with the amplitude signal of the kinesthetic stimulation (Stim), C) oxygen saturation (SaO$_2$) and D) instantaneous heart rate (HR), as detected from the ECG. "A" and "B" represents apnea or hypopnea detections respectively.

Quantitative analysis results of the 10 patients included in this phase of the study in terms of event duration, HR response, delivered energy and SaO$_2$ levels are presented in figure 7.9. The set of parameters implemented for each patient are presented in table 7.3. Since there is not enough data to perform statistical analyses on the obtained results, we based the selection of the set of control coefficients on direct observation. After discarding patients with few number of respiratory events, the best compromise in performance was found for patients 3 and 9. These patients presented the lowest values for event duration and delivered stimulation energy, while conserving relatively high SaO$_2$ and HR response levels. Although patient 4 presented convenient results, it was discarded for not having enough events to analyze.

Thus, the selected control coefficients were: $a_1 = 0.01, c_1 = 0.10, c_2 = -2.00$. Note that this decision was a combination of the sets applied for the previously mentioned patients, based on the analysis of the event-by-event response of each signal influenced by its corresponding coefficient. Moreover, other important aspects that were taken into account apart from the physiological response were the prevention of the saturation of the stimulation and the stability of the controller.
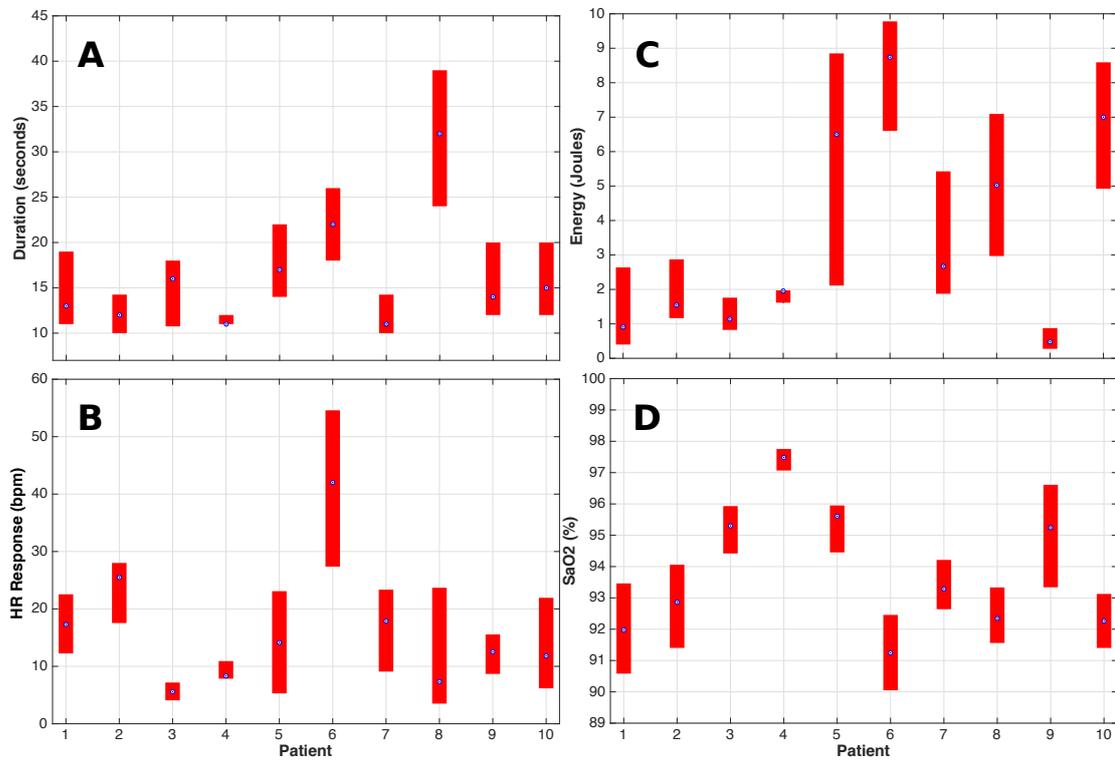
Figure 7.9: Boxplots of the quantitative results for the patients included in the first phase of the EKINOX study. A) Event duration (seconds), B) HR response (bpm), C) Delivered stimulation energy (Joules) and D) SaO_2 levels (%).

Table 7.3: Set of control coefficients of each patient implemented for the closed-loop controller

Patient	a_1	c_1	c_2
1	0.01	-0.01	2.00
2	0.01	-0.01	2.00
3	0.03	0.10	-2.00
4	0.03	0.10	-2.00
5	0.03	0.10	-2.00
6	0.03	0.10	-2.00
7	0.03	0.10	-2.00
8	0.01	-0.01	2.00
9	0.01	-0.01	2.00
10	0.03	0.10	-2.00

7.3.3. Acceleration evaluation

This section shows preliminary results from the analyses that are currently ongoing in the context of another thesis of our team where the mechanical coupling between the actuator and the skin of the patient is estimated with an accelerometer attached to the

actuator (see section 7.2.1.2) in order to improve the application of the therapy. A novel coupling index have been implemented to compare with a rule-based threshold system if the mechanical coupling has the quality needed to apply the therapy correctly. Three threshold levels have been defined: i) Floating (no mechanical coupling), ii) minimum coupling and iii) good coupling. Figure 7.10 presents results for a complete night of recording where the mechanical coupling is estimated. The black, red and violet lines represent the different coupling thresholds while the color-bar represent the three different body positions that the patient can have (yellow = the head of the patient rests on top of the actuator, green = neutral position where the actuator is on one side of the head without any other contact and blue = the actuator is on the opposite side to the resting place of the head of the patient). As described in chapter 5, the therapy efficacy strongly depends of this mechanical coupling; in this example, it is observed that the coupling decrease during night and it is influenced by the patient body position. This behavior can be observed in figure 7.10 in the first hour where the head of the patient rests on top of the actuator and the best coupling is found. Note that floating coupling is observed after the fifth hour of recording due to the body position and the deterioration of the adhesive used to attach the actuator.

7.4.   Discussion

Previous works have studied the possibility of using kinesthetic stimulation to treat sleep apnea, both in adults and infants (HERNÁNDEZ et al., 2007a; HERNÁNDEZ et al., 2016). Although results from these studies suggest that this therapy may be useful, some limitations persist in order to be applicable in clinical practice. One of these limitations is related to the stimulation parameters that should be used and, in particular, to the stimulation amplitude. Indeed, if a very large stimulation amplitude is used, respiratory events may be stopped more easily but the sleep of the patient can be significantly fragmented, while a too low amplitude will provoke no effect on respiratory events. An optimal stimulation amplitude should be defined between these extreme values. In this chapter, we have shown the difficulty of the parameters selection for a closed-loop control algorithm in biomedical applications due to the need of patients recruitment in order to be able to empirically test the control parameters. For obvious reasons, this need results in a great limitation to determine an optimal set of parameters. Further analyses in the context of another thesis of our team are currently ongoing for the development of mathematical models that represent the physiopathology underlying in patients suffering from SAS. The results of those analyses may be relevant for the determination of the optimal set of parameters since these models would allow in-bench optimization like those performed for the respiratory event detector in section 7.2.1.1.

In this first study phase, we determinate that the control coefficients should be in the range of $a_1 = [0.01, 0.03], c_1 = [-0.01, 0.10], c_2 = [-2.00, 2.00]$. However, for the accurate estimation of these coefficients, further statistical event-by-event analyses should be performed. These analyses would permit the characterization and classification of the
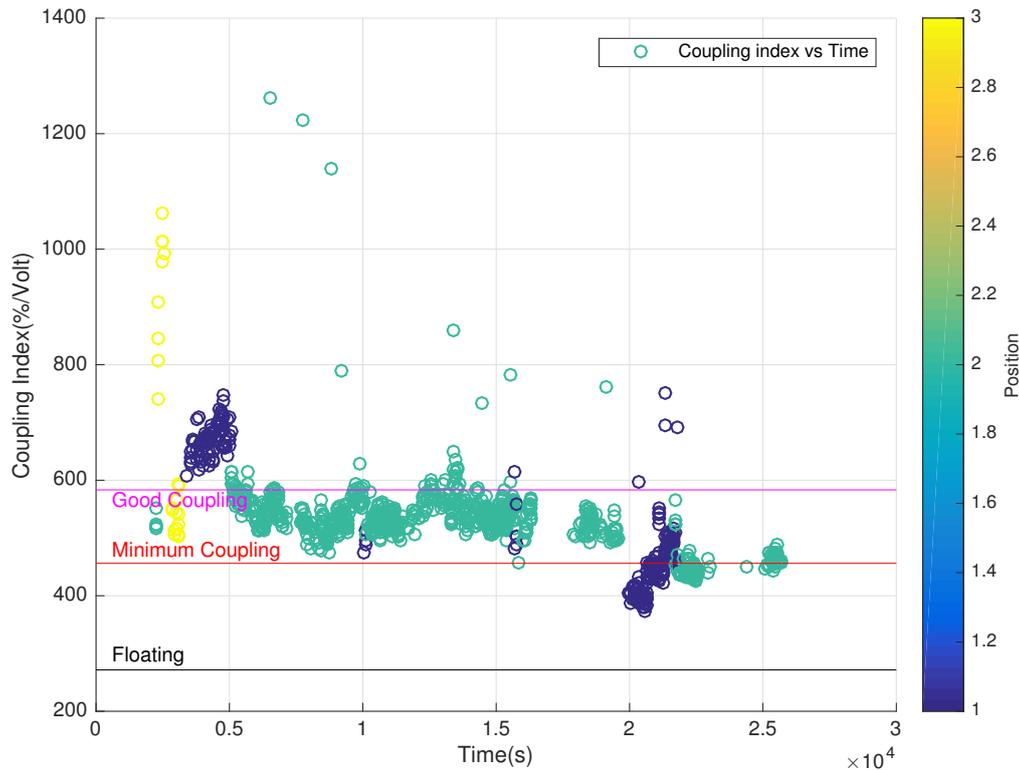
Figure 7.10: Example of mechanical coupling estimation for a complete night of recording. The black, red and violet lines represent the different coupling thresholds. Body positions are represented by a color-bar, 1) yellow = the head of the patient rests on top of the actuator, 2) green = neutral position where the actuator is on one side of the head without any other contact and 3) blue = the actuator is on the opposite side to the resting place of the head of the patient.

physiological responses associated with the sort of stimulation applied.

Note that although the closed-loop control algorithm is capable of taking the HR signal as a control variable, in this phase, due to the scarce information in the literature on the HR responses to kinesthetic stimulation, we limited the analyses to the coefficients related to NP and SaO$_2$ signals (a_1, c_1 and c_2). Prospective event-by-event analyses of these HR responses due to kinesthetic stimulation amplitude over the patients enrolled in this first phase will be performed in order to estimated coefficients b_1 and b_2 for the next study phase.

In our previous works (see chapter 4), stimulation parameters were constant for all patients and these parameters were defined heuristically from a test population. It seems obvious from previous results that each patient responds differently to a given set of kinesthetic stimulation parameters, implying the need of patient-specific stimulation values. Moreover, changes in patient sleep stages and position during the night may have consequences on the optimal stimulation amplitude.

In this work, qualitative results showed that the controller is technically capable of adapting the stimulation and converging to a minimum patient-specific amplitude, which is sufficient to elicit the desired physiological response. These results are encouraging concerning the feasibility of implementing this controller in therapy. However, further studies are necessary to evaluate the effect of the therapy, performing a statistical comparison in the duration and frequency of the SAS events, as well as an analysis of the sleep structure of these patients. These analyses will be performed after the second phase of the EKINOX study.

Regarding the optimization of the respiratory event detector results (section 7.3.1.), an improvement in performance of 10.3% and 10.2% in terms of sensitivity for apneas and hypopneas respectively along with an increase in specificity of 10.1% for hypopneas have been obtained. However, PPV values in particular for hypopneas remained rather low. These results present a significant concern since the performance of the control loop is intrinsically linked to the number of correct respiratory event detections. Briefly, if the detector yields to a significant amount of false positives detections, the control-loop algorithm will translate this behavior into a "no-response", leading to important increases of the stimulation amplitude that can cause amplitude saturation. Instability problems are also of concern in this situation. We acknowledge that this limitation could affect the results for the next study phase. Yet, since the main objective of this study was the validation of the closed-loop controller, we decided to integrate the already tested (see chapter 4, HYPNOS study) respiratory event detector. Future developments will be focused on the improvement of this detector through probabilistic detection algorithms (ALTUVE et al., 2011; CRUZ et al., n.d.; SONG et al., 2016).

An important aspect that was observed during phase 1 is that the effectiveness of the therapy decreases as the night progresses. We hypothesize that the reason of this loss of effectiveness is due to a reduction of the mechanical coupling between the actuator and the skin of the patient throughout the night (see section 7.3.3).

7.5.   Conclusion

In this chapter, a novel control system for real-time detection and adaptive therapy delivery through kinesthetic stimulation, directed to patients suffering from SAS was proposed. First, by the adaptation and improvement of the previously validated PASITHEA system (see chapter 4). Improvements were incorporated into each of the different parts constituting the system: an optimization of the respiratory event detector implemented in the first study of this project (HYPNOS study), hardware and firmware adaptation of the kinesthetic stimulation device, and several modifications of the real-time control application in order to integrate all the new features included in this phase were also proposed and validated.

Moreover, the proposed closed-loop controller functioning was validated on 10 patients included in the first phase of the EKINOX study, and it was shown that the controller is

capable of delivering an adaptive kinesthetic stimulation in function of the patient-specific responses. In addition, qualitative results, demonstrate that the control algorithm tends to minimize the delivered stimulation amplitude, while eliciting the desired physiological response.

Although the main objective of this study to validate the functioning of the controller was accomplished, some technical concerns, as the high false positive detection rate of the event respiratory detector (see section 7.4) and the estimation of the mechanical coupling between the actuator and the skin of the patient, remained as limitations. However, these concerns are currently under evaluation and future developments will be focused on the improvement of the current event respiratory detector through probabilistic detection algorithms. Mechanical coupling estimation algorithms are also in development.

The preliminary results of the effect of the adaptive stimulation presented in this chapter are very encouraging and they offer valuable information on the feasibility of the implementation of this controller in the therapy. Further works are directed to the clinical evaluation of this device on a second phase with the inclusion of 30 patients. Characterization of the patient response to therapy with the inclusion of the validated control algorithm will be also perform.

References

ALTUVE, M., G. CARRAULT, A. BEUCHEE, P. PLADYS, and A. I. HERNANDEZ (2011). "On-line apnea-bradycardia detection using hidden semi-Markov models". In: *Engineering in Medicine and Biology Society, EMBC, 2011 Annual International Conference of the IEEE*. IEEE, pp. 4374–4377.

CHENG, J. Y. and T. MAILUND (2015). "Ancestral population genomics using coalescence hidden Markov models and heuristic optimisation algorithms". In: *Computational biology and chemistry* 57, pp. 80–92.

CRUZ, J., A. I. HERNANDEZ, S. WONG, G. CARRAULT, and A. BEUCHEE. "Algorithm fusion for the early detection of apnea-bradycardia in preterm infants". In: *Computers in Cardiology, 2006*, pp. 473–476.

DOYEN, M. (2018). "Méthodes probabilistes pour le monitoring cardio-respiratoire des nouveau-nés prématurés". PhD thesis. Rennes 1.

FEUERSTEIN, D., L. GRAINDORGE, A. AMBLARD, A. TATAR, G. GUERRERO, S. CHRISTOPHLE-BOULARD, C. LOIODICE, A. I. HERNANDEZ, et al. (2015). "Real- time detection of sleep breathing disorders". In: *2015 Computing in Cardiology Conference (CinC)*. IEEE, pp. 317–320.

GOLDBERG, D. E. and J. H. HOLLAND (1988). "Genetic algorithms and machine learning". In: *Machine learning* 3.2, pp. 95–99.

HERNÁNDEZ, A., J. CRUZ, and G. GARRAULT (2007a). *Device for supervision and stimulation intended to fight sleep apnea*. Tech. rep. WO Patent App. PCT/EP2007/055,723.

HERNÁNDEZ, A., G. GUERRERO, D. FEUERSTEIN, L. GRAINDORGE, D. PEREZ, A. AMBLARD, P. MABO, J.-L. PÉPIN, and L. SENHADJI (2016). "PASITHEA: An Integrated Monitoring and Therapeutic System for Sleep Apnea Syndromes Based on Adaptive Kinesthetic Stimulation". In: *IRBM* 37.2, pp. 81–89.

LE ROLLE, V., A. BEUCHEE, J.-P. PRAUD, N. SAMSON, P. PLADYS, and A. I. HERNÁNDEZ (2015). "Recursive identification of an arterial baroreflex model for the evaluation of cardiovascular autonomic modulation". In: *Computers in biology and medicine* 66, pp. 287–294.

LE ROLLE, V., D. OJEDA, and A. I. HERNÁNDEZ (2011). "Embedding a cardiac pulsatile model into an integrated model of the cardiovascular regulation for heart failure followup". In: *IEEE transactions on biomedical engineering* 58.10, pp. 2982–2986.

OJEDA, D., V. LE ROLLE, M. HARMOUCHE, A. DROCHON, H. CORBINEAU, J.-P. VERHOYE, and A. I. HERNÁNDEZ (2014). "Sensitivity analysis and parameter estimation of a coronary circulation model for triple-vessel disease". In: *IEEE Transactions on Biomedical Engineering* 61.4, pp. 1208–1219.

PÉREZ, D., G. GUERRERO, D. FEUERSTEIN, L. GRAINDORGE, A. AMBLARD, J.-L. PÉPIN, L. SENHADJI, and A. HERNÁNDEZ (2016). "Closed-loop kinesthetic stimulation for the treatment of sleep apnea syndromes". In: *Computing in Cardiology Conference (CinC), 2016.* IEEE, pp. 841–844.

SONG, C., K. LIU, X. ZHANG, L. CHEN, and X. XIAN (2016). "An obstructive sleep apnea detection approach using a discriminative hidden Markov model from ECG signals". In: *IEEE Transactions on Biomedical Engineering* 63.7, pp. 1532–1542.

CHAPTER 8 ■

Conclusion

Sleep apnea syndrome (SAS) is a common disease characterized by repeated episodes of upper airway obstruction during sleep, causing intermittent hypoxia (IH) and impaired sleep continuity and quality (LÉVY et al., 2014). SAS is a growing health concern affecting up to 5% of middle-aged men and women (HEINZER et al., 2015; JENNUM et al., 2009). SAS is recognized as an important and independent risk factor for hypertension, coronary heart diseases, stroke and cardiovascular complications in the long term (SOMERS et al., 2008; STANSBURY et al., 2015). The deleterious effects of SAS on cardiovascular outcomes are mainly triggered by IH severity and the subsequent activation of the autonomic nervous system (DRAGER et al., 2010; KASAI et al., 2011). To date, the gold standard therapy in the management of moderate to severe SAS is the continuous positive airway pressure (CPAP) (BERKANI et al., 2015; MARIN et al., 2005). However, recent studies have proved that this therapy has a 15% initial refusal rate, along with average adherence rates between 36% and 50% (CRAIG et al., 2012; KUSHIDA et al., 2012). Other therapies have been proposed as alternative strategies for the treatment of SAS. Recently, stimulation approaches dedicated to augment neural output to upper airway dilator muscles (e.g., hypoglossal nerve stimulation) and direct stimulation of the phrenic nerve have gained interest in the treatment of obstructive and central apnea. Nonetheless, although promising, they remain under clinical evaluation (PENGO et al., 2016; PONIKOWSKI et al., 2011; STROLLO JR et al., 2014).

In this thesis, we proposed a novel real-time monitoring and therapeutic neuromodulation system for SAS, based on triggered kinesthetic stimulation. The hypothesis underlying this therapy was that burst of kinesthetic stimulation delivered during the early phase of the respiratory events (apnea or hypopnea), may elicit a controlled startle response that can activate sub-cortical centers controlling upper airway muscles and the autonomic nervous system, stopping respiratory events without generating a cortical arousal. Since SAS consequences are mainly linked to the IH severity and the subsequent autonomic activations, the first part of this thesis work was focused on the assessment of the physiological

responses to the application of the previously described therapy.

Novel approaches better accounting for the complexity and multifactorial nature of the available biomedical signals were developed. They were applied on clinical databases composed of polysomnography (PSG) data from subjects that underwent a whole night of recording where the kinesthetic stimulation was evaluated. The physiological responses and the patient selection profile were evaluated by two main approaches:

- Characterization of the effects of the triggered kinesthetic stimulation therapy in respiratory event duration, oxygen saturation levels, sleep fragmentation and number of micro-arousals for patients suffering for SAS.

- Comparison of the ANS function based on heart rate variability (HRV) and heart rate complexity (HRC) parameters between SAS patients with different responses to kinesthetic stimulation therapy, in order to prove the relevance of the ANS function for a more accurate selection of patients to whom the proposed therapy should be applied.

According to the analysis of the effects of kinesthetic stimulation, 75% of patients included in this first part of the project demonstrated a significant reduction (5 seconds approximately) in the duration of apneas or hypopneas. Moreover, although non-significant improvements were found in terms of ODI4 and mean SaO_2 when comparing the whole group of patients, a new method based on $\delta SaO2$ analysis has shown a statistically significant reduction in more than half of the patients, 55.4% decrease for apnea and 37.61% for hypopnea events. Regarding sleep analysis, no statistically significant differences were found for any sleep stage when comparing active and inactive stimulation periods. Neither significant differences were found concerning micro-arousal index results.

Results from the analyses of the ANS function have shown that when comparing the ANS function between SAS patients classified as responders and non-responders to kinesthetic stimulation in terms of reduction in respiratory events duration, a statistically significant decrease in HF_{nu} was noted in non-responder patients in relation to responders, suggesting that this greater vagal modulation found in responder patients may be related to a healthier ANS condition (TRINDER et al., 2001). Furthermore, a statistically significant increase in α_1 was also noted in non-responders, indicating that these patients present a more correlated RR series than the fractal-like dynamics associated with healthy subjects. A significant reduction in cardiac complexity according to $SampEn$ and HFD was also found in non-responder patients, evidencing an impaired heart condition. These results suggest that the key mechanism underlying the effectiveness of this therapy is the presence of a properly-functioning ANS. Therefore, the previously observed lack of response to kinesthetic stimulation may be due to an inappropriate patient selection that should have included a complete HRV and HRC analysis.

Findings from these analyses indicate that kinesthetic stimulation therapy is capable of decreasing the duration of the respiratory events and, when applied early during these

events, important reductions on SaO_2 levels may also be avoided. Moreover, results suggest that the effectiveness of this therapy depends on the ANS condition of the patient. Therefore, this aspect should be included as clinical criteria for an appropriate patient selection. Concerning sleep analyses, although preliminary results were presented, we acknowledge that, by design, this first study did not allow a robust assessment of the impact of kinesthetic stimulation on a whole night sleep architecture.

The results of this first part of the thesis also provided important information about the technical improvement needed for the second phase. These technical aspects were: i) an optimization of the respiratory event detector that decreases the detection time delay, ii) the inclusion of an accelerometer attached to the stimulator in order to estimate the mechanical coupling between the stimulator and the skin of the patient, and iii) the implementation of a novel real-time adaptive closed-loop control algorithm for delivering kinesthetic stimulation.

The second part of the thesis was focused on the improvements made on these aspects. Moreover, a complete description of the preliminary results obtained from a second clinical protocol aimed to evaluate the performance of the novel adaptive control algorithm was presented. Results from the optimization of the respiratory event detector showed an improvement in performance of more than 10% in terms of sensitivity for apneas and hypopneas. However, PPV values remained rather low for hypopneas which represents a significant concern for the global effectiveness of the therapy since the performance of the control loop is intrinsically linked to the number of correct respiratory event detections. Regarding mechanical coupling analysis, a new method based on a coupling index that identifies, with a rule-based threshold system, if the mechanical coupling has the quality needed to correctly apply the therapy, was also proposed in the context of another thesis. Preliminary results show that the coupling quality depends on two main factors: the body position of the patient and the time instant of the night, since the mechanical coupling tends to decrease throughout night due to deterioration of the adhesive used to attach the stimulator.

A closed-loop control system integrating concurrent, coupled proportional-derivative (PD) controllers was proposed in order to manage the kinesthetic stimulation amplitude delivered to the patient. Ten patient underwent a full PSG recording night in order to stabilize and evaluate the proposed controller. Although the correct functioning of the controller was validated, there were still some limitations related to the optimal stimulation control parameters that should be used. As described in the introduction of this thesis, one of the difficulties of parameter selection in biomedical applications is the need of patient recruitment to empirically test these control parameters. In this study, we determinate that the control coefficients should be in the range of $a_1 = [0.01, 0.03], c_1 = [-0.01, 0.10], c_2 = [-2.00, 2.00]$. However, for the accurate estimation of these coefficients, further statistical event-by-event analyses should be performed. On the other hand, further analyses in the context of another thesis are currently ongoing for the development of new mathematical models that represent the physiopathology underlying SAS. The results of those analyses

could provide relevant information for the selection of the optimal set of parameters since these models would allow in-bench optimization.

Future work will be focused on the analysis of the physiological responses obtained from adaptive kinesthetic stimulation in the second phase of the ongoing clinical protocol including 30 more SAS patients. Event-by-event analyses of the HR response of patients enrolled in this study will be performed in order to estimate the remained control coefficients b_1 and b_2. Finally, new control and detection probabilistic algorithms will be evaluated for their inclusion in a third version of the system. Indeed, the limitation of the need of patient recruitment for the evaluation of new control algorithms remains, but, with the implementation of the mathematical models that are currently ongoing, new possibilities for the development of more advanced control systems using methods such as Markov chains and neural networks are foreseen.

References

BERKANI, K. and J. DIMET (2015). "[Acceptability and compliance to long-term continuous positive pressure treatment]". In: *Revue des maladies respiratoires* 32.3, pp. 249–255.

CRAIG, S. E., M. KOHLER, D. NICOLL, D. J. BRATTON, A. NUNN, R. DAVIES, and J. STRADLING (2012). "Continuous positive airway pressure improves sleepiness but not calculated vascular risk in patients with minimally symptomatic obstructive sleep apnoea: the MOSAIC randomised controlled trial". In: *Thorax*, thoraxjnl–2012.

DRAGER, L. F., J. C. JUN, and V. Y. POLOTSKY (2010). "Metabolic consequences of intermittent hypoxia: relevance to obstructive sleep apnea". In: *Best practice & research Clinical endocrinology & metabolism* 24.5, pp. 843–851.

HEINZER, R., S. VAT, P. MARQUES-VIDAL, H. MARTI-SOLER, D. ANDRIES, N. TOBBACK, V. MOOSER, M. PREISIG, A. MALHOTRA, G. WAEBER, et al. (2015). "Prevalence of sleep-disordered breathing in the general population: the HypnoLaus study". In: *The Lancet Respiratory Medicine* 3.4, pp. 310–318.

JENNUM, P. and R. L. RIHA (2009). "Epidemiology of sleep apnoea/hypopnoea syndrome and sleep-disordered breathing". In: *European Respiratory Journal* 33.4, pp. 907–914.

KASAI, T. and T. D. BRADLEY (2011). "Obstructive sleep apnea and heart failure: pathophysiologic and therapeutic implications". In: *Journal of the American College of Cardiology* 57.2, pp. 119–127.

KUSHIDA, C. A., D. A. NICHOLS, T. H. HOLMES, S. F. QUAN, J. K. WALSH, D. J. GOTTLIEB, R. D. SIMON JR, C. GUILLEMINAULT, D. P. WHITE, J. L. GOODWIN, et al. (2012). "Effects of continuous positive airway pressure on neurocognitive function in obstructive sleep apnea patients: the Apnea Positive Pressure Long-term Efficacy Study (APPLES)". In: *Sleep* 35.12, pp. 1593–1602.

LÉVY, P., M. KOHLER, W. T. McNICHOLAS, F. BARBÉ, R. D. McEVOY, V. K. SOMERS, L. LAVIE, and J.-L. PEPIN (2014). "Obstructive sleep apnoea syndrome." In: *Nature reviews. Disease primers* 1, pp. 15015–15015.

MARIN, J. M., S. J. CARRIZO, E. VICENTE, and A. G. AGUSTI (2005). "Long-term cardiovascular outcomes in men with obstructive sleep apnoea-hypopnoea with or without treatment with continuous positive airway pressure: an observational study". In: *The Lancet* 365.9464, pp. 1046–1053.

PENGO, M. F., S. XIAO, C. RATNESWARAN, K. REED, N. SHAH, T. CHEN, A. DOUIRI, N. HART, Y. LUO, G. F. RAFFERTY, et al. (2016). "Randomised sham-controlled trial of transcutaneous electrical stimulation in obstructive sleep apnoea". In: *Thorax*, thoraxjnl–2016.

PONIKOWSKI, P., S. JAVAHERI, D. MICHALKIEWICZ, B. A. BART, D. CZARNECKA, M. JASTRZEBSKI, A. KUSIAK, R. AUGOSTINI, D. JAGIELSKI, T. WITKOWSKI, et al. (2011). "Transvenous phrenic nerve stimulation for the treatment of central sleep apnoea in heart failure". In: *European heart journal* 33.7, pp. 889–894.

SOMERS, V. K., D. P. WHITE, R. AMIN, W. T. ABRAHAM, F. COSTA, A. CULEBRAS, S. DANIELS, J. S. FLORAS, C. E. HUNT, L. J. OLSON, et al. (2008). "Sleep apnea and cardiovascular disease: An American heart association/American college of cardiology foundation scientific statement from the American heart association council for high blood pressure research professional education committee, council on clinical cardiology, stroke council, and council on cardiovascular nursing in collaboration with the national heart, lung, and blood institute national center on sleep disorders research (national institutes of health)". In: *Journal of the American College of Cardiology* 52.8, pp. 686–717.

STANSBURY, R. C. and P. J. STROLLO (2015). "Clinical manifestations of sleep apnea". In: *Journal of thoracic disease* 7.9, E298.

STROLLO JR, P. J., R. J. SOOSE, J. T. MAURER, N. DE VRIES, J. CORNELIUS, O. FROYMOVICH, R. D. HANSON, T. A. PADHYA, D. L. STEWARD, M. B. GILLESPIE, et al. (2014). "Upper-airway stimulation for obstructive sleep apnea". In: *New England Journal of Medicine* 370.2, pp. 139–149.

TRINDER, J., J. KLEIMAN, M. CARRINGTON, S. SMITH, S. BREEN, N. TAN, and Y. KIM (2001). "Autonomic activity during human sleep as a function of time and sleep stage". In: *Journal of sleep research* 10.4, pp. 253–264.

List of associated publications

International journals

Hernández, Alfredo I, **Pérez, Diego**, D. Feuerstein, C. Loiodice, L. Graindorge, G. Guerrero, N. Limousin, F. Gagnadoux, Y. Dauvilliers, R. Tamisier, et al. (2018). "Kinesthetic stimulation for obstructive sleep apnea syndrome: An "on-off" proof of concept trial. **AH and DP contributed equally to this work**". In: *Scientific reports* 8.1, p. 3092.

Hernandez, A., G. Guerrero, D. Feuerstein, L. Graindorge, D. Perez, A. Amblard, P. Mabo, J.-L. Pépin, and L. Senhadji (2016). "Pasithea: An integrated monitoring and therapeutic system for sleep apnea syndromes based on adaptive kinesthetic stimulation". In: *IRBM* 37.2, pp. 81–89.

International conferences

Pérez, D., G. Guerrero, D. Feuerstein, L. Graindorge, A. Amblard, J.-L. Pépin, L. Senhadji, and A. Hernández (2016). "Closed-loop kinesthetic stimulation for the treatment of sleep apnea syndromes". In: *Computing in Cardiology Conference (CinC), 2016*. IEEE, pp. 841–844.

International abstracts

Hernández, A. I., D. O. P. Trenard, D. Feuerstein, C. Loiodice, L. Graindorge, G. Guerrero, N. Limousin, F. Gagnadoux, Y. Dauvilliers, R. Tamisier, et al. (2017). "Kinesthetic stimulation for obstructive sleep apnea syndrome: an "on-off" proof of concept trial". In: European Respiratory Society. Eur Respiratory Soc.

Software registration

PÉREZ, D., A. I. HERNÁNDEZ, T. JANVIER, and G. GUERRERO. *Design électronique de hardware SALTH et firmware associée (V1.a, V1.b et V2).*

Kinesthetic stimulation therapy of sleep apnea syndrome: duration, acute SaO$_2$ and sleep analyses results

This appendix contains the results of the durations, acute SaO$_2$ and sleep analyses presented in chapter 5. Tables of the results for each patient presenting the median, Q1 and Q3 quartiles of the time spent at each sleep stage (Awake, REM, Stage1, Stage2 and Stage3) as well as the micro-arousals indices, during cycles $Ther_{en}$, $Ther_{dis}$ and during the whole night (41 markers in total for each patient) are presented in this appendix for the sleep analysis.

B.1. Event durations

Table B.1: Mean, Q1 and Q3 for the apnea duration results (24 patients).

Apnea durations (seconds).

Patient	$Ther_{en}$			$Ther_{dis}$			p-value
	Median	Q1	Q3	Median	Q1	Q3	
1	11.5	11	12	13	12	14	0.14
2	10	9	13	17	12	24.5	<0.01
3	13	10.75	13	14	12.5	17.75	0.12
4	12	10.5	13.5	18	16	20.5	<0.01
5	11.5	10.5	13	11.5	11	14	0.31
6	12	11.25	13.75	23	18.75	28	<0.01
7	13	11.25	13.75	20	16	23	<0.01
8	12	11	13	25	18.5	27	<0.01
9	12	10	14	14	12	16	0.02
10	10	10	13	13	11	16	0.01
11	13	11	14.5	13	11	15	0.25
12	12	11	16	15	13	18	<0.01
13	12	10.75	14	17.5	16	21	<0.01
14	12	11	15.75	14	11	19	0.01
15	13	10.5	17	23	18	27	<0.01
16	12	12	19.5	20.5	16.5	22.5	0.13
17	17	15.5	18.5	15.5	13	23	0.58
18	16	12.25	21.25	18	15	21.75	0.049
19	16	12	26	22	17	25	0.01
20	25	17	31.25	16	11	23	1.00
21	28.5	24	33	28	22	33	0.81
22	33	28	40	30	25	36	0.99
23	36	27	41.25	33	27	40	0.76
24	NaN	NaN	NaN	38.5	25.5	44	NaN

Table B.2: Mean, Q1 and Q3 for the hypopnea duration results (24 patients).

Hypopnea durations (seconds).

Patient	$Ther_{en}$			$Ther_{dis}$			p-value
	Median	Q1	Q3	Median	Q1	Q3	
1	21.5	15.5	17	18	14	16	0.02
2	23	14	18	18.25	15	16	0.19
3	43.25	17	29	18	14	16	<0.01
4	31	15	21	16.25	14	15	0.01
5	29	18	21	21	17	18	<0.01
6	36.25	18.75	25	21	15.75	17	<0.01
7	18	15	17	38.75	20	37	1.00
8	16	16	16	18.25	13	16	0.75
9	19	14	15.5	16	14	14.5	0.38
10	20	14	16	16	13	14	0.01
11	17	13	15	17.75	13.25	16	0.71
12	28.75	15	22	21	15	18	0.01
13	28	16	22	16	14	15	<0.01
14	24	15	18	26	14.5	17	0.34
15	35	21	29	26.5	15	17	<0.01
16	21	15	17	18	14	15.5	0.045
17	37	21	27	40	24	29	0.91
18	23	17	20	27	17	21	0.97
19	23	16	20	33.5	15	17	0.31
20	17.5	14	15	28	16.25	18	0.94
21	35.5	24	30	35.75	26	29	0.51
22	25	15	18	24.5	16.25	21	0.66
23	45.5	22.5	33.5	60.25	36.75	44	1.00
24	34.5	18	24	21	15	18.5	<0.01

B.2. Local, acute SaO$_2$ results

Table B.3: Mean, Q1 and Q3 for the apnea δSaO$_2$ results (24 patients).

Apnea δSaO$_2$ (%).

Patient	$Ther_{en}$			$Ther_{dis}$			p-value
	Median	Q1	Q3	Median	Q1	Q3	
1	3.06	1.32	4.32	0.50	-0.05	1.04	0.93
2	1.58	1.00	2.00	2.65	1.37	4.43	<0.01
3	0.98	0.77	1.75	4.00	3.13	5.60	0.01
4	2.30	1.83	2.91	4.06	3.41	4.68	<0.01
5	3.89	2.27	4.53	2.49	1.74	3.73	0.88
6	2.82	0.83	3.99	3.38	1.01	4.89	0.28
7	1.63	0.70	2.10	3.60	1.99	6.77	<0.01
8	8.18	7.20	10.17	4.44	3.47	7.64	0.92
9	2.27	1.33	3.47	3.07	2.65	4.87	0.01
10	2.74	0.36	3.22	3.92	2.90	5.77	<0.01
11	1.83	0.03	3.00	1.23	0.14	2.35	0.85
12	1.88	0.76	3.10	0.96	-0.19	2.37	0.97
13	4.04	0.00	5.00	7.61	7.00	7.93	<0.01
14	4.24	2.73	7.38	4.05	2.61	7.14	0.54
15	2.19	1.03	4.49	5.55	3.16	7.00	<0.01
16	1.00	0.51	1.95	7.76	2.65	8.45	0.02
17	0.60	0.15	0.90	0.23	0.00	3.96	0.50
18	1.00	0.00	2.21	2.06	0.89	4.00	0.01
19	2.48	0.69	3.67	1.73	0.57	3.25	0.80
20	1.11	-0.38	3.56	1.07	-0.39	2.68	0.58
21	0.96	0.00	1.58	0.58	0.00	1.70	0.40
22	2.47	0.17	3.61	2.06	0.53	3.43	0.61
23	1.06	-0.78	3.09	1.20	-1.91	3.94	0.58
24	NaN	NaN	NaN	6.78	2.05	13.63	NaN

Table B.4: Mean, Q1 and Q3 for the hypopnea δSaO$_2$ results (24 patients).

Hypopnea δSaO$_2$ (%).

Patient	$Ther_{en}$			$Ther_{dis}$			p-value
	Median	Q1	Q3	Median	Q1	Q3	
1	1.95	0.49	3.74	2.00	1.08	3.02	0.54
2	0.98	0.33	1.79	1.57	0.55	2.43	0.04
3	1.66	1.08	3.38	2.71	1.44	3.49	0.22
4	2.89	1.16	3.37	2.05	1.00	3.16	0.77
5	1.59	0.78	2.46	1.85	0.74	3.32	0.29
6	0.90	0.02	2.32	1.96	0.79	3.17	0.02
7	1.62	0.33	2.51	2.56	1.09	3.02	0.14
8	5.76	5.76	5.76	4.07	4.07	4.07	1.00
9	0.87	0.52	1.28	1.51	0.14	2.45	0.37
10	1.47	0.88	2.77	2.00	0.96	3.00	0.19
11	1.26	0.04	2.00	0.71	0.04	1.51	0.91
12	1.93	0.72	3.16	1.83	0.83	3.30	0.46
13	2.33	1.65	3.89	2.90	1.97	3.80	0.27
14	1.35	-0.12	3.24	2.66	1.28	4.37	<0.00
15	1.80	0.29	3.30	2.44	1.29	3.67	0.04
16	1.38	0.67	2.10	1.90	0.90	3.00	0.16
17	1.76	0.55	3.07	1.00	0.00	2.44	0.93
18	1.00	0.00	1.75	1.00	0.00	2.00	0.09
19	1.03	0.38	2.20	1.20	0.53	2.11	0.42
20	1.16	-0.07	2.16	2.58	1.66	5.71	0.11
21	1.00	0.00	1.51	0.67	0.00	1.68	0.55
22	1.32	-0.14	2.65	1.59	0.71	2.70	0.29
23	1.58	0.25	3.00	1.33	-0.68	4.13	0.49
24	2.11	1.20	3.00	2.83	1.72	3.97	0.04

B.3. Sleep stage

Table B.5: Time spent in awake for $Ther_{en}$ and $Ther_{dis}$ periods (24 patients).

	Awake (time in minutes)						
	$Ther_{en}$			$Ther_{dis}$			
Patient	Median	Q1	Q3	Median	Q1	Q3	p-value
1	0.00	0.00	3.86	0.75	0.00	30.00	0.70
2	21.82	17.45	28.05	3.50	1.31	16.97	0.06
3	1.50	1.50	15.33	0.50	0.00	8.00	0.35
4	8.01	6.39	13.68	4.87	0.50	24.50	1.00
5	28.00	1.63	29.50	21.75	17.56	30.00	0.67
6	5.03	3.25	9.75	1.96	1.25	2.72	**0.02**
7	15.30	5.70	19.20	2.42	1.25	4.27	0.23
8	30.00	22.98	30.00	30.00	21.63	30.00	0.34
9	22.24	9.50	26.27	11.29	1.00	20.26	0.24
10	1.50	0.53	5.97	0.57	0.13	1.90	0.41
11	23.50	5.91	29.00	23.16	14.21	27.00	0.81
12	1.42	0.90	8.75	0.00	0.00	8.07	0.30
13	7.21	3.07	10.83	3.36	2.37	5.61	0.31
14	3.19	2.33	4.36	5.44	3.50	10.00	0.25
15	4.56	2.50	29.01	2.00	1.13	11.37	0.56
16	1.36	0.00	10.82	1.04	0.25	5.21	0.85
17	1.25	0.25	3.71	2.00	0.00	5.13	0.91
18	4.38	0.50	14.56	2.50	0.75	7.76	0.76
19	3.50	0.75	7.74	4.00	2.38	6.90	0.83
20	20.00	3.02	30.00	24.96	4.38	30.00	0.99
21	0.50	0.13	1.76	1.06	0.00	2.50	0.90
22	1.25	1.00	3.50	0.50	0.00	1.36	0.08
23	0.00	0.00	14.47	0.00	0.00	1.03	0.80
24	4.00	1.00	29.51	2.86	0.38	11.19	0.51

Table B.6: Time spent in REM for $Ther_{en}$ and $Ther_{dis}$ periods (24 patients).

REM (time in minutes)

Patient	$Ther_{en}$			$Ther_{dis}$			p-value
	Median	Q1	Q3	Median	Q1	Q3	
1	0.00	0.00	16.64	0.00	0.00	0.00	0.45
2	0.00	0.00	0.08	0.00	0.00	2.87	0.56
3	0.17	0.00	5.59	9.86	0.00	13.78	0.52
4	1.84	0.00	9.46	0.00	0.00	1.84	0.42
5	0.00	0.00	0.00	0.00	0.00	0.00	0.93
6	2.01	0.78	9.72	11.65	4.03	16.75	0.31
7	0.00	0.00	9.91	0.00	0.00	1.39	0.86
8	0.00	0.00	0.00	0.00	0.00	0.00	NaN
9	0.00	0.00	0.27	2.87	0.00	10.23	0.32
10	0.00	0.00	0.00	9.73	0.13	19.56	NaN
11	0.00	0.00	0.00	0.00	0.00	0.00	NaN
12	0.00	0.00	14.87	0.00	0.00	8.29	1.00
13	0.85	0.00	12.32	6.44	0.00	7.70	0.70
14	0.00	0.00	4.38	0.00	0.00	0.00	NaN
15	0.00	0.00	0.00	0.00	0.00	6.68	0.54
16	8.17	0.00	11.55	1.93	0.00	8.97	0.47
17	3.71	0.00	16.97	0.00	0.00	13.08	0.65
18	6.00	0.00	14.02	0.00	0.00	3.28	0.33
19	0.00	0.00	1.14	0.00	0.00	0.00	0.73
20	0.00	0.00	9.48	0.00	0.00	6.02	0.80
21	11.53	0.01	25.97	5.47	0.00	25.93	0.86
22	0.49	0.00	19.76	0.00	0.00	22.88	0.95
23	3.57	0.00	9.15	2.39	0.49	10.99	0.80
24	0.00	0.00	8.50	0.00	0.00	15.64	0.83

Table B.7: Time spent in stage 1 for $Ther_{en}$ and $Ther_{dis}$ periods (24 patients).

	Stage 1 (time in minutes)						
	$Ther_{en}$			$Ther_{dis}$			
Patient	Median	Q1	Q3	Median	Q1	Q3	p-value
1	0.00	0.00	0.00	0.00	0.00	1.50	0.73
2	4.12	1.87	8.49	10.09	8.68	14.49	0.11
3	3.25	1.75	5.00	0.50	0.00	1.75	0.24
4	6.00	3.50	7.04	3.00	0.00	5.34	0.22
5	0.50	0.13	3.13	2.97	0.00	5.00	0.63
6	5.97	3.46	8.28	3.54	2.04	7.25	0.51
7	4.50	2.25	5.47	4.43	3.07	6.10	0.86
8	0.00	0.00	7.03	0.00	0.00	1.75	0.86
9	3.62	1.50	6.50	6.53	4.52	8.00	0.48
10	11.93	7.34	15.79	3.49	2.63	4.04	0.07
11	4.36	1.00	6.25	3.00	1.00	7.05	0.98
12	7.56	4.88	10.35	1.50	0.00	2.63	**0.03**
13	4.75	3.58	6.47	3.73	2.73	5.91	0.74
14	8.00	5.60	14.88	4.09	0.41	6.50	0.18
15	7.50	1.00	13.50	4.11	0.88	8.51	0.84
16	2.38	0.00	3.00	0.75	0.00	3.18	0.64
17	6.04	1.75	7.71	3.50	0.00	4.29	0.24
18	4.10	0.75	9.50	3.90	1.76	8.40	0.80
19	14.51	7.25	17.01	16.50	5.43	24.63	0.53
20	1.24	0.00	4.50	0.00	0.00	7.62	0.98
21	1.00	0.13	11.14	3.50	0.00	6.81	0.86
22	5.99	2.28	19.50	7.50	1.13	14.98	1.00
23	2.00	0.38	6.40	4.50	2.06	7.38	0.60
24	0.75	0.00	7.64	0.86	0.21	2.93	0.93

Table B.8: Time spent in stage 2 for $Ther_{en}$ and $Ther_{dis}$ periods (24 patients).

	Stage 2 (time in minutes)						
	$Ther_{en}$			$Ther_{dis}$			
Patient	Median	Q1	Q3	Median	Q1	Q3	p-value
1	10.00	5.50	11.63	5.50	0.00	17.13	0.78
2	0.00	0.00	4.07	6.00	4.35	10.13	0.17
3	10.92	5.34	18.09	8.50	5.83	11.97	0.90
4	6.00	3.73	10.27	6.50	0.00	7.65	0.53
5	0.00	0.00	14.87	3.09	0.00	8.98	1.00
6	7.00	3.50	13.00	5.39	1.00	11.50	0.46
7	3.71	0.93	5.80	18.15	14.21	20.43	0.06
8	0.00	0.00	0.00	0.00	0.00	6.62	NaN
9	1.14	0.00	3.74	5.64	1.74	8.26	0.26
10	7.51	5.37	15.01	11.00	3.17	11.83	1.00
11	0.00	0.00	15.88	0.25	0.00	3.25	0.83
12	9.80	8.02	11.64	5.78	2.26	11.43	0.22
13	14.62	8.50	19.32	9.83	7.68	11.29	0.42
14	15.80	6.25	16.81	18.73	12.20	21.02	0.33
15	6.25	0.11	9.50	8.00	1.22	17.78	0.56
16	9.15	2.30	16.96	10.75	5.00	23.28	0.75
17	12.47	6.03	20.51	14.00	0.00	18.88	0.98
18	8.92	2.80	14.49	15.27	8.31	21.50	0.17
19	0.00	0.00	7.00	0.50	0.00	8.13	0.69
20	0.01	0.00	9.27	0.00	0.00	2.24	0.49
21	11.45	0.25	20.98	5.72	0.00	21.76	0.69
22	4.75	0.00	8.25	0.50	0.00	20.50	0.81
23	22.04	3.24	26.87	20.03	14.26	25.63	0.97
24	9.43	0.00	12.50	7.19	2.04	13.48	0.94

Table B.9: Time spent in stage 3 for $Ther_{en}$ and $Ther_{dis}$ periods (24 patients).

	Stage 3 (time in minutes)						
	$Ther_{en}$			$Ther_{dis}$			
Patient	Median	Q1	Q3	Median	Q1	Q3	p-value
1	8.50	0.50	13.15	4.94	0.00	11.13	0.70
2	0.00	0.00	0.00	0.00	0.00	0.00	NaN
3	0.00	0.00	7.41	7.00	3.76	15.09	0.27
4	0.00	0.00	1.83	0.00	0.00	10.06	0.69
5	0.00	0.00	0.00	0.00	0.00	0.00	NaN
6	0.00	0.00	3.78	0.00	0.00	6.71	0.93
7	0.00	0.00	12.38	2.60	0.00	8.80	1.00
8	0.00	0.00	0.00	0.00	0.00	0.00	NaN
9	0.00	0.00	0.00	3.67	0.00	6.00	0.24
10	0.00	0.00	11.02	1.47	0.00	8.40	0.80
11	0.00	0.00	1.39	0.00	0.00	1.33	0.96
12	0.00	0.00	1.45	4.00	0.00	22.18	0.29
13	0.25	0.00	0.50	7.50	0.00	10.80	0.16
14	0.00	0.00	0.00	0.00	0.00	4.50	NaN
15	0.00	0.00	0.50	0.81	0.00	5.81	0.52
16	0.52	0.00	1.50	0.24	0.00	6.73	1.00
17	0.00	0.00	0.00	0.00	0.00	2.39	0.39
18	0.00	0.00	0.00	0.00	0.00	2.25	0.53
19	0.00	0.00	6.61	1.02	0.00	4.80	0.80
20	0.00	0.00	0.00	0.00	0.00	0.00	NaN
21	0.00	0.00	0.00	0.00	0.00	0.00	NaN
22	0.00	0.00	0.00	0.00	0.00	0.00	NaN
23	0.00	0.00	0.00	0.00	0.00	0.00	NaN
24	1.18	0.00	2.86	5.64	0.00	12.15	0.44

B.4.   Micro-arousal

Table B.10: MicroArousal Index results for $Ther_{en}$ and $Ther_{dis}$ periods (24 patients).

MicroArousal Index (number/hours of sleep)

Patient	$Ther_{en}$			$Ther_{dis}$			p-value
	Median	Q1	Q3	Median	Q1	Q3	
1	18.00	9.50	33.71	16.00	7.00	41.53	0.90
2	61.42	29.59	65.86	32.37	27.90	45.08	0.39
3	20.00	9.47	36.83	6.49	4.69	23.78	0.90
4	26.03	8.00	35.57	15.48	4.00	32.69	0.65
5	2.08	0.00	31.11	32.91	23.53	59.35	0.12
6	21.29	7.41	31.67	16.98	9.96	38.33	0.88
7	21.82	5.45	90.71	73.29	54.93	84.67	0.63
8	140.93	140.93	140.93	96.79	96.79	96.79	1.00
9	9.67	0.00	43.32	12.16	5.22	12.41	0.89
10	40.72	28.94	76.26	22.61	13.97	27.15	0.20
11	40.08	0.00	57.85	29.78	18.91	46.52	0.66
12	66.08	46.24	84.16	28.84	18.00	53.30	0.10
13	20.34	12.42	28.17	14.35	13.03	25.00	0.82
14	63.87	52.65	89.98	57.94	30.88	66.00	0.43
15	39.54	0.00	72.31	30.03	16.22	43.20	0.78
16	16.38	7.39	30.78	23.13	13.23	44.72	0.41
17	8.40	0.00	32.28	3.74	0.00	27.14	1.00
18	44.00	34.41	56.92	52.36	36.64	56.88	0.65
19	30.00	12.29	51.99	50.76	17.19	72.00	0.32
20	88.42	72.00	137.14	82.49	62.91	Inf	0.98
21	40.71	4.58	54.36	32.57	5.00	50.42	0.79
22	29.60	6.22	57.21	20.00	6.60	65.37	0.67
23	59.99	49.57	63.49	62.00	55.55	73.02	0.26
24	16.55	6.21	44.14	14.39	13.30	24.44	1.00

B.5.   Whole night sleep overview

Table B.11: Time spent in each sleep stage for the whole night (24 patients).

Time spent in each sleep stage (time in minutes)

Patient	Awake	REM	Stage1	Stage2	Stage3
1	153.00	45.12	12.00	129.03	107.02
2	148.98	10.97	92.58	48.62	0.00
3	127.00	58.62	22.50	93.53	102.52
4	167.13	72.40	64.00	97.63	67.50
5	334.00	14.00	45.48	117.50	13.00
6	132.50	141.00	86.00	129.98	72.50
7	84.00	16.00	36.20	89.35	37.00
8	222.83	0.00	15.38	13.82	0.00
9	198.67	33.30	80.02	58.50	40.52
10	45.90	80.88	89.28	146.35	61.42
11	293.85	15.98	62.50	65.00	33.00
12	64.87	70.87	64.53	131.40	54.50
13	97.78	60.60	60.47	147.48	66.50
14	85.00	17.82	93.50	180.02	21.50
15	151.50	35.13	135.02	101.50	41.02
16	101.47	90.32	37.25	176.13	52.00
17	131.50	125.35	91.00	216.02	20.50
18	121.87	86.02	103.95	226.33	24.50
19	106.50	45.70	219.13	51.00	71.50
20	348.52	107.97	54.98	52.02	0.00
21	60.05	186.73	74.00	185.50	3.00
22	77.00	161.50	192.13	129.00	6.00
23	71.40	68.10	63.98	267.02	0.00
24	160.50	67.15	43.50	118.00	63.02

List of Figures

List of Tables